

ANNALES ACADEMIÆ SCIENTIARUM FENNICÆ

MATHEMATICA

DISSERTATIONES

149

DIRECT AND INVERSE SCATTERING
FOR BELTRAMI FIELDS

SIMOPEKKA VÄNSKÄ



HELSINKI 2006
SUOMALAINEN TIEDEKATEMIA

Editor: OLLI MARTIO
Department of Mathematics and Statistics
P.O. Box 68
FI-00014 University of Helsinki
Finland

ANNALES ACADEMIÆ SCIENTIARUM FENNICÆ

MATHEMATICA

DISSERTATIONES

149

DIRECT AND INVERSE SCATTERING
FOR BELTRAMI FIELDS

SIMOPEKKA VÄNSKÄ

University of Helsinki, Department of Mathematics and Statistics

*To be presented, with the permission of the Faculty of Science of the
University of Helsinki, for public criticism in Auditorium CK112,
Exactum, on December 19th, 2006, at 12 o'clock noon.*

HELSINKI 2006
SUOMALAINEN TIEDEAKATEMIA

Copyright © 2006 by
Academia Scientiarum Fennica
ISSN 1239-6303
ISBN 951-41-0987-2

Received 17 November 2006

2000 Mathematics Subject Classification:
Primary 35R30; Secondary 47A40, 78A46, 65N21.

YLIOPISTOPAINO
HELSINKI 2006

Abstract

We consider an obstacle scattering problem for linear Beltrami fields. A vector field u is a linear Beltrami field if $\nabla \times u = ku$ with a constant $k > 0$. We study the obstacles that are of Neumann type, that is, the normal component of the total field vanishes on the boundary of the obstacle. We prove the unique solvability for the corresponding exterior boundary value problem, in other words, the direct obstacle scattering model. For the inverse obstacle scattering problem, we deduce the formulas that are needed to apply the singular sources method. The numerical examples are computed for the direct scattering problem and for the inverse scattering problem.

Tiivistelmä

Työssä tarkastellaan lineaaristen Beltrami-kenttien sirontaa esteestä. Vektorikenttä u on lineaarinen Beltrami-kenttä, mikäli $\nabla \times u = ku$ jollakin vakiolla $k > 0$. Tarkasteltavat esteet ovat Neumann-tyyppiä, ts. kentän normaalikomponenttien vaaditaan katoavan esteen reunalla. Työssä osoitetaan, että vastaava ulkoalueen reuna-arvotettava on yksikäsitteisesti ratkeava, eli käytettävissä on suoran sironnan malli. Työssä johdetaan kaavat, jotka tarvitaan, jotta singulaaristen lähteiden menetelmää voidaan soveltaa esteen sironnan inversio-ongelman ratkaisemiseen Beltrami kenttien tapauksessa. Työssä esitetään numeerisia esimerkkejä sekä suoralle että käänteiselle sirontatehtävälle.

Acknowledgements

For the financial support I am indebted to the Graduate School of Applied Electromagnetism, Väisälä Foundation, Academy of Finland, Rolf Nevanlinna Institute and the Department of Mathematics and Statistics of Helsinki University.

I would like to express my deepest gratitude to my supervisor Petri Ola for guiding me to the inverse problems and for his friendly and patient guidance with this long-term project. I am also grateful to Matti Lassas for his guidance and encouragement.

I am grateful to Professor, Grand Ambassador of the Finnish Inverse Problems Society, Lassi Päivärinta for the inspirational and supportive working environment in our Inverse Problems group.

I thank Professor Jukka Sarvas who hired me to the Rolf Nevanlinna Institute and helped to get all this started.

I am grateful to the pre-examiners, Professors Masaru Ikehata and Samuli Siltanen, for reading carefully the manuscript and making valuable comments and suggestions.

I would like to thank Matti Taskinen for his guidance to the world of numerics and for the constant help with computers.

I thank Professors Andreas Kirsch and Rainer Kress for sending their articles and for discussions.

I thank Tuula Blåfield for checking and correcting the language.

I am deeply indebted to my colleagues. There are so many of you who have affected the accomplishment of this work one way or another! Particularly, I want to mention the Höris study group of early days, the coffee company of the Rolf Nevanlinna Institute and the SanDIke project group.

I am grateful to my wife Saara for her support and for pushing me over the final lines.

Finally, I would like to thank God for making all this possible, and especially, for computing wonderful direct problems so that we have challenging inverse problems to solve.

Helsinki, November 2006

Simopekka Vänskä

Contents

1	Introduction	9
2	Direct and inverse scattering problems	11
2.1	The Helmholtz equation and the radiation condition	12
2.2	An acoustic inverse obstacle scattering problem	19
2.2.1	Linear sampling method	21
2.2.2	Factorization method	24
2.2.3	Singular sources method	25
3	Direct obstacle scattering for Beltrami fields	29
3.1	Preliminaries	31
3.1.1	Basic definitions	31
3.1.2	Radiation condition	33
3.1.3	Integration by parts	35
3.1.4	Representation formulas	37
3.2	Exterior Neumann boundary value problem	41
3.2.1	Scattering of plane waves from a plane	42
3.2.2	Uniqueness	44
3.2.3	Existence	45
4	An inverse obstacle scattering problem for Beltrami fields	51
4.1	Uniqueness of the inverse obstacle scattering problem	52
4.1.1	A singular Beltrami field	52
4.1.2	Herglotz waves	56
4.1.3	Neumann-to-far-field mapping	58
4.1.4	The uniqueness result	59
4.2	Singular sources method for Beltrami fields	60
4.2.1	Mixed reciprocity	60
4.2.2	Approximating fields	62
4.2.3	Translating the singularity point	64
5	Numerical experiments	67
5.1	The far field solver	67
5.1.1	Discretized obstacles and boundary functions	68
5.1.2	Solving the boundary integral equation	69
5.1.3	The far field	72
5.2	Reconstructing the obstacle	73
5.2.1	Solving the Herglotz density of the singular source	74
5.2.2	Constructing the indicator function with a given approximation domain	76

5.2.3	Some scanning algorithms	78
5.3	Test cases	79
5.3.1	Forward problem	82
5.3.2	Inverse problem	84
6	Conclusions	96

1 Introduction

The direct obstacle scattering problem is to compute the scattered wave when an obstacle and an incident wave are given. A scattered wave has a certain decay when propagating. The shape of a scattered wave at infinity is called the *far field pattern*. The inverse obstacle scattering problem is to reconstruct the obstacle, or the obstacles, when the far field patterns of the scattered waves are known with given incident fields. The far field patterns can, in principle, be measured by sending in some incident fields and by measuring the corresponding scattered fields.

We consider obstacle scattering problems for Beltrami fields. A vector field u in \mathbb{R}^3 is a Beltrami field if

$$\nabla \times u = ku.$$

We study the case where $k > 0$ is a constant. This means that the Beltrami field is linear and the chirality right-handed.¹ Beltrami fields appear in plasma physics, electromagnetics and fluid mechanics [14, 30, 40, 4]. The boundary condition for an obstacle is defined by posing the Neumann boundary condition, that is, the normal component of the total field u vanishes on the boundary. For more background of Beltrami fields, see Chapter 3.

The direct obstacle scattering problem is a classical one. Recently, the inverse obstacle scattering problem and its modifications with different boundary values have been studied in acoustics and in electromagnetics [13, 9]. The inverse obstacle scattering problem is heavily ill-posed since the measurement operator is an infinitely smoothing operator. However, several numerical methods have been proposed to reconstruct an approximation for the obstacle. The algorithms can be divided into *iterative*, *decomposition* and *sampling/probe methods*; see [28].

Iterative methods, for example, *the Newton method*, require solving the forward problem iteratively many times and can, therefore, be computationally intensive.

Decomposition algorithms split the inverse problem into an ill-posed part and a well-posed part. A representative of these algorithms is the technique of Kirsch and Kress [23], in which one reconstructs the scattered field from its far-field pattern (ill-posed part) and then determines the scatterer by locating zeros of the total field.

In sampling methods one tests if a given point, or a region, is in or out of the scatterer. One often determines the boundary of the scatterer to be at where some indicator function

¹The case with negative and constant k is left-handed and similar. The non-linear case is when $k = k(x)$ is not constant, see [26, 5]. Note that the differential equation is linear also with the non-linear Beltrami fields.

blows up. Widely known sampling methods are the *linear sampling method* [11] and the *factorization method* [20], the latter being theoretically more satisfactory. In the *singular source method* [36], the indicator function is an approximation for the reflection of the singular source at the point of singularity. In Ikehata's *probe method* [19], one computes the indicator function along “needles”, and with the *enclosure method* [18] one can determine the convex hull of the obstacle. The blow-up of the indicator function is now based on the hyper-singularity (non-integrability) of the gradient field of the singular source. In the *no-response test* one samples with fields that are small in given test domains and then compares the corresponding far-field patterns [28]. We present the acoustic case and three sampling type reconstruction methods – linear sampling method, factorization method and the singular sources method – with more details in Chapter 2.

The interior Neumann boundary value problem for the Beltrami fields has been studied in [25, 33, 26, 5], also for non-constant k (non-linear Beltrami fields). However, as far as we know, the mathematical theory of the exterior Neumann boundary value problem is not so well understood. In [5] the authors proved that there are no exterior solution in certain weighted Sobolev spaces. In [3] the representation formula for the exterior solution is obtained if the solutions satisfy certain radiation condition. In [27, 3], it was also noted that the zero field is the only solution if the tangential boundary value of the total field is zero. Hence, there is no scattering theory for obstacles with vanishing tangential boundary values.

There are two main results in this work: We give a proof for the unique solvability of the exterior Neumann boundary value problem for the Beltrami fields with the correct radiation condition. Also, we show that for Beltrami fields the inverse obstacle scattering problem has a unique solution and obtain the formulas that are needed to apply the singular sources method [36] in reconstructing an approximation for the obstacle. To present numerical examples, we have implemented the boundary integral equation of the Neumann problem and the Neumann-to-far-field mapping. Also, we show some reconstructions that are made with the singular sources method. All computations are made in 3D.

The thesis is organized as follows. We begin by discussing the basics of the scattering phenomena and relate the Beltrami field scattering to a well-known acoustic situation. We also discuss the three sampling type reconstruction algorithms mentioned above. Chapter 3 is about the direct scattering problem for Beltrami fields. As the main result of the chapter, we prove the unique solvability for the exterior Neumann boundary value problem. In Chapter 4 we study the inverse obstacle scattering problem for Beltrami fields. We show that the singular sources method can be applied for this problem. Numerical examples are given in Chapter 5.

Throughout the work, we have tried to keep the mathematical framework as simple as possible. Although Beltrami fields appear in different areas of physics, the author has had no particular application in his mind for the inverse scattering problem. The work lies somewhere between theoretical studies and applications. We denote an obstacle by

Ω and assume $\Omega \subset \mathbb{R}^3$ is a smooth bounded domain with a connected complement. Interpreting the boundary integral operators as pseudodifferential operators and computing their symbols, which is our basic tool in solving the forward problem, is simple when the obstacles are smooth. The exterior domain is denoted² by

$$\Omega^s = \mathbb{R}^3 \setminus \bar{\Omega}.$$

A large part of the work is formulated for smooth functions: Because the incident fields are smooth functions, one has to be able to solve the direct boundary value problem with smooth obstacles only for smooth boundary functions. However, since the solvability of the boundary value problem is obtained with the Fredholm theory, one has to formulate the problem in such function spaces for which the compact imbedding is available. Also, one needs to consider mapping properties of the operators in order to deduce the reconstruction algorithms, particularly the factorization method. Hence, where it is necessary, we have used L^2 -based Sobolev spaces.

2 Direct and inverse scattering problems

Consider a wave that is propagating in space. The wave can, for example, be a sound wave or an electromagnetic wave. When the space is homogeneous, in other words, there is nothing that interacts with the wave, the wave just propagates freely. But suppose there is an inhomogeneity, a *scatterer*, that interacts with the wave. For example, in the sound wave case, the sound speed could differ from the basic background sound speed in some part of the media — a very concrete example is a fish (scatterer) in water (media). When the original wave, called an *incident wave*, hits the inhomogeneity, the wave scatters, and the *total wave* is thereafter a sum of the incident wave and the *scattered wave*.

The *direct scattering problem* is to determine the scattered wave when the incident wave and the material parameters of the homogeneous background and of the scatterer are given. The direct problem corresponds to what nature does. When one sends an incident wave, the nature “computes” the scattered wave automatically. Hence, if the physical model approximates nature well enough, one should get unique solvability for the direct scattering problem.

The *inverse scattering problem* is to determine the scatterer when one is measuring the scattered wave. Actually, there is a huge collection of different inverse scattering problems. First, what are we measuring? Can we measure the scattered wave anywhere, or are we limited to some points or directions? If we are using a sonar to find fish in a sea, then we can send the waves into the sea only from one point (the ship) and receive the scattered wave at the same point. But when we are trying to locate the cracks of a construction pole, we might be able to locate our measurement equipment all around the

²The motivation for the s -notation is that the scattered fields are defined in the exterior domain, “the scattering domain”.

pole and measure from any direction. Secondly, what do we mean by determining the scatterer? Is it enough to find the location of the scatterer (where the fishes are), or do we need the values of the inhomogeneous parameters (what species or size the fishes are)? The solvability of the inverse scattering problem differs a lot depending on what is really the question and what is the measurement.

The inverse problem that we are studying is the one in which we are able to produce a *plane wave* in any direction as an incident field and measure the corresponding *far-field pattern*. It turns out that a scattered field has a certain decay at infinity. The far-field pattern of a scattered field tells about the intensity and phase of the decay in each direction. The scatterer is assumed to be an obstacle, which means that on the boundary the total wave vanishes (in some component). The task is to find an algorithm to compute the shape of the scatterer.

2.1 The Helmholtz equation and the radiation condition

In this section, we have collected some basic facts concerning solutions of the Helmholtz equation. For a more detailed study of the Helmholtz equation and the acoustic scattering theory, we refer to [13].

Helmholtz equation Let $V : \mathbb{R}_x^3 \times \mathbb{R}_t \rightarrow \mathbb{C}$ satisfy the wave equation

$$\Delta V - \frac{1}{c^2} \frac{\partial^2 V}{\partial t^2} = 0,$$

where c is the speed of propagation. We consider only *time-harmonic* waves, namely waves of the form

$$(2.1) \quad V(x, t) = v(x)e^{-i\omega t},$$

where ω is a positive frequency. The corresponding physical wave is the real part of V . Throughout the work, we assume that the *wave number* $k = \omega/c$ is a positive constant. The *spatial part* $v = v(x)$ satisfies the *Helmholtz equation*

$$(2.2) \quad \Delta v + k^2 v = 0.$$

A basic example of a solution of the Helmholtz equation is a *plane wave*

$$v = v(x) = v(x, \xi) = e^{ikx \cdot \xi}, \quad \xi \in S^2.$$

The corresponding physical time-dependent field is

$$\operatorname{Re}(e^{ikx \cdot \xi} e^{-i\omega t}) = \cos(kx \cdot \xi - \omega t),$$

which at any moment is constant in each plane that is perpendicular to the propagation direction $\xi \in S^2$, explaining why these are called plane waves.

Fundamental solution The fundamental solution Φ is a field whose source term is the unit point source (Dirac's delta) at the origin,

$$(2.3) \quad -(\Delta + k^2)\Phi = \delta.$$

A straightforward computation shows that the only radially symmetric fundamental solutions, for which the *energy*

$$\int_{\partial B(0,R)} |\Phi(x)|^2 dS(x)$$

is independent of R , are

$$\Phi_{\pm}(x) = \frac{1}{4\pi} \frac{e^{\pm ik|x|}}{|x|}.$$

The corresponding physical time-dependent fields are

$$\operatorname{Re}(\Phi_{\pm}(x)e^{-i\omega t}) = \frac{1}{4\pi} \frac{1}{|x|} \cos(\pm k|x| - \omega t),$$

so if we choose the $+$ -sign, the waves are propagating away from the origin as time t grows. From now on, we always consider only the *outgoing* fundamental solution Φ ,

$$(2.4) \quad \Phi(x) = \frac{1}{4\pi} \frac{e^{ik|x|}}{|x|}.$$

Denote the translated fundamental solution by

$$(2.5) \quad \Phi_z(x) = \Phi(x - z), \quad z \in \mathbb{R}^3,$$

and similarly,

$$(2.6) \quad \delta_z(x) = \delta(x - z).$$

Now

$$-(\Delta + k^2)\Phi_z = \delta_z.$$

With the fundamental solution, one can represent a solution of the Helmholtz equation in terms of its Cauchy data. Suppose $v \in C^\infty(\overline{\Omega})$ solves the Helmholtz equation in Ω . Then, see [13],

$$(2.7) \quad \int_{\partial\Omega} \Phi_x(y) \frac{\partial v}{\partial n}(y) dS(y) - \int_{\partial\Omega} \frac{\partial \Phi_x}{\partial n}(y) v(y) dS(y) = \begin{cases} v(x), & x \in \Omega, \\ 0, & x \in \Omega^s. \end{cases}$$

Here, and from now on, $n = n(y)$ is the unit outer normal at point $y \in \partial\Omega$.

Sommerfeld radiation condition Suppose v solves the Helmholtz equation in an exterior domain Ω^s , $v \in C^\infty(\overline{\Omega^s})$. Let $x \in \mathbb{R}^3$. By applying the representation formula (2.7) in the domain $\Omega_R = \Omega^s \cap B(0, R)$, where $R > |x|$ is such that $\overline{\Omega} \subset B(0, R)$, we get the representation

$$\int_{\partial\Omega_R} \Phi_x(y) \frac{\partial v}{\partial n_R}(y) dS(y) - \int_{\partial\Omega_R} \frac{\partial \Phi_x}{\partial n_R}(y) v(y) dS(y) = \begin{cases} 0, & x \in \Omega, \\ v(x), & x \in \Omega^s. \end{cases}$$

Here $n_R = n_R(y)$ is the unit outer normal at $y \in \partial\Omega_R$. Now, the integral over the exterior part $\partial B(0, R)$ of the boundary $\partial\Omega_R$ vanishes, if v satisfies the *Sommerfeld radiation condition*

$$(2.8) \quad \hat{x} \cdot \nabla v(x) - ikv(x) = o\left(\frac{1}{|x|}\right), \quad \hat{x} = \frac{x}{|x|},$$

uniformly in all directions as $|x| \rightarrow \infty$, see [13]. Such v is called *radiating*, and we have the exterior representation formula

$$(2.9) \quad \int_{\partial\Omega} \Phi_x(y) \frac{\partial v}{\partial n}(y) dS(y) - \int_{\partial\Omega} \frac{\partial \Phi_x}{\partial n}(y) v(y) dS(y) = \begin{cases} 0, & x \in \Omega, \\ -v(x), & x \in \Omega^s. \end{cases}$$

Note that a straightforward calculation shows that the fundamental solution Φ_z and its derivative $\partial\Phi_z/\partial x_j$ satisfy the Sommerfeld radiation condition (2.8).

Far field pattern Every radiating solution v of the Helmholtz equation is of the form

$$(2.10) \quad v(x) = \Phi(x)v_\infty(\hat{x}) + o\left(\frac{1}{|x|}\right)$$

as $|x| \rightarrow \infty$. The function v_∞ is called the *far field pattern*³ of v or, shortly, the *far field* of v . From now on, we use the subscript ∞ notation to denote the far field of a function. By formula (2.10), the decay of each radiating solution is similar to the outgoing field of a point source when we are far away from the origin, and hence every radiating solution is outgoing.

The formula (2.10) can be obtained as follows. Suppose v is a radiating solution in an exterior domain Ω^s . Since

$$|x - z| = |x| - \hat{x} \cdot z + o(1)$$

for a fixed point $z \in \mathbb{R}^3$, we get

$$(2.11) \quad \Phi_z(x) = \Phi(x)e^{-ik\hat{x} \cdot z} + o\left(\frac{1}{|x|}\right).$$

³In many cases, the factor $\frac{1}{4\pi}$ is part of the far field, but we keep it as part of the fundamental solution. This causes some 4π -factor differences in some formulas when compared to, for example, [13].

Similarly, from

$$(2.12) \quad \nabla\Phi_z(x) = \Phi_z(x) \left(ik - \frac{1}{|x-z|} \right) \frac{x-z}{|x-z|}$$

and (2.11), it follows that

$$(2.13) \quad \nabla\Phi_z(x) = \Phi(x)e^{-ik\hat{x}\cdot z} ik\hat{x} + o\left(\frac{1}{|x|}\right).$$

Now, by the representation formula (2.9) and decays (2.11) and (2.13), we get (2.10) with

$$(2.14) \quad v_\infty(\hat{x}) = - \int_{\partial\Omega} e^{-ik\hat{x}\cdot y} \frac{\partial v}{\partial n}(y) dS(y) - ik \int_{\partial\Omega} e^{-ik\hat{x}\cdot y} n(y) \cdot \hat{x} v(y) dS(y).$$

Particularly, by (2.11) and (2.13), we get a formula for the far field of Φ_z and for its derivative,

$$(2.15) \quad \Phi_{z,\infty}(\hat{x}) = e^{-ik\hat{x}\cdot z},$$

and

$$(2.16) \quad \partial_j \Phi_{z,\infty}(\hat{x}) = ik\hat{x}_j e^{-ik\hat{x}\cdot z}.$$

Note that $\Phi_{z,\infty}$ is a plane wave in direction $-\hat{x}$ as a function of z .

Single layer Define the *single layer potential* of density $f \in C^\infty(\partial\Omega)$ by

$$(2.17) \quad S_A f(x) = \int_{\partial\Omega} \Phi_y(x) f(y) dS(y), \quad x \in A, \quad A \subset \mathbb{R}^3.$$

In the interior domain, $S_\Omega f$ and its derivative $\partial_j S_\Omega f$ solve the Helmholtz equation. In the exterior domain, $S_{\Omega^s} f$ and its derivative $\partial_j S_{\Omega^s} f$ are radiating solutions of the Helmholtz equation with far fields

$$(2.18) \quad (S_{\Omega^s} f)_\infty(\hat{x}) = \int_{\partial\Omega} e^{-ik\hat{x}\cdot y} f(y) dS(y),$$

$$(2.19) \quad (\partial_j S_{\Omega^s} f)_\infty(\hat{x}) = ik\hat{x}_j \int_{\partial\Omega} e^{-ik\hat{x}\cdot y} f(y) dS(y),$$

by (2.15), (2.16) and the compactness of $\partial\Omega$. Denote

$$(2.20) \quad S_\infty f = (S_{\Omega^s} f)_\infty.$$

Denote the limits onto the boundary as

$$(2.21) \quad v|_{\partial\Omega}^-(x) := \lim_{h \searrow 0} v(x - hn(x)), \quad v|_{\partial\Omega}^+(x) := \lim_{h \searrow 0} v(x + hn(x)),$$

where $n(x)$ is the unit outer normal at $x \in \partial\Omega$. The single layer and its derivative can be extended continuously onto the boundary as

$$(2.22) \quad (S_\Omega f)|_{\partial\Omega}^-(x) = S_{\partial\Omega} f(x) = (S_{\Omega^s} f)|_{\partial\Omega}^+(x),$$

and

$$(2.23) \quad (\partial_j S_\Omega f)|_{\partial\Omega}^-(x) = \partial_j S_{\partial\Omega} f(x) + \frac{1}{2} f(x) n_j(x),$$

$$(2.24) \quad (\partial_j S_{\Omega^s} f)|_{\partial\Omega}^+(x) = \partial_j S_{\partial\Omega} f(x) - \frac{1}{2} f(x) n_j(x).$$

These are the *jump formulas*, [12, Thm 2.12 and Thm 2.17]. For $x \in \partial\Omega$, the operator $S_{\partial\Omega} f$ and $\partial_j S_{\partial\Omega} f$ are defined with the integral kernel $\Phi_y(x)$ and $\partial_j \Phi_y(x)$, respectively. For $\partial_j \Phi_y(x)$ the integral exists in Cauchy principal value sense. Note that the jump formulas are valid in the trace sense also for the Sobolev spaces, see [29, Theorem 6.11].

Herglotz waves A function

$$(2.25) \quad v_g(x) = \int_{S^2} e^{ikx \cdot \xi} g(\xi) dS(\xi), \quad x \in \mathbb{R}^3,$$

is the *Herglotz wave function* in \mathbb{R}^3 with the *Herglotz density* $g \in L^2(S^2)$. A Herglotz wave function satisfies the Helmholtz equation in \mathbb{R}^3 , and they will serve us as the basic incident waves.

Denote the restriction of the Herglotz wave function onto the boundary of an obstacle Ω by

$$(2.26) \quad Hg(x) = v_g|_{\partial\Omega}, \quad g \in L^2(S^2).$$

The L^2 -adjoint of H is

$$(2.27) \quad H^* f(\xi) = \int_{\partial\Omega} e^{-ikx \cdot \xi} f(x) dS(x),$$

which, by (2.18), is the far field of the single layer potential $S_{\Omega^s} f$, in other words,

$$(2.28) \quad H^* f = S_\infty f.$$

Lemmata The next three lemmata will be used frequently in our work. A consequence of Rellich's Lemma is that the far field pattern determines the scattered field uniquely. The proof of Rellich's Lemma is based on the asymptotic behaviour of the spherical Hankel functions, see [13, Lemma 2.11]. The second lemma is an L^2 -density result of the Herglotz waves in the space of boundary functions, see [13, Theorem 5.5]. The third lemma gives an L^2 -estimate for the solutions of the Helmholtz equation in terms of their boundary values, [13, Theorem 5.4].

Lemma 2.1 (*Rellich's Lemma*) Suppose $u \in C^2(\Omega^s)$ solves the Helmholtz equation with

$$(2.29) \quad \lim_{R \rightarrow \infty} \int_{\partial B_R} |u(x)|^2 dS(x) = 0.$$

Then $u = 0$.

Rellich's Lemma is not *a priori* asking u to be radiating. For a radiating solution u , the far field u_∞ is defined, and the lemma can be rewritten in the form

$$(2.30) \quad u_\infty = 0 \quad \Rightarrow \quad u = 0,$$

because

$$\lim_{R \rightarrow \infty} \int_{\partial B_R} |u(x)|^2 dS(x) = \frac{1}{4\pi} \int_{S^2} |u_\infty(\hat{x})|^2 dS(\hat{x}).$$

Lemma 2.2 Suppose k^2 is not a Dirichlet eigenvalue⁴ of Ω . Then the Herglotz waves Hf , $f \in L^2(S^2)$, form a dense subspace of $L^2(\partial\Omega)$.

Proof. By the linearity of H , the Herglotz waves form a subspace.

Let $g \in L^2(\partial\Omega)$ be such that

$$(Hf, g)_{L^2(\partial\Omega)} = 0$$

for every $f \in L^2(S^2)$. We will show $g = 0$, implying

$$\{Hf \mid f \in L^2(S^2)\}^\perp = \{0\},$$

namely, the claim. Denote the single layer potential by

$$v(x) = Sg(x)$$

for $x \in \mathbb{R}^3$. Now v is a radiating solution in Ω^s with far field

$$v_\infty = H^*g$$

by (2.28), and so for every $f \in L^2(S^2)$,

$$(f, v_\infty)_{L^2(S^2)} = (Hf, g)_{L^2(\partial\Omega)} = 0$$

by the assumption. Hence,

$$v_\infty = 0,$$

or

$$v = 0$$

⁴Constant λ is a Dirichlet eigenvalue for Ω if there exists a non-trivial v with $v|_{\partial\Omega} = 0$ such that $-\Delta v = \lambda v$ in Ω . The Dirichlet eigenvalues are positive and form a numerable discrete set, [29].

in Ω^s by Rellich's Lemma. By the continuity of the single layer over the boundary (in the trace sense),

$$0 = v|_{\partial\Omega}^+ = (S_{\Omega^s}g)^+|_{\partial\Omega} = (S_{\Omega}g)|_{\partial\Omega}^- = v|_{\partial\Omega}^-.$$

Since k^2 is not a Dirichlet eigenvalue,

$$v = 0$$

also in Ω , and so by the jump formulas

$$0 = \frac{\partial v}{\partial n}\Big|_{\partial\Omega}^- - \frac{\partial v}{\partial n}\Big|_{\partial\Omega}^+ = g,$$

which is the claim. □

Lemma 2.3 *For any compact subset $K \subset \Omega$ and multi-index α , there exists a finite constant $C_{K,\alpha}$ such that*

$$(2.31) \quad \sup_{x \in K} |\partial^\alpha u(x)| \leq C_{K,\alpha} \|u\|_{L^2(\partial\Omega)},$$

for every $u \in C^\infty(\overline{\Omega})$ that solves the Helmholtz equation in Ω . The constant $C_{K,\alpha}$ is related to the distance of K and $\partial\Omega$ as

$$C_{K,\alpha} \sim d(K, \partial\Omega)^{-|\alpha|-2}.$$

Proof. (See the proof of Theorem 5.4 in [13]) The solution u can be represented with the double layer potential D ,

$$u(x) = (D\phi)(x) = \int_{\partial\Omega} \frac{\partial\Phi_x}{\partial n}(y) \phi(y) dS(y),$$

where

$$\phi = \left(\frac{1}{2}I - D\right)^{-1} u|_{\partial\Omega}^-,$$

and $(\frac{1}{2}I - D)^{-1}$ is defined and bounded in $L^2(\partial\Omega)$. Now,

$$|\partial^\alpha u(x)| \leq \sup_{y \in \partial\Omega} \left| \frac{\partial^\alpha \partial\Phi_x}{\partial x^\alpha \partial n}(y) \right| \int_{\partial\Omega} |\phi(y)| dS(y).$$

By the Hölder inequality,

$$\begin{aligned} \int_{\partial\Omega} |\phi(y)| dS(y) &\leq \sqrt{|\partial\Omega|} \|\phi\|_{L^2(\partial\Omega)} \\ &\leq \sqrt{|\partial\Omega|} \|(\frac{1}{2}I - D)^{-1}\| \cdot \|u\|_{L^2(\partial\Omega)}. \end{aligned}$$

Hence,

$$|\partial^\alpha u(x)| \leq C_{K,\alpha} \|u\|_{L^2(\partial\Omega)}$$

with constant

$$C_{K,\alpha} = \sqrt{|\partial\Omega|} \cdot \sup_{\substack{x \in K \\ y \in \partial\Omega}} \left| \frac{\partial^\alpha \partial \Phi_x}{\partial x^\alpha \partial n(y)}(y) \right| \cdot \left\| \left(\frac{1}{2}I - D \right)^{-1} \right\|,$$

which is finite since

$$K \times \partial\Omega \ni (x, y) \mapsto \frac{\partial \Phi_x}{\partial n}(y)$$

is a C^∞ mapping. The estimate for $C_{K,\alpha}$ follows from

$$\left| \frac{\partial^\alpha \partial \Phi_x}{\partial x^\alpha \partial n(y)}(y) \right| \leq C_\alpha \cdot \frac{1}{|x - y|^{|\alpha|+2}}.$$

□

2.2 An acoustic inverse obstacle scattering problem

In this section, we outline an acoustic inverse obstacle scattering problem for sound-soft obstacles. This will serve as a reference case later. An acoustic sound-soft obstacle is such that the total field vanishes on the boundary of the obstacle. We sketch the proof for the unique solvability of the inverse problem and discuss three different obstacle reconstruction methods.

For an acoustic sound-soft obstacle, the direct scattering problem is the following, [13, p. 46]:

Direct Acoustic Obstacle Scattering Problem *Given an incident field v^i ,*

$$\Delta v^i + k^2 v^i = 0 \quad \text{in } \mathbb{R}^3,$$

find the scattered field v^s that is a radiating solution of the Helmholtz equation in the exterior domain Ω^s and for which the total field

$$v = v^i + v^s$$

satisfies the boundary condition

$$v = 0 \quad \text{on } \partial\Omega.$$

The direct obstacle scattering problem is uniquely solvable, e.g., [29]. In fact, for an incident field it is enough to be a solution of the Helmholtz equation in a neighbourhood of the scatterer. The incident field could be, for example, the field of a point source Φ_z with $z \in \Omega^s$.

Denote by

$$(2.32) \quad v_\infty^s(\cdot, \xi)$$

the far field pattern of the unique scattered field, when the incident field is the plane wave propagating in direction ξ , $\xi \in S^2$,

$$(2.33) \quad v^i = v^i(x, \xi) = e^{ikx \cdot \xi}.$$

Inverse Acoustic Obstacle Scattering Problem *Given the far field pattern $v_\infty^s(\cdot, \xi)$ for each incoming plane wave $v^i(\cdot, \xi)$, $\xi \in S^2$, and assuming the scatterer is a sound-soft obstacle, determine the scatterer Ω .*

The inverse acoustic obstacle scattering problem has a unique solution. Namely, if the far field patterns of the incident plane waves coincide for two sound-soft obstacles Ω_1 and Ω_2 , then $\Omega_1 = \Omega_2$. We sketch the proof which is based on the “screaming close to wall” effect. For more details, see [24, 20]. In [13], there is a slightly different approach.

Assume that the far field patterns corresponding to incoming plane waves equal for Ω_1 and Ω_2 . Denote by E the unbounded component of the exterior $\mathbb{R}^3 \setminus (\overline{\Omega_1} \cup \overline{\Omega_2})$. Fix $z \in E$. Denote by G_j the *Dirichlet-to-far-field mapping*, the operator that maps the Dirichlet’s boundary values on $\partial\Omega_j$ of the scattered field to the corresponding far field,

$$G_j(v^s|_{\partial\Omega_j}) = v_\infty^s.$$

The operator G_j can be considered as a bounded linear operator from $H^{1/2}(\partial\Omega_j)$ to $L^2(S^2)$ [2].

First, we will show that if $\Phi_{z,j}^s$ is the radiating solution of

$$(2.34) \quad \begin{cases} \Delta\Phi_{z,j}^s + k^2\Phi_{z,j}^s = 0, & \text{in } \Omega_j^s, \\ \Phi_{z,j}^s = -\Phi_z & \text{on } \partial\Omega_j, \end{cases}$$

$j = 1, 2$, then

$$\Phi_{z,1}^s = \Phi_{z,2}^s \quad \text{in } E.$$

To this end, choose a domain $A_z \subset \mathbb{R}^3$ such that $z \notin \overline{A_z}$,

$$(2.35) \quad \overline{\Omega_1 \cup \Omega_2} \subset A_z,$$

and for which k^2 is not a Dirichlet eigenvalue. By the density, Lemma 2.2, there is a sequence

$$v_n \in \text{span}\{v^i(\cdot, \xi)\}$$

with

$$v_n|_{\partial A_z} \rightarrow \Phi_z|_{\partial A_z} \quad \text{in } L^2(\partial A_z).$$

But now, v_n and Φ_z are both solutions to the Helmholtz equation in A_z , and so by the estimate (2.31) in Lemma 2.3,

$$v_n \rightarrow \Phi_z, \quad \nabla v_n \rightarrow \nabla \Phi_z,$$

uniformly in a compact subset $\overline{\Omega_1} \cup \overline{\Omega_2} \subset A_z$. Hence,

$$v_n|_{\partial\Omega_j} \rightarrow \Phi_z|_{\partial\Omega_j}$$

in $H^{1/2}(\partial\Omega_j)$, and by the continuity of G_j ,

$$\Phi_{z,j,\infty}^s = -G_j(\Phi_z|_{\partial\Omega_j}) = -G_j(\lim v_n|_{\partial\Omega_j}) = -\lim G_j(v_n|_{\partial\Omega_j}).$$

Since the far fields corresponding to the incident plane waves coincide and G_j 's are linear,

$$G_1(v_n|_{\partial\Omega_1}) = G_2(v_n|_{\partial\Omega_2}).$$

Now we get

$$\Phi_{z,1,\infty}^s = -\lim G_1(v_n|_{\partial\Omega_1}) = -\lim G_2(v_n|_{\partial\Omega_2}) = \Phi_{z,2,\infty}^s.$$

Hence, by Rellich's Lemma 2.1, $\Phi_{z,1}^s = \Phi_{z,2}^s$ in E .

Suppose then that $\Omega_1 \neq \Omega_2$. We may assume that there is a $z_0 \in \partial\Omega_1$ such that z_0 can be approached by $z \in E$ and that the distance $d(z, \Omega_2)$ stays bounded below by some positive constant. But then, for example, by the mirror source principle⁵,

$$(2.36) \quad |\Phi_{z,1}^s(z)| \rightarrow \infty \quad \text{as } z \rightarrow z_0,$$

while $|\Phi_{z,2}^s(z)|$ stays bounded by the representation formula since $\Phi_z|_{\partial\Omega_2}$ and $\nabla\Phi_z|_{\partial\Omega_2}$ stay bounded. This is impossible since $\Phi_{z,1}^s = \Phi_{z,2}^s$ in E , a contradiction. Hence,

$$\Omega_1 = \Omega_2,$$

and the unique solvability of the inverse problem is proved.

Basicly, the proof consists of two steps. First, the far field data determines Φ_z^s , the scattered field when the incident field is the field of the point source, and secondly, $|\Phi_z^s(z)|$ becomes unbounded as z approaches the boundary. Neither of these steps is limited only to the Dirichlet boundary condition. If the v_n 's are as in the proof, then the whole Cauchy data of v_n approaches uniformly the Cauchy data of Φ_z on $\partial\Omega$. Hence, Φ_z^s is determined if the far fields of the scattered waves depend continuously on some combination of the Cauchy data of the incident wave. If the boundary condition is such that $|\Phi_z^s(z)|$ becomes unbounded close to the boundary, then also the second step works. Hence, with small modifications, the same proof works also for different boundary conditions, for example, for the Neumann boundary condition.

2.2.1 Linear sampling method

The measurement of the inverse acoustic obstacle scattering problem can be interpreted in the operator theoretic setting by introducing the *far field operator*,

$$(2.37) \quad Fg(\hat{x}) = \int_{S^2} v_\infty^s(\hat{x}, \xi)g(\xi)dS(\xi),$$

⁵Let \tilde{z} be the mirror point with respect to the boundary $\partial\Omega$ of $z \in \Omega^s$ when z is close to $\partial\Omega$. By the mirror source principle, also called the image source principle, the asymptotics of Φ_z^s can be estimated by $\Phi_{\tilde{z}}$ when z tends to the boundary $\partial\Omega$.

where $v_\infty^s(\cdot, \xi)$ is the far field of the scattered wave when the incident field is the plane wave $v^i(\cdot, \xi)$, see (2.32), (2.33). By the linearity of the direct problem, Fg is the far field when the incident field is the Herglotz wave function v_g^i with the Herglotz density g .

For sound-soft obstacles,

$$(2.38) \quad F = -GH,$$

where G is the Dirichlet-to-far field mapping, the operator that maps the boundary values of the scattered waves to the far field pattern, and H is the restriction of the Herglotz wave onto the boundary (2.26). The operators H , G and F are considered between the following spaces,

$$\begin{aligned} H &: L^2(S^2) \rightarrow H^{1/2}(\partial\Omega), \\ G &: H^{1/2}(\partial\Omega) \rightarrow L^2(S^2), \\ F &: L^2(S^2) \rightarrow L^2(S^2). \end{aligned}$$

They are all compact injective linear operators with dense images [2]. For the density, it has to be assumed that k^2 is not a Dirichlet eigenvalue of Ω . By using Rellich's Lemma 2.1 in the same way as in the proof of the unique solvability of the inverse problem, one can obtain a relation for the scatterer and the factor G of the far field mapping F , [11],

$$(2.39) \quad z \in \Omega \Leftrightarrow \Phi_{z,\infty} \in \mathcal{R}(G).$$

In the linear sampling method, the criteria to decide when $z \in \Omega$, or $z \in \Omega^s$, is to look at the norm of the regularized solution $g = g_z$ for

$$(2.40) \quad Fg = \Phi_{z,\infty}.$$

For $z \in \Omega$ the norm $\|g_z\|$ is small but for $z \in \Omega^s$ it is large. The linear sampling method has been motivated with theorems of the following type, [11, 2]:

Theorem 2.4 *Suppose k^2 is not a Dirichlet eigenvalue of Ω . Let $z \in \Omega$ and $\epsilon > 0$. There exists a solution $g_z^\epsilon \in L^2(S^2)$ of the inequality*

$$\|Fg_z^\epsilon - \Phi_{z,\infty}\|_{L^2} < \epsilon,$$

such that as $z \rightarrow \partial\Omega$, we have

$$\|g_z^\epsilon\|_{L^2} \rightarrow \infty,$$

and for the Herglotz wave function v_g^i of $g = g_z^\epsilon$,

$$\|v_g^i\|_{H^1(\Omega)} \rightarrow \infty.$$

Even though the linear sampling method has been observed to work in practice by several numerical tests in different situations, [11, 1, 10], the previous theorem does not prove the method; compare to the discussion in [11, after Example 2.2]. A problem is that there is no guarantee that the regularized solution of (2.40) is the function g_z^ϵ of Theorem 2.4. In fact, it can be proven that one can always find Theorem 2.4-type “singular” Herglotz densities, also when approaching other points besides $\partial\Omega$; see the next lemma. Moreover, the theorem says nothing about points $z \in \Omega^s$.

Lemma 2.5 *Let X, Y, Z be infinite-dimensional Hilbert spaces, and let*

$$H : X \rightarrow Y, \quad G : Y \rightarrow Z,$$

be compact linear operators with dense images. Let

$$F = GH.$$

Then for any $z \in Z$ and for any $\epsilon > 0$ and $M > 0$, there exists a solution $x \in X$ of the inequality

$$\|Fx - z\| < \epsilon,$$

such that

$$\|x\| > M, \quad \text{and} \quad \|Hx\| > M.$$

Proof. Let $z \in Z$ and $\epsilon > 0$. Since G is compact, the preimage $U = G^{-1}B(z, \epsilon)$ is an open and unbounded set in Y and non-empty since the image of G is dense. Take $y \in U$ with

$$\|y\| > M + 1,$$

and let $\delta, 0 < \delta < 1$, be such that

$$B(y, \delta) \subset U.$$

Now, the set $H^{-1}B(y, \delta)$ is an open, non-empty and unbounded set. Take

$$x \in H^{-1}B(y, \delta),$$

such that $\|x\| > M$. But now $Hx \in B(y, \delta)$, and so also

$$\|Hx\| > \|y\| - \delta > M + 1 - 1 = M,$$

and it holds that

$$Fx = GHx \in GB(y, \delta) \subset GU \subset B(z, \epsilon).$$

□

What is the relation between (2.39) and the regularized solutions of (2.40)? In [2], Arens has recently shown that the linear sampling method works if the factorization

method ([20]) works, that is, there is a proof for the linear sampling method in those cases where there is a proof also for the factorization method. In this case, the regularization method for (2.40) can be understood as a regularizing method for

$$(2.41) \quad G\phi = \Phi_{z,\infty},$$

and this is the reason why the linear sampling method works. Roughly speaking, if R is a regularizer of F , then for $\tilde{R} = -HR$, and for Hg (Herglotz waves are dense in $H^{1/2}(\partial\Omega)$),

$$\tilde{R}G(Hg) = -HRGHg = HRFg \approx Hg,$$

and so \tilde{R} is a regularizer for G . The rigorous proof uses the Riesz base relations of the singular systems of operators F , G and H , which is the key in proving the factorization method, too.

As a conclusion, the linear sampling method has been proven to work when the factorization method works. This is the case in the acoustic scattering with sound-soft obstacles, but not, for example, with the electromagnetic scattering problems, although in the numerical tests the linear sampling method seems to work also in these cases.

2.2.2 Factorization method

In [20], Kirsch proved a relation between the ranges of F and G ,

$$(2.42) \quad \mathcal{R}(G) = \mathcal{R}(|F|^{1/2}).$$

Then, by (2.39), z is in Ω if and only if the equation

$$(2.43) \quad |F|^{1/2}g = \Phi_{z,\infty}$$

is solvable. This is called the *factorization method*. Equation (2.43) is ill-posed since F is a compact operator, and hence, one is looking for a regularized solution of (2.43).

The starting point in proving the relation (2.42) is the factorization

$$F = -GS_{\partial\Omega}^*G^*,$$

which follows from (2.38) and

$$Gf = (S_{\Omega^s}S_{\partial\Omega}^{-1}f)_{\infty} = H^*S_{\partial\Omega}^{-1}f.$$

To get the relation (2.42), it is crucial that the middle operator in the factorization is coercive, or at most compact perturbation of a coercive operator, see [20, Theorem 3.4], [22, Theorem 3.3]. This is satisfied in the sound-soft and sound-hard acoustic obstacle scattering but fails in the electromagnetic scattering case, [2, 21].

As numerical methods, both the factorization method and the linear sampling method are quick and simple. It is enough to solve the regularizer for discretized $|F|^{1/2}$, or F ,

only once. Thereafter, one applies the regularizer for $\Phi_{z,\infty}$ to get $g = g_z$ and computes the norm of g . Another possibility is to apply the formula

$$\mathcal{R}(A) = \left\{ f \mid \sum_j \frac{|(f, \psi_j)|^2}{|a_j|^2} < \infty \right\},$$

where A is a compact operator with the singular system (a_j, ϕ_j, ψ_j) , and apply this for $A = |F|^{1/2}$, or for $A = F$, and for $f = \Phi_{z,\infty}$ with each z . This means that one needs to compute the singular value decomposition of the matrix of the discretized far field operator only once.

2.2.3 Singular sources method

The singular sources method, introduced by Potthast in [36], follows strictly the ideas of the unique solvability proof for the inverse problem. As in the proof, the ‘‘Screaming close to wall’’ effect is also the key idea for the numerical singular sources method. One constructs an approximation for the scattered field of a point source at the source point, denoted by $\Phi_z^s(z)$. When point z approaches the boundary of the scatterer (from outside), the function $|\Phi_z^s(z)|$ becomes large.

The *indicator function* of the singular sources method is

$$(2.44) \quad I(z) = \left| \int_{S^2} F g_z(-\xi) g_z(\xi) dS(\xi) \right|,$$

where g_z is such that the Herglotz wave with density g_z approximates⁶ Φ_z on the boundary $\partial\Omega$,

$$(2.45) \quad H g_z \approx \Phi_z|_{\partial\Omega}.$$

The indicator function approximates $|\Phi_z^s(z)|$, which is based on the density of the Herglotz wave functions, Lemma 2.2 and the *mixed reciprocity relation*, [37, 16, 35]. This is described briefly in the following.

The mixed reciprocity relation between the scattered fields of a point source and of a plane wave is

$$(2.46) \quad \Phi_{z,\infty}^s(\xi) = v^s(z, -\xi), \quad \xi \in S^2, \quad z \in \Omega^s.$$

If the incident field is a Herglotz wave function v_g with density g , then the scattered field at $z \in \Omega^s$ is

$$v_g^s(z) = \int_{S^2} v^s(z, \xi) g(\xi) dS(\xi) = \int_{S^2} \Phi_{z,\infty}^s(-\xi) g(\xi) dS(\xi)$$

by the mixed reciprocity. Now,

$$\Phi_{z,\infty}^s(\xi) = -G(\Phi_z|_{\partial\Omega})(\xi) \approx -G(H g_z)(\xi) = \int_{S^2} v_\infty^s(\xi, \eta) g_z(\eta) dS(\eta),$$

⁶The meaning of \approx will be studied in the Beltrami field case more carefully. Here we just briefly give the idea.

where g_z satisfies (2.45), and hence,

$$v_g^s(z) \approx \int_{S^2} \int_{S^2} v_\infty^s(-\xi, \eta) g_z(\eta) g(\xi) dS(\xi) dS(\eta).$$

By choosing $g = g_z$,

$$\Phi_z^s(z) \approx v_{g_z}^s(z) \approx \int_{S^2} \int_{S^2} v_\infty^s(-\xi, \eta) g_z(\eta) g_z(\xi) dS(\xi) dS(\eta),$$

and the absolute value of the right-hand side is $I(z)$.

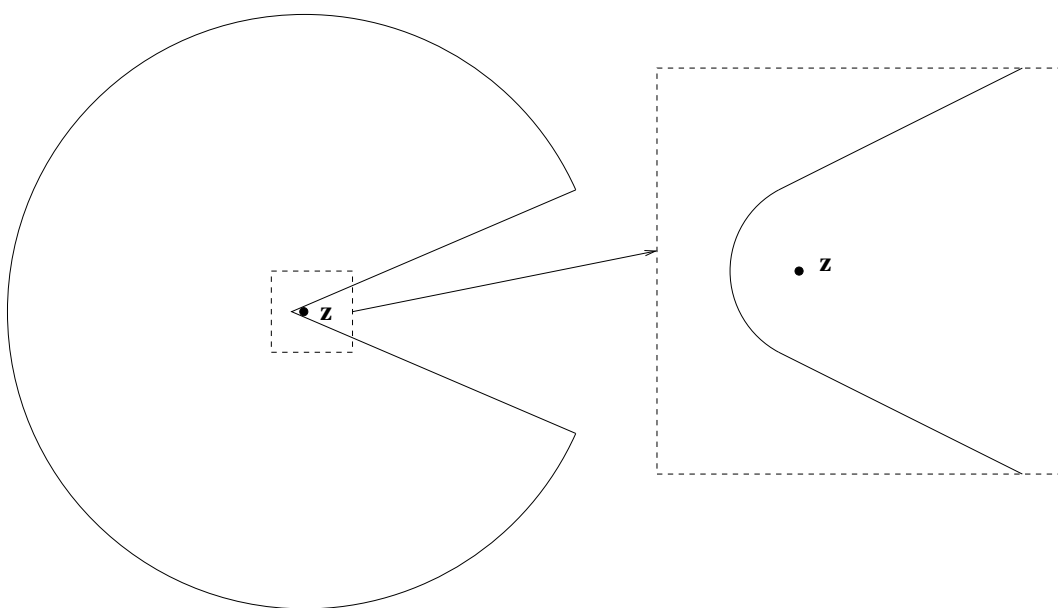


Figure 1: A cone domain is one possibility for the approximation domain. The corners are smoothed on a small scale.

Scanning procedures The Herglotz density g_z of (2.45) for $z \in \Omega^s$ is obtained through an approximation domain. A bounded smooth domain A_z is an *approximation domain* for point $z \in \Omega^s$ if

$$(2.47) \quad z \notin \overline{A_z}, \quad \overline{\Omega} \subset A_z.$$

Now, g_z is defined as a regularized solution for

$$(2.48) \quad Hg_z = \Phi_z$$

on ∂A_z . Then by the estimate (2.31), the Herglotz wave with density g_z approximates Φ_z also on $\partial\Omega$. The idea is to choose the approximation domains A_z so that z can approach $\partial\Omega$. Since the scatterer Ω is unknown, the points z and the corresponding approximation domains have to be chosen by an appropriate procedure. We call this a *scanning procedure*.

One straightforward possibility for the scanning procedure is the following. Assume that the scatterer is located in some big ball $B = B(0, R)$. Suppose also that the boundary of the scatterer is such that every point on the boundary can be approached in some direction $\xi \in S^2$ with a cone domain, see Figure 1. Let A_0 be a cone domain with $z = 0$ such that the radius of the ball is $3R$, say. Fix a direction $\xi_1 \in S^2$ and rotate A_0 so that the cone is pointing in the direction ξ_1 . To get the value of the indicator function (2.44) at $z \in B$, we translate the ξ_1 -directed cone domain to z . Scan the ball B starting from the ξ_1 side, until the indicator function (2.44) becomes large, in other words, we come close to the boundary. Note that until z becomes close to the boundary, the condition (2.47) is satisfied. This way, we can determine the part of the boundary that has access from the ξ_1 direction from infinity. Then choose another direction ξ_2 and do the same, and so on. Then, after choosing all, in practice, several different scanning directions ξ , we get the whole boundary determined. We consider other scanning procedures later.

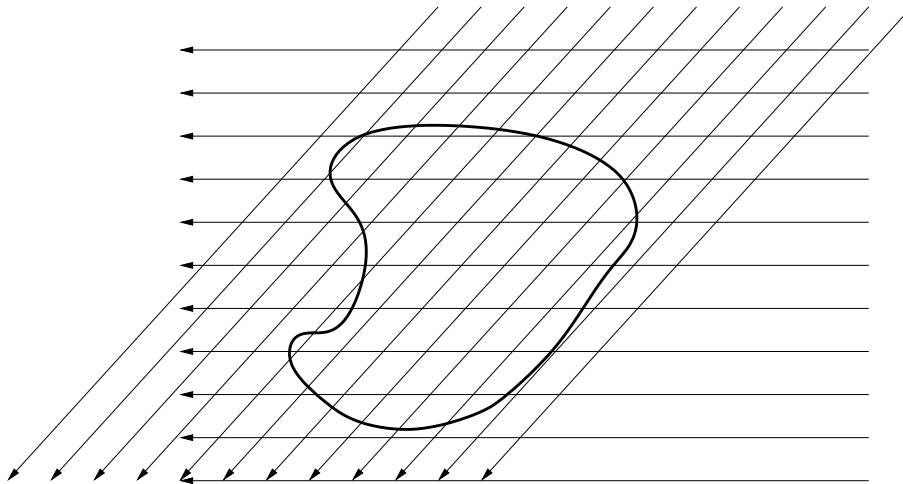


Figure 2: Scanning the boundary from two different directions.

Notice the fundamental difference in the visualization between the factorization method and the singular sources method. In the factorization method one can plot the function

$$z \mapsto \|g_z\|.$$

But in the singular sources method the value of the indicator function $I(z)$ also depends on the choice for the approximation domain, that is, one has to scan the computational domain by computing the indicator function (2.44) for each z , according to the scanning procedure. The computational complexity depends heavily on the used scanning procedure. To get the method faster in practice, the approximation domain A_z for each z has to be such that A_z is just a translation and/or rotation of some fixed basic approximation domain A_0 . Then, if g_0 is the solution of (2.48) for A_0 , the function g_z can be computed from g_0 without solving the equation separately for each z . The question how to visualize the singular sources method is discussed shortly in the numerical part of the work.

Indicator function of the probe method The probe method, introduced by Ikehata [16, 17, 19], is also a scanning type method. The inverse problem considered in [17] is slightly different: *Let B be a ball in which the scatterer Ω is located. Given $\Phi_z^s|_{\partial B}$ for every $z \in \partial B$, determine the scatterer Ω .*

In the probe method scanning is done with *needles* σ that are curves in B starting from the boundary, $\sigma(0) \in \partial B$. Denote

$$\Omega_B = B \setminus \overline{\Omega}.$$

Define the following Dirichlet-to-Neumann mappings:

$$\Lambda_\Omega f = \frac{\partial u}{\partial n} \Big|_{\partial B}, \quad \Lambda_0 f = \frac{\partial u_0}{\partial n} \Big|_{\partial B},$$

where

$$(2.49) \quad \begin{cases} (\Delta + k^2)u = 0 & \text{in } \Omega_B, \\ u = f & \text{on } \partial B, \\ u = 0 & \text{on } \partial\Omega, \end{cases}$$

and

$$(2.50) \quad \begin{cases} (\Delta + k^2)u_0 = 0 & \text{in } B, \\ u_0 = f & \text{on } \partial B. \end{cases}$$

Let f_t^n be such that the solution u_t^n of (2.50) with the boundary value $f = f_t^n$ approximates $\Phi_{c(t)}$ in B except shrinking small neighborhoods V_t^n of $\sigma[0, t]$. The indicator function of the probe method is

$$(2.51) \quad I(t) = \lim_n \int_{\partial B} (\Lambda_\Omega f_t^n - \Lambda_0 f_t^n) \overline{f_t^n} dS.$$

This blows up when $\sigma(t)$ approaches the boundary:

Set

$$S_t f(x) = \int_{\partial B} (\Phi_x(y) + \Phi_x^s(y)) f(y) dS(y), \quad x \in \partial B,$$

which is a modified single-layer potential with total field as the integral kernel. It can be shown [17, Proposition 9] that

$$\Lambda_\Omega - \Lambda_0 = S_t^{-1} - S_{\partial B}^{-1},$$

and hence, (2.51) is computable from data.

If u and u_0 are the solutions of (2.49) and (2.50), respectively, then

$$(2.52) \quad \begin{aligned} \int_{\partial B} (\Lambda_\Omega f - \Lambda_0 f) \overline{f} dS &= \int_\Omega (|\nabla u_0|^2 - k^2 |u_0|^2) dx \\ &\quad + \int_{\Omega_B} (|\nabla(u - u_0)|^2 - k^2 |u - u_0|^2) dx \end{aligned}$$

which follows from

$$\begin{aligned} 0 &= \int_{\partial\Omega_B} \frac{\partial}{\partial n} (u - u_0) \bar{u}_0 dS - \int_{\partial\Omega_B} (u - u_0) \frac{\partial \bar{u}_0}{\partial n} dS \\ &= \int_{\partial B} (\Lambda_\Omega - \Lambda_0) f \bar{f} dS - \int_{\partial\Omega_B} \frac{\partial}{\partial n} (u - u_0) \overline{(u - u_0)} dS - \int_{\partial\Omega} u_0 \frac{\partial \bar{u}_0}{\partial n} dS. \end{aligned}$$

For $f = f_t^n$, (2.52) blows up since $|\nabla\Phi_z|^2$ with $z = c(t)$ becomes hypersingular. In fact, since the solution u_t^n becomes rapidly changing on whole $\sigma[0, t]$ as the neighborhood V_t^n shrinks to $\sigma[0, t]$, it can be shown that the indicator function is large also when z is inside the scatter or when $\sigma[0, t]$ is passing through the scatterer. This has been proved in [19] provided k is sufficiently small.

3 Direct obstacle scattering for Beltrami fields

A vector field u in \mathbb{R}^3 is a linear right-handed Beltrami field if

$$(3.1) \quad \nabla \times u = ku,$$

where $k > 0$ is a constant. In this work we call these simply Beltrami fields. By taking the divergence from the equation (3.1), we see

$$\nabla \cdot u = 0,$$

and so u solves also the Helmholtz equation,

$$-\Delta u = (\nabla \times)^2 u - \nabla \nabla \cdot u = k^2 u.$$

There are corresponding left-handed Beltrami fields that satisfy

$$\nabla \times u = -ku.$$

We write the theorems only for right-handed fields to avoid the unnecessary mess of \pm signs. Of course, the same results can be obtained also in the left-handed case. An obstacle is defined by asking the Neumann boundary condition, that is, the normal component of the Beltrami field vanishes. Notice that fixing the tangential component of the Beltrami field will lead to an overdetermined problem, [27]. This will be also seen from the representation formulas.

There is a one-to-one correspondence between electromagnetic fields and Beltrami field pairs with different handednesses. If (E, H) is a solution of the (reduced) Maxwell equations

$$\begin{cases} \nabla \times E = ikH, \\ \nabla \times H = -ikE, \end{cases}$$

then

$$U = E + iH$$

solves

$$\nabla \times U = \nabla \times E + i\nabla \times H = k(iH + E) = kU,$$

in other words, U is a right-handed Beltrami field. Similarly,

$$V = E - iH$$

is a left-handed Beltrami field. Note that, when the Maxwell equations are written for the Beltrami fields, the equations are decoupled,

$$\begin{cases} \nabla \times U &= kU, \\ \nabla \times V &= -kV, \end{cases}$$

but the boundary values of U and V are coupled, for instance, for an electric obstacle with vanishing $n \times E$,

$$\frac{1}{2}n \times (U + V) = 0.$$

In contrast, in this work we study the Neumann boundary value problem for a single Beltrami field. A vanishing Neumann boundary value for a Beltrami field U alone,

$$n \cdot U = n \cdot (E + iH) = 0,$$

does not determine an electromagnetic boundary value problem since this gives no information about V , so fixing one component is not enough for the Maxwell equations.

In plasma physics, when auroras are produced on the polar sky region, the magnetic flow B is parallel with the current density j , called *Birkeland current*, [39]. When the electromagnetic effects are neglected, Ampere's law gives

$$\nabla \times B = j,$$

and because $j \parallel B$,

$$\nabla \times B = \alpha B,$$

that is, the magnetic field B is then a Beltrami field.

In this section, we consider the direct problem of Beltrami field scattering with the Neumann boundary condition. We first study some preliminaries, such as plane waves. We obtain the well-known representation formulas, [3], by using an enlarged Beltrami system with the correct radiation condition; compare to [32, 34, 38] where this enlarging approach has been used for the Maxwell equations. Then we turn to the obstacle scattering. This leads to the question of the unique solvability of the exterior Neumann boundary value problem. After one uses the Helmholtz decomposition for the boundary functions, the uniqueness can be obtained in a standard way — the zero boundary value implies that the far field vanishes, and Rellich's Lemma gives the uniqueness. The existence is proved with the boundary integral equation approach using the Fredholm theory. The Fredholm properties are obtained by considering the boundary integral operators as pseudo-differential operators and by computing their symbols.

3.1 Preliminaries

3.1.1 Basic definitions

Plane waves In the following, one gets a motivation for the Beltrami field plane waves and later for the singular fields from the corresponding electric plane waves and the field of an electric dipole, see [13],

$$E_0(x) = -(\xi \times)^2 p e^{ik\xi \cdot x},$$

and

$$E_{z,p}(x) = \nabla \times (\Phi_z(x)p).$$

A plane wave

$$u(x) = p e^{ikx \cdot \xi}, \quad \xi \in S^2, \quad p \in \mathbb{C}^3,$$

is a Beltrami field if and only if the polarization vector p satisfies

$$i\xi \times p = p.$$

For any $q \in \mathbb{R}^n$, the vector

$$p = -(\xi \times)^2 q + i\xi \times q$$

satisfies the equation for the polarization, and so

$$(3.2) \quad u(x, \xi, q) = \left(-(\xi \times)^2 q + i\xi \times q \right) e^{ikx \cdot \xi}, \quad x \in \mathbb{R}^3, \quad \xi \in S^2, \quad q \in \mathbb{R}^3$$

is a Beltrami field plane wave. The real part of the plane wave is

$$\operatorname{Re} u(x, \xi, q) = -(\xi \times)^2 q \cos(kx \cdot \xi) - \xi \times q \sin(kx \cdot \xi),$$

so the plane wave is circularly polarized and right-handed.

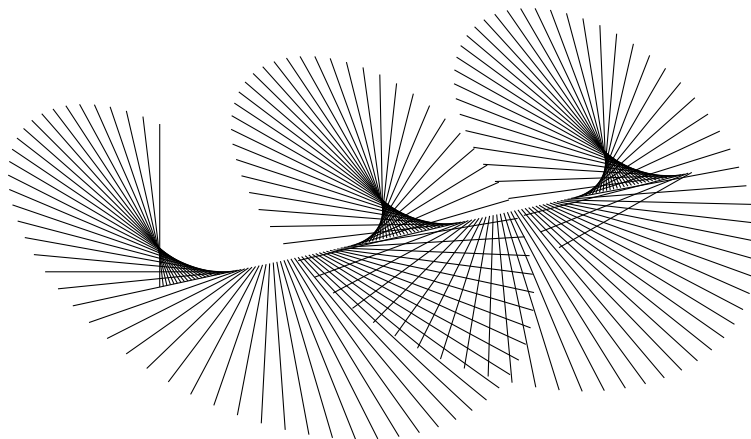


Figure 3: The real part of a Beltrami field plane wave is plotted on a half-axis starting from the origin (left-end point) in the propagation direction. The polarization vector q is pointing upwards. If the time dependency $e^{-i\omega t}$ is included, the picture will rotate clockwise around the axis.

Smoothness Since the singular support of the fundamental solution of the Helmholtz equation is $\{0\}$, a Beltrami field $u \in \mathcal{D}'(\mathbb{R}^3)^3$ is an infinitely smooth function, [15] Theorem 4.4.1. If a Beltrami field $u \in H^s(\Omega)$, then $\nabla \times u, \Delta u \in H^s(\Omega)$ also. Hence, if $u \in H^1(\Omega)$, then we are able to take the boundary values in the trace sense of $u, \nabla \times u$ and Δu into $H^{1/2}(\partial\Omega)$.

Beltrami system To obtain the representation formulas easily, we introduce the following Beltrami system where we add the divergence of u as an extra scalar field; compare to the Picard system in electromagnetics [32, 34, 38].

Let

$$(3.3) \quad A(p) = \begin{pmatrix} p \times & -p \\ p \cdot & 0 \end{pmatrix} = \begin{pmatrix} 0 & -p_3 & p_2 & -p_1 \\ p_3 & 0 & -p_1 & -p_2 \\ -p_2 & p_1 & 0 & -p_3 \\ p_1 & p_2 & p_3 & 0 \end{pmatrix}, \quad p \in \mathbb{R}^3.$$

Note

$$A(p)^T = -A(p), \quad A(p)^T A(p) = \begin{pmatrix} -(p \times)^2 + pp \cdot & 0 \\ 0 & p \cdot p \end{pmatrix} = |p|^2 I.$$

We say

$$U = \begin{pmatrix} u \\ \phi \end{pmatrix}$$

solves the *Beltrami system* if

$$(3.4) \quad A(\nabla)U = kU.$$

The relation between the Beltrami system and the Beltrami field is the following.

Lemma 3.1 *Let*

$$U = \begin{pmatrix} u \\ \phi \end{pmatrix}$$

solve the Beltrami system. Then u is a Beltrami field if and only if $\phi = 0$.

Proof. The Beltrami system for u and ϕ is

$$\begin{cases} \nabla \times u - \nabla \phi = ku, \\ \nabla \cdot u = k\phi. \end{cases}$$

If u is a Beltrami field, then the lower equation gives $\phi = 0$. If $\phi = 0$, then the upper equation is the equation (3.1). \square

The advantage of the Beltrami system is that it factors the Helmholtz operator,

$$(A(\nabla) - kI)(A(\nabla) + kI) = -(\Delta + k^2)I.$$

Now, the matrix

$$G = (A(\nabla) + kI)(\Phi I) = A(\nabla\Phi) + k\Phi I,$$

where Φ is the fundamental solution of the Helmholtz equation, satisfies

$$(A(\nabla) - kI)G = \delta I.$$

Denote also

$$G_z = A(\nabla\Phi_z) + k\Phi_z I,$$

where $\Phi_z(x) = \Phi(x - z)$. Since

$$A(\nabla_z\Phi_x(z)) + k\Phi_x(z)I = -A(\nabla_x\Phi_z(x)) + k\Phi_z(x)I,$$

we have the reciprocity relation

$$(3.5) \quad G_x(z) = G_z(x)^T$$

3.1.2 Radiation condition

To get the representation formula in the exterior domain and to have hope for the uniqueness of any direct scattering problem, we need to have a correct radiation condition. Since the components satisfy the Helmholtz equation, it is natural to try to obtain the radiation condition starting from the Sommerfeld radiation condition (2.8). It turns out that the obtained one is equivalent with the Sommerfeld radiation condition for each component.

Lemma 3.2 *Suppose v is a radiating solution of the Helmholtz equation in an exterior domain Ω^s . Then $\partial_j v$ is also a radiating solution with far field*

$$(3.6) \quad (\partial_j v)_\infty(\hat{x}) = ik\hat{x}_j v_\infty(\hat{x}).$$

Proof. A single layer potential

$$S\phi(x) = \int_{\partial\Omega} \Phi_y(x)\phi(y)dS(y),$$

has the far field

$$(3.7) \quad (S\phi)_\infty(\hat{x}) = \int_{\partial\Omega} e^{-ik\hat{x}\cdot y}\phi(y)dS(y).$$

By (2.12), we see

$$(\partial_j\Phi_y)_\infty(\hat{x}) = ik\hat{x}_j e^{-ik\hat{x}\cdot y},$$

and so

$$(\partial_j S\phi)_\infty(\hat{x}) = \int_{\partial\Omega} (\partial_j\Phi_y)_\infty(\hat{x})\phi(y)dS(y) = ik\hat{x}_j (S\phi)_\infty(\hat{x}).$$

Thus, the claim holds for the single layer potentials. But, any radiating solution can be represented as a single layer potential: Choose $R > 0$ such that k^2 is not Dirichlet's eigenvalue of the ball $B = B(0, R)$ and that $\bar{\Omega} \subset B$. Then

$$v = S\phi,$$

where the single layer is of the boundary ∂B , and

$$\phi = S_{\partial B}^{-1}v|_{|x|=R}.$$

Note that $S_{\partial B}$ is invertible since k^2 is not Dirichlet's eigenvalue. □

Lemma 3.3 *Let*

$$P = P(D) = \sum_{j=1}^3 P^j \partial_j$$

be a linear first-order differential operator with constant (matrix) coefficients P^j , $j = 1, \dots, 3$. Suppose v solves the Helmholtz equation in an exterior domain and satisfies the Sommerfeld radiation condition. If v solves the equation

$$v = P(D)v,$$

then

$$v(x) - ikP(\hat{x})v(x) = o\left(\frac{1}{|x|}\right)$$

uniformly in \hat{x} as $|x| \rightarrow \infty$.

Proof. First, by the previous lemma,

$$0 = [P(D)v - v]_{\infty}(\hat{x}) = ikP(\hat{x})v_{\infty}(\hat{x}) - v_{\infty}(\hat{x}).$$

Hence, as $|x| \rightarrow \infty$,

$$v(x) - ikP(\hat{x})v(x) = \Phi(x)(v_{\infty}(\hat{x}) - ikP(\hat{x})v_{\infty}(\hat{x})) + o\left(\frac{1}{|x|}\right) = o\left(\frac{1}{|x|}\right).$$

□

A solution U of the Beltrami system solves also the Helmholtz equation. If we assume U satisfies the Sommerfeld radiation condition (2.8), then Lemma 3.3 applied with

$$P(D) = \frac{1}{k}A(\nabla)$$

implies that U satisfies the radiation condition

$$(3.8) \quad U(x) - iA(\hat{x})U(x) = o\left(\frac{1}{|x|}\right)$$

uniformly in all directions as $|x| \rightarrow \infty$. In the Beltrami field case,

$$U = \begin{pmatrix} u \\ 0 \end{pmatrix},$$

the radiation condition (3.8) implies

$$\begin{pmatrix} u \\ 0 \end{pmatrix} - i \begin{pmatrix} \hat{x} \times u \\ \hat{x} \cdot u \end{pmatrix} = o\left(\frac{1}{|x|}\right).$$

Note that the lower condition follows from the upper one. Hence, we define the radiation condition for the Beltrami field by (compare [3])

$$(3.9) \quad u - i\hat{x} \times u = o\left(\frac{1}{|x|}\right).$$

This could have been obtained also directly from Lemma 3.3.

3.1.3 Integration by parts

When deriving the representation formulas, one integrates the fundamental solution with the following interpretation.

Lemma 3.4 *Let $f \in \mathcal{D}'(\mathbb{R}^3)$ with compact $\text{singsupp}(f)$. Suppose f is smooth in a neighbourhood of $\partial\Omega$, i.e.,*

$$d(\text{singsupp}(f), \partial\Omega) > 0.$$

Then

$$(3.10) \quad \int_{\Omega} \partial_j f dx = \int_{\partial\Omega} n_j f dS.$$

Remark. The left-hand side has to be interpreted as

$$(3.11) \quad \int_{\Omega} \partial_j f dx := \langle \partial_j f, \psi \chi_{\Omega} \rangle + \int_{\Omega} (1 - \psi) \partial_j f dx,$$

where χ_{Ω} is the characteristic function of Ω , and for $\psi \in C_0^{\infty}(\mathbb{R}^3)$ it holds

$$\psi = \begin{cases} 1 & \text{in a neighbourhood of } \text{singsupp}(f), \\ 0 & \text{in a neighbourhood of } \partial\Omega. \end{cases}$$

The proof shows that the definition is independent of the choice of ψ .

Proof. Choose the function ψ as in the remark. The first term in the right-hand side of (3.11) is

$$\langle \partial_j f, \psi \chi_{\Omega} \rangle = -\langle f, \partial_j(\psi \chi_{\Omega}) \rangle = -\int_{\Omega} f \partial_j(\psi \chi_{\Omega}) dx$$

by the definition of the distribution derivative and because $\partial_j(\psi\chi_\Omega)$ vanishes in some neighbourhoods of $\text{singsupp}(f)$ and $\partial\Omega$. Since

$$\chi_\Omega\partial_j\psi = \partial_j(\psi\chi_\Omega),$$

we get

$$\chi_\Omega\partial_j[(1-\psi)f] = \chi_\Omega(1-\psi)\partial_jf - f\partial_j(\psi\chi_\Omega),$$

where all terms are functions, and so

$$\int_\Omega(1-\psi)\partial_jf dx = \int_\Omega f\partial_j(\psi\chi_\Omega) dx + \int_\Omega\partial_j[(1-\psi)f] dx.$$

Hence,

$$\langle\partial_jf, \psi\chi_\Omega\rangle + \int_\Omega(1-\psi)\partial_jf dx = \int_\Omega\partial_j[(1-\psi)f] dx,$$

for which we can apply the integration rule of smooth functions to obtain

$$\int_\Omega\partial_j[(1-\psi)f] dx = \int_{\partial\Omega} n_j(1-\psi)f dS = \int_{\partial\Omega} n_jf dS.$$

□

Consider linear differential operators of the form

$$(3.12) \quad L(\nabla) = \sum_j L^j\partial_j,$$

where the coefficient matrices $L^j = (L^j_{\alpha\beta})$ are constant. For $L = \nabla \times$, for example,

$$\begin{aligned} \nabla \times &= \begin{pmatrix} 0 & -\partial_3 & \partial_2 \\ \partial_3 & 0 & -\partial_1 \\ -\partial_2 & \partial_1 & 0 \end{pmatrix} \\ &= \begin{pmatrix} 0 & 0 & 0 \\ 0 & 0 & -1 \\ 0 & 1 & 0 \end{pmatrix} \partial_1 + \begin{pmatrix} 0 & 0 & 1 \\ 0 & 0 & 0 \\ -1 & 0 & 0 \end{pmatrix} \partial_2 + \begin{pmatrix} 0 & -1 & 0 \\ 1 & 0 & 0 \\ 0 & 0 & 0 \end{pmatrix} \partial_3. \end{aligned}$$

By L^T we mean

$$L(\nabla)^T = \sum_j (L^j)^T \partial_j,$$

and so, for example,

$$(\nabla \times)^T = -\nabla \times.$$

Lemma 3.5 *Let $L = L(\nabla)$ be a linear differential operator of the form (3.12). Let $A = A(x)$ and $B = B(x)$ be smooth matrices with such sizes that the matrix products below are defined. Then*

$$(3.13) \quad \int_\Omega (L(\nabla)A)^T B dx = \int_{\partial\Omega} (L(n)A)^T B dS(x) - \int_\Omega A^T L(\nabla)^T B dx.$$

Proof. By the scalar integration by parts, it holds for a single derivative that

$$\begin{aligned} \int_{\Omega} ((\partial_j A)B)_{\alpha\beta} dx &= \sum_{\gamma} \int_{\Omega} (\partial_j A_{\alpha\gamma}) B_{\gamma\beta} dx \\ &= \sum_{\gamma} \left(\int_{\partial\Omega} n_j A_{\alpha\gamma} B_{\gamma\beta} dS - \int_{\Omega} A_{\alpha\gamma} \partial_j B_{\gamma\beta} dx \right) \\ &= \left(\int_{\partial\Omega} n_j AB dS - \int_{\Omega} A \partial_j B dx \right)_{\alpha\beta}, \end{aligned}$$

or,

$$\int_{\Omega} (\partial_j A) B dx = \int_{\partial\Omega} n_j AB dS - \int_{\Omega} A \partial_j B dx$$

for any matrices A and B that are compatible with each other. Apply this to get

$$\begin{aligned} \int_{\Omega} (L(\nabla)A)^T B dx &= \sum_j \int_{\Omega} (\partial_j A^T) (L^j)^T B dx \\ &= \sum_j \int_{\partial\Omega} n_j A^T (L^j)^T B dS - \sum_j \int_{\Omega} A^T \partial_j ((L^j)^T B) dx \\ &= \int_{\partial\Omega} (L(n)A)^T B dS - \int_{\partial\Omega} A^T L(\nabla)^T B dx \end{aligned}$$

since $\partial_j((L^j)^T B) = (L^j)^T \partial_j B$. □

3.1.4 Representation formulas

Theorem 3.6 *Let $U \in C^\infty(\overline{\Omega})^4$ satisfy*

$$A(\nabla)U = kU$$

in Ω . Then

$$(3.14) \quad \int_{\partial\Omega} G_y(x) A(n(y)) U(y) dS(y) = \begin{cases} -U(x), & x \in \Omega, \\ 0, & x \in \Omega^s. \end{cases}$$

Proof. We integrate against δ_x to get

$$\begin{aligned} \left. \begin{array}{l} x \in \Omega : U(x) \\ x \in \Omega^s : 0 \end{array} \right\} &= \int_{\Omega} [(A(\nabla_y) - kI)G_x(y)]^T U(y) dy \\ &= \int_{\partial\Omega} [A(n)G_x(y)]^T U(y) dS(y) - \int_{\Omega} G_x(y)^T [A(\nabla_y)^T + kI] U(y) dy \\ &= - \int_{\partial\Omega} G_y(x) A(n) U(y) dS(y) \end{aligned}$$

by reciprocity (3.5). □

We can rewrite

$$(3.15) \quad \int_{\partial\Omega} G_y(x) A(n) U(y) dS(y) = (A(\nabla) + kI) S[A(n)U](x),$$

where S is the single layer. Note that

$$A(n)U = \begin{pmatrix} n \times u - n\phi \\ n \cdot u \end{pmatrix}, \quad U = \begin{pmatrix} u \\ \phi \end{pmatrix}.$$

Corollary 3.7 *Let $u \in C^\infty(\overline{\Omega})^3$ be a Beltrami field in Ω . Then*

$$(3.16) \quad \left. \begin{array}{l} x \in \Omega : -u(x) \\ x \in \Omega^s : 0 \end{array} \right\} = \nabla \times S(n \times u)(x) + \frac{1}{k} (\nabla \times)^2 S(n \times u)(x).$$

Proof. We apply Theorem 3.6 for

$$U = \begin{pmatrix} u \\ 0 \end{pmatrix}.$$

The lower equation of (3.14) gives the relation

$$\nabla \cdot S(n \times u) + kS(n \cdot u) = 0.$$

When we substitute this into the upper equation of (3.14), it gives

$$\begin{aligned} \left. \begin{array}{l} x \in \Omega : -u(x) \\ x \in \Omega^s : 0 \end{array} \right\} &= \nabla \times S(n \times u)(x) - \nabla S(n \cdot u) + kS(n \times u) \\ &= \nabla \times S(n \times u)(x) + \frac{1}{k} \nabla \nabla \cdot S(n \times u) - \frac{1}{k} \Delta S(n \times u) \\ &= \nabla \times S(n \times u)(x) + \frac{1}{k} (\nabla \times)^2 S(n \times u)(x). \end{aligned}$$

□

The representation formula for the exterior domain follows from the interior one since we have the correct radiation condition.

Lemma 3.8 *i) Let $U \in C^\infty(\overline{\Omega^s})^4$ solve the Beltrami system in the exterior domain Ω^s with the radiation condition (3.8). Then*

$$(3.17) \quad \lim_{R \rightarrow \infty} \int_{\partial B(0,R)} |U|^2 dS = i \int_{\partial\Omega} (A(n)U)^T \bar{U} dS.$$

ii) Let $u \in C^\infty(\overline{\Omega^s})^3$ be a Beltrami field in the exterior domain Ω^s that satisfies the radiation condition (3.9). Then

$$(3.18) \quad \lim_{R \rightarrow \infty} \int_{\partial B(0,R)} |u|^2 dS = i \int_{\partial\Omega} (n \times u)^T \bar{u} dS.$$

Proof. i) Let $R > 0$ be large such that $\overline{\Omega} \subset B(0, R)$. It holds, since $A(\hat{x})^T A(\hat{x}) = I$,

$$\begin{aligned} \int_{\partial B(0,R)} |(I - iA(\hat{x}))U(x)|^2 dS &= 2 \int_{\partial B(0,R)} (|U|^2 - i(A(\hat{x})U)^T \overline{U}) dS \\ &= 2 \int_{\partial B(0,R)} |U|^2 dS - 2i \int_{\partial \Omega} (A(n)U)^T \overline{U} dS. \end{aligned}$$

The left-hand side tends to zero by the radiation condition (3.8) as $R \rightarrow \infty$.

ii) Apply i) with

$$U = \begin{pmatrix} u \\ 0 \end{pmatrix}.$$

□

Remark. The proof above holds also for weak solutions $U \in H_{loc}^1(\Omega^s)^4$ of the Beltrami system that satisfy the radiation condition since it is just an integration by parts argument. Recall $H_{loc}^1(\Omega^s)$ consists of such functions u that $\phi u \in H^1(\Omega^s)$ for all compactly supported smooth functions ϕ .

Theorem 3.9 *Let $U \in C^\infty(\overline{\Omega^s})^4$ solve the Beltrami system in the exterior domain Ω^s with the radiation condition (3.8). Then*

$$(3.19) \quad \int_{\partial \Omega} G_y(x) A(n(y)) U(y) dS(y) = \begin{cases} 0, & x \in \Omega, \\ U(x), & x \in \Omega^s. \end{cases}$$

Proof. First, we study the far field of the fundamental solution matrix. Since

$$G_z(x) = A(\nabla \Phi_z) + k \Phi_z I,$$

we get

$$G_z(x) = \Phi(x) G_{z,\infty}(\hat{x}) + o\left(\frac{1}{|x|}\right),$$

where

$$(3.20) \quad G_{z,\infty}(\hat{x}) = k(iA(\hat{x}) + I) \Phi_{z,\infty}(\hat{x}),$$

by (3.6). Now

$$(I - iA(\hat{x})) G_{z,\infty}(\hat{x}) = 0,$$

and so

$$(I - iA(\hat{x})) G_z(x) = o\left(\frac{1}{|x|}\right).$$

Let $x \in \mathbb{R}^3 \setminus \partial \Omega$, and let $R > |x|$ be large such that $\overline{\Omega} \subset B(0, R)$. Set

$$\Omega_R = \Omega^s \cap B(0, R),$$

and denote by n_R the unit outer normal of $\partial\Omega_R$. Here n is the unit outer normal of $\partial\Omega$. By the representation formula of interior solutions applied to Ω_R ,

$$\begin{aligned} \left. \begin{array}{l} x \in \Omega : \quad 0 \\ x \in \Omega^s : \quad U(x) \end{array} \right\} &= - \int_{\partial\Omega_R} G_y(x) A(n_R) U(y) dS(y) \\ &= \int_{\partial\Omega} G_y(x) A(n) U(y) dS(y) - \int_{\partial B(0,R)} G_y(x) A(\hat{y}) U(y) dS(y). \end{aligned}$$

The latter integrand tends to zero as R grows: By (3.5) and (3.20), the integrand is

$$\begin{aligned} G_y(x) A(\hat{y}) U(y) &= G_x(y)^T A(\hat{y}) U(y) \\ &= ik\Phi(y)\Phi_{x,\infty}(\hat{y})(I - iA(\hat{y}))U(y) + U(y)o\left(\frac{1}{R}\right) \\ &= o\left(\frac{1}{R^2}\right) + U(y)o\left(\frac{1}{R}\right) \end{aligned}$$

by the radiation condition (3.8). Hence, by the Cauchy-Schwartz inequality,

$$\left| \int_{\partial B(0,R)} G_y(x) A(\hat{y}) U(y) dS(y) \right| \leq o(1) + \left(\int_{\partial B(0,R)} |U|^2 dS \right)^{1/2} o(1),$$

and

$$\int_{\partial B(0,R)} |U|^2 dS$$

is bounded as $R \rightarrow \infty$ by the previous Lemma 3.8. \square

Corollary 3.10 *Let $u \in C^\infty(\overline{\Omega^s})^3$ be a Beltrami field in the exterior domain Ω^s that satisfies the radiation condition (3.9). Then*

$$(3.21) \quad \left. \begin{array}{l} x \in \Omega : \quad 0 \\ x \in \Omega^s : \quad u(x) \end{array} \right\} = \nabla \times S(n \times u)(x) + \frac{1}{k} (\nabla \times)^2 S(n \times u)(x).$$

Proof. Now

$$U = \begin{pmatrix} u \\ 0 \end{pmatrix}$$

solves the Beltrami system in the exterior domain and satisfies the radiation condition (3.8), so we can apply Theorem 3.9. The normal component $n \cdot u$ can be eliminated in the same way as in the interior case. \square

Earlier, in Section 3.1.2, we saw that the Sommerfeld radiation condition (2.8) implies the radiation condition (3.8) for Beltrami systems and (3.9) for Beltrami fields. Now, we assumed that the radiation condition (3.8), or (3.9), holds, and then we got a representation in terms of the radiating fundamental solution Φ of the Helmholtz equation. Hence,

the radiation conditions (3.8) and (3.9) are equivalent with the Sommerfeld radiation condition.

From the representation formula (3.21) it follows that the tangential component alone determines the Beltrami field u , and hence, fixing the tangential component would lead to an overdetermined problem. If one tries to ask a tangential boundary condition

$$n \times u^s + n \times u^i = 0$$

for a scattering phenomenon, then by the representation formula of the exterior domain

$$\begin{aligned} u^s(x) &= \nabla \times S(n \times u^s)(x) + \frac{1}{k}(\nabla \times)^2 S(n \times u^s)(x) \\ &= -\nabla \times S(n \times u^i)(x) - \frac{1}{k}(\nabla \times)^2 S(n \times u^i)(x) \\ &= 0, \end{aligned}$$

and $u^s \equiv 0$. But then on the boundary,

$$n \times u^i = -n \times u^s = 0,$$

and so also $u^i \equiv 0$ by the representation formula for interior solutions. Hence, the zero field is the only “scattering field” for the obstacles with tangential boundary conditions, that is, there are no such obstacles.

3.2 Exterior Neumann boundary value problem

The exterior Neumann boundary value problem is to find a solution $u \in H_{loc}^1(\Omega^s)^3$ for

$$(3.22) \quad \begin{cases} \nabla \times u = ku, & \text{in } \Omega^s, \\ n \cdot u|_{\partial\Omega}^+ = g, \end{cases}$$

where u is a radiating solution satisfying (3.9) and $g \in H^{1/2}(\partial\Omega)$. For g we also ask

$$(3.23) \quad \int_{\partial\Omega_j} g dS = 0$$

over each component Ω_j of Ω , which corresponds to the domain Ω to be source free. Define

$$(3.24) \quad H_0^{1/2}(\partial\Omega) = \left\{ g \in H^{1/2}(\partial\Omega) \mid \int_{\partial\Omega_j} g dS = 0 \text{ for each component } \Omega_j \right\}.$$

Notice that

$$H^{1/2}(\partial\Omega) = H_0^{1/2}(\partial\Omega) \oplus \text{span}\{\chi_{\partial\Omega_1}\} \oplus \dots \oplus \text{span}\{\chi_{\partial\Omega_N}\},$$

where N is the number of components of $\partial\Omega$ and $\chi_{\partial\Omega_j}$ is the characteristic function on the boundary component $\partial\Omega_j$, $j = 1, \dots, N$,

$$\chi_{\partial\Omega_j}(x) = \begin{cases} 1, & x \in \partial\Omega_j, \\ 0, & x \in \partial\Omega \setminus \partial\Omega_j. \end{cases}$$

3.2.1 Scattering of plane waves from a plane

Scattering of Beltrami fields is not as simple as one could imagine. To get some intuition, study first how plane waves scatter from the plane

$$n \cdot x = 0, \quad n \in S^2.$$

Note that scattering from a plane corresponds to what happens locally with more complicated boundaries.

Let

$$u^i(x, \xi, q) = \left(-(\xi \times)^2 q + i\xi \times q \right) e^{ikx \cdot \xi}, \quad \xi \in S^2, \quad q \in \mathbb{R}^3,$$

where for ξ we ask

$$\xi_n = n \cdot \xi < 0.$$

Define

$$\xi_T = -(n \times)^2 \xi,$$

so

$$\xi = \xi_T + \xi_n n.$$

The task is to find a plane wave

$$u^s(x, \tilde{\xi}, \tilde{q}) = \left(-(\tilde{\xi} \times)^2 \tilde{q} + i\tilde{\xi} \times \tilde{q} \right) e^{ikx \cdot \tilde{\xi}},$$

for which

$$(3.25) \quad n \cdot u^s + n \cdot u^i = 0$$

on the plane $n \cdot x = 0$, and where the natural choice for the propagation direction $\tilde{\xi}$ is, see Figure 4,

$$(3.26) \quad \tilde{\xi} = \xi_T - \xi_n n.$$

If one thinks about the symmetry over the plane $n \cdot x = 0$, then one might prefer to choose

$$\tilde{q} = -q_n n + q_T.$$

But for this choice,

$$(n \cdot u^s + n \cdot u^i)(x) = 2i(n \times \xi_T) \cdot q e^{ikx_T \cdot \xi_T},$$

which is not usually zero and so (3.25) is not satisfied. However, if one defines a left-handed plane wave with this polarization \tilde{q} ,

$$v^s(x, \tilde{\xi}, \tilde{q}) = \left(-(\tilde{\xi} \times)^2 \tilde{q} - i\tilde{\xi} \times \tilde{q} \right) e^{ikx \cdot \tilde{q}},$$

then

$$n \cdot v^s + n \cdot u^i = 0$$

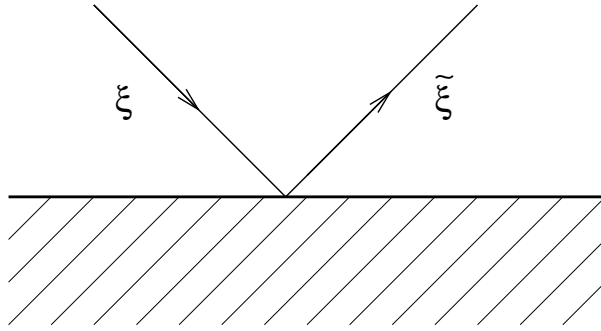


Figure 4: Propagating direction of the incident wave and the scattered wave.

on the plane $n \cdot x = 0$.

To get a right-handed scattered plane wave, we have to analyze u^i more carefully. Now,

$$\begin{aligned} n \cdot u^i(x, \xi, q)|_{n \cdot x = 0} &= (n \cdot q - \xi_n \xi \cdot q + i n \cdot (\xi \times q)) e^{ikx_T \cdot \xi_T} \\ &= \left((1 - \xi_n^2) n \cdot q - \xi_n \xi_T \cdot q + i(n \times \xi_T) \cdot q \right) e^{ikx_T \cdot \xi_T}, \end{aligned}$$

and

$$n \cdot u^s(x, \tilde{\xi}, \tilde{q})|_{n \cdot x = 0} = \left((1 - \tilde{\xi}_n^2) n \cdot \tilde{q} + \tilde{\xi}_n \tilde{\xi}_T \cdot \tilde{q} + i(n \times \tilde{\xi}_T) \cdot \tilde{q} \right) e^{ikx_T \cdot \tilde{\xi}_T}.$$

For $\xi \neq \pm n$, the vector triple

$$(n, \hat{\xi}_T, n \times \hat{\xi}_T), \quad \hat{\xi}_T = \frac{\xi_T}{|\xi_T|},$$

defines an orthonormal basis in \mathbb{R}^3 . If we represent q in these coordinates,

$$q = (q \cdot n)n + (q \cdot \hat{\xi}_T)\hat{\xi}_T + (q \cdot (n \times \hat{\xi}_T)) \cdot (n \times \hat{\xi}_T),$$

then we easily see that choosing

$$(3.27) \quad \tilde{q} = -(q \cdot n)n + (q \cdot \hat{\xi}_T)\hat{\xi}_T - (q \cdot (n \times \hat{\xi}_T))(n \times \hat{\xi}_T)$$

the boundary condition (3.25) is satisfied.

In case $\xi = \pm n$, the normal component of u^i disappears,

$$n \cdot u^i(\cdot, \xi, q) = 0$$

identically everywhere, and particularly on plane $n \cdot x = 0$. Since the same is true also for $u^s(\cdot, \tilde{\xi}, \tilde{q})$, the condition (3.25) is satisfied with any choice $\tilde{q} \in \mathbb{R}^3$.

3.2.2 Uniqueness

To prove uniqueness it is enough to show that the exterior field for $g = 0$ vanishes. This is usually obtained from the vanishing of the far field via Rellich's lemma. The problem here is that the formula (3.18) relating the far field to boundary values does not directly involve $n \cdot u$ but $n \times u$ instead. We can progress by representing the right-hand side of (3.18) with the Hodge-Helmholtz decomposition.

Recall the basic surface differential operators. Suppose that Γ is the smooth boundary of an open set of \mathbb{R}^3 . The surface divergence $Div : TL^2(\Gamma) \rightarrow H^{-1}(\Gamma)$ is defined via the duality

$$\langle Div(f), \phi \rangle = -\langle f, \nabla_T \phi \rangle, \quad f \in TL^2(\Gamma), \quad \phi \in H^1(\Gamma),$$

where $\nabla_T : H^1(\Gamma) \rightarrow TL^2(\Gamma)$ is the surface gradient. The surface curl $Curl : TL^2(\Gamma) \rightarrow H^{-1}(\Gamma)$ is defined

$$\langle Curl(f), \phi \rangle = -\langle f, n \times \nabla_T \phi \rangle, \quad f \in TL^2(\Gamma), \quad \phi \in H^1(\Gamma),$$

where n is the unit outer normal to Γ . Now,

$$Curl(f) = -Div(n \times f),$$

and

$$Curl(\nabla_T \phi) \equiv 0, \quad Div(n \times \nabla_T \phi) \equiv 0.$$

It holds that

$$\nabla_T \phi = -(n \times)^2 \nabla \phi, \quad Curl(f) = n \cdot (\nabla \times f),$$

when ϕ and f are extended away from the boundary Γ . If Γ is simply connected, in other words, there are neither handles nor holes, and if $f \in TL^2(\Gamma)$ with

$$Curl(f) = 0,$$

then there exists $\psi \in H^1(\Gamma)$ such that

$$f = \nabla_T \psi,$$

see [13], [6, Lemma 1], and [7, Proposition 3.1] also for non-smooth boundaries.

Theorem 3.11 *Suppose that each component of the boundary $\partial\Omega$ is simply connected. Let $u \in H_{loc}^1(\Omega^s)^3$ be a radiating solution of the exterior Neumann boundary value problem (3.22) with zero boundary value,*

$$n \cdot u|_{\partial\Omega}^+ = 0.$$

Then u is zero.

Proof. Now $u|_{\partial\Omega}^+ \in TL^2(\partial\Omega)$ and

$$\text{Curl}(u|_{\partial\Omega}^+) = n \cdot (\nabla \times u) = kn \cdot u = 0,$$

so there is a potential $\psi \in H^1(\partial\Omega)$ with

$$u|_{\partial\Omega}^+ = \nabla_T \psi.$$

Note that for this we need the topological assumption of $\partial\Omega$. By (3.18), it holds that

$$\begin{aligned} \lim_{R \rightarrow \infty} \int_{\partial B(0,R)} |u|^2 dS &= i \int_{\partial\Omega} (n \times \nabla_T \psi) \cdot \overline{\nabla_T \psi} dS \\ &= i \int_{\partial\Omega} \text{Div}(\overline{\psi}(n \times \nabla_T \psi)) dS \\ &= 0. \end{aligned}$$

Hence, $u = 0$ by Rellich's lemma. □

Remark. We conjecture that the presence of handles and holes will induce finite-dimensional non-uniqueness for the solution as is the case with the potential for a tangential curl free field. A detailed study of this topic is left out from this work.

Corollary 3.12 *Suppose that each component of the boundary $\partial\Omega$ is simply connected. The exterior Neumann boundary value problem of Beltrami fields (3.22) has at most one radiating solution.*

3.2.3 Existence

For the existence of the solution to the Neumann boundary value, we make an ansatz and show that it leads to a boundary integral equation, to which we apply the Fredholm theory.

We seek a suitable ansatz in several steps. First, let

$$u = \nabla \times v + kv.$$

Now

$$\nabla \times u - ku = (\nabla \times)^2 v - k^2 v = -(\Delta + k^2)v + \nabla \nabla \cdot v,$$

so u solves the Beltrami equation, if v satisfies Helmholtz equation with

$$\nabla \cdot v = 0.$$

If we define v as a single layer potential,

$$v = S_{\Omega^s} f, \quad f = n \times \nabla_T \phi,$$

v solves the Helmholtz equation. Note that

$$\nabla \cdot S_{\Omega^s} h = S_{\Omega^s} \text{Div}(h)$$

for $h \in TL^2(\partial\Omega)$, because

$$\int_{\partial\Omega} \nabla_x \Phi_y(x) \cdot h(y) dS(y) = - \int_{\partial\Omega} \nabla_y \Phi_y(x) \cdot h(y) dS(y) = \int_{\partial\Omega} \Phi_x(y) \text{Div}(h)(y) dS(y).$$

Since $\text{Div}(n \times \nabla_T) = 0$,

$$\nabla \cdot v = S_{\Omega^s} \text{Div}(f) = 0,$$

and hence u is a Beltrami field.

Let

$$(3.28) \quad u = (\nabla \times + kI) S_{\Omega^s} (n \times \nabla_T \phi)$$

be the full ansatz, which looks pretty complicated, but now u satisfies the desired properties. First, u is automatically a Beltrami field. Since the ansatz is in terms of the single layer potential, the Sommerfeld radiation condition is satisfied, and hence also (3.9) by Lemma 3.3. Also, the unknown is a scalar function ϕ , whereas we have a scalar valued boundary value, too, the normal component.

The jump formulas (2.22)-(2.24) imply that the traces from the exterior domain are

$$(\nabla \times S_{\Omega^s} f)|_{\partial\Omega}^+ = \nabla \times S_{\partial\Omega} f + \frac{1}{2} n \times f,$$

and

$$(S_{\Omega^s} f)|_{\partial\Omega}^+ = S_{\partial\Omega} f,$$

and so the condition for the normal component gives the boundary integral equation

$$g = n \cdot u|_{\partial\Omega}^+ = -\text{Div}(n \times S_{\partial\Omega} f) + kn \cdot S_{\partial\Omega} f,$$

or

$$(3.29) \quad -\text{Div}(n \times S_{\partial\Omega} n \times \nabla_T \phi) + kn \cdot S_{\partial\Omega} n \times \nabla_T \phi = g.$$

Hence, if $\phi \in H^{1/2}(\partial\Omega)$ satisfies the equation (3.29), then u defined by (3.28) gives the solution for the Neumann boundary value problem (3.22).

Next, we want to show that (3.29) is solvable for $g \in H_0^{1/2}(\partial\Omega)$. In fact, we show this for a larger space

$$(3.30) \quad H_0^{-1/2}(\partial\Omega) = \left\{ g \in H^{-1/2}(\partial\Omega) \mid \langle g, \chi_{\partial\Omega_j} \rangle = 0 \text{ for each component } \Omega_j \right\}.$$

Now

$$H^{-1/2}(\partial\Omega) = H_0^{-1/2}(\partial\Omega) \oplus \text{span}\{\chi_{\partial\Omega_1}\} \oplus \dots \oplus \text{span}\{\chi_{\partial\Omega_N}\},$$

where $\chi_{\partial\Omega_j}$ is the characteristic function on the boundary component $\partial\Omega_j$, $j = 1, \dots, N$. Note that $H_0^{-1/2}(\partial\Omega)$ and $H_0^{1/2}(\partial\Omega)$ have the same codimension N .

Simplify the notation by defining

$$(3.31) \quad T\phi = -\text{Div}(n \times S_{\partial\Omega} n \times \nabla_T \phi),$$

and

$$(3.32) \quad K\phi = kn \cdot S_{\partial\Omega} n \times \nabla_T \phi.$$

The boundary integral equation (3.29) can now be rewritten by

$$(T + K)\phi = g.$$

Theorem 3.13 *Suppose k^2 is not a Dirichlet eigenvalue and k is not a Neumann eigenvalue for the curl in Ω . Suppose that each component of the boundary $\partial\Omega$ is simply connected. Then*

$$(3.33) \quad (T + K)\phi = g,$$

is uniquely solvable in $H_0^{1/2}(\partial\Omega)$ for $g \in H_0^{-1/2}(\partial\Omega)$, and

$$u = (\nabla \times + kI)S(n \times \nabla_T \phi)$$

is the unique solution of the Neumann boundary value problem of Beltrami fields in both the interior and the exterior domain (choose $S = S_\Omega$, or $S = S_{\Omega^s}$, respectively) with

$$n \cdot u|_{\partial\Omega}^- = g = n \cdot u|_{\partial\Omega}^+.$$

Proof. We prove the following steps:

i) The operator

$$T + K : H^{1/2}(\partial\Omega) \rightarrow H^{-1/2}(\partial\Omega)$$

is a Fredholm operator with index zero.

ii) $\dim \text{Ker}(T + K) = N$.

iii) $R(T + K) \subset H_0^{-1/2}(\partial\Omega)$.

iv) $R(T + K) = H_0^{-1/2}(\partial\Omega)$.

v) $T + K$ is injective on $H_0^{1/2}(\partial\Omega)$.

i) We will show that $T + K$ is the sum of a coercive operator and a compact operator, which proves the claim, see [29, Theorem 2.34]. The coercivity is with $L^2(\partial\Omega)$ acting as a pivot space,

$$H^{1/2}(\partial\Omega) \subset L^2(\partial\Omega) \subset H^{-1/2}(\partial\Omega).$$

Consider T and K as pseudodifferential operators. If a pseudodifferential operator is of order m , then it maps the Sobolev space H^s to H^{s-m} , [43], and compactness can be obtained from the Rellich theorem of compact imbeddings, [29].

Computing the principal parts is based on the following two properties. First, a principal symbol of a pseudodifferential operator can be computed locally via a partition of the unity since the non-local remainder term is smoothing. Second, it holds that

$$\sigma_{pr}(A \circ B) = \sigma_{pr}(A)\sigma_{pr}(B)$$

for the principal symbols of pseudodifferential operators A and B . We consider the local coordinates in the form

$$\tilde{\psi}(x) = (x, \psi(x)) \in \partial\Omega, \quad x \in \mathbb{R}^2,$$

around $x = 0$. We can assume

$$(3.34) \quad \nabla\psi(0) = 0.$$

The principal part of the single layer in these coordinates is

$$(S\phi)_{pr}(x) = \frac{1}{4\pi} \int_{\mathbb{R}^2} \frac{1}{|x-y|} \tilde{\phi}(y) dy = \left(\frac{1}{|\cdot|} * \tilde{\phi} \right)(x),$$

where ϕ is assumed to be supported near $\tilde{\psi}(0)$ and $\tilde{\phi} = \phi \circ \psi$. Since for the Fourier transform it holds that

$$\widehat{\frac{1}{|\cdot|} * \tilde{\phi}} = \widehat{\frac{1}{|\cdot|}} \cdot \widehat{\tilde{\phi}},$$

and the principal symbol of the single layer is

$$(3.35) \quad \sigma_{-1}(S) = \widehat{\frac{1}{|\cdot|}} = \frac{1}{|\xi|}, \quad \xi \in \mathbb{R}^2.$$

The tangential gradient ∇_T is in the local coordinates

$$\nabla_T = g^{-1}\nabla,$$

where

$$g = (g_{ij}), \quad g_{ij} = \partial_i \tilde{\psi} \cdot \partial_j \tilde{\psi},$$

is the fundamental matrix of the geometry, see [13] and [8]; so the principal symbol is

$$(3.36) \quad \sigma_1(\nabla_T) = ig^{-1} \begin{pmatrix} \xi_1 \\ \xi_2 \end{pmatrix}, \quad \xi \in \mathbb{R}^2.$$

The surface divergence is

$$\operatorname{Div} F = \frac{1}{\sqrt{\det(g)}} \nabla \cdot (\sqrt{\det(g)} F) = \nabla \cdot F + \frac{1}{\sqrt{\det(g)}} \nabla(\sqrt{\det(g)}) \cdot F,$$

and so the principal symbol is

$$(3.37) \quad \sigma_1(\operatorname{Div}) = i \begin{pmatrix} \xi_1 & \xi_2 \end{pmatrix}.$$

Since we assumed (3.34), the symbol of $n \times$ is

$$(3.38) \quad \sigma_0(n \times) = \begin{pmatrix} 0 & -1 \\ 1 & 0 \end{pmatrix}.$$

By (3.35)-(3.38), the principal symbol of T is

$$\sigma_{pr}(T) = \sigma_1(T) = -i \begin{pmatrix} \xi_1 & \xi_2 \end{pmatrix} \begin{pmatrix} 0 & -1 \\ 1 & 0 \end{pmatrix} \frac{1}{|\xi|} \begin{pmatrix} 0 & -1 \\ 1 & 0 \end{pmatrix} i g^{-1} \begin{pmatrix} \xi_1 \\ \xi_2 \end{pmatrix} = -\frac{\xi^T g^{-1} \xi}{|\xi|}.$$

Now

$$\xi^T g^{-1} \xi \geq c |\xi|^2$$

with global $c > 0$ because $\partial\Omega$ is smooth and compact. Hence, the principal part of $-T$ is strongly elliptic and of degree 1,

$$\sigma(-T_{pr}) \geq c |\xi|,$$

and by Gårding's inequality [41] there exist C_1 and C_2 with

$$\operatorname{Re} \langle -T_{pr} \phi, \phi \rangle \geq C_1 \|\phi\|_{H^{1/2}(\partial\Omega)}^2 - C_2 \|\phi\|_{L^2(\partial\Omega)}^2,$$

that is, $-T$ is coercive. Hence,

$$\operatorname{ind}(T) = 0.$$

The operator

$$K = kn \cdot S_{\partial\Omega} n \times \nabla_T$$

is of order 0, and so K is a compact mapping

$$K : H^{1/2}(\partial\Omega) \rightarrow H^{1/2}(\partial\Omega) \hookrightarrow H^{-1/2}(\partial\Omega).$$

Hence,

$$\operatorname{ind}(T + K) = \operatorname{ind}(T) = 0.$$

ii) Suppose

$$(T + K)\phi = 0, \quad \phi \in H^{1/2}(\partial\Omega),$$

and let

$$f = n \times \nabla_T \phi$$

as before. Now for u defined by the ansatz (3.28), it holds that

$$u = 0 \quad \text{in } \Omega^s.$$

Note that the same ansatz (3.28) defines a Beltrami field also in the interior domain Ω , if we just change S_{Ω^s} to S_Ω . The boundary value is now

$$u|_{\partial\Omega}^- = (\nabla \times S_{\partial\Omega})f - \frac{1}{2}n \times f + kS_{\partial\Omega}f,$$

and so

$$(3.39) \quad n \cdot u|_{\partial\Omega}^- = (T + K)\phi = 0.$$

Since k is not a Neumann eigenvalue for the interior boundary value problem

$$u = 0 \quad \text{in } \Omega.$$

But then,

$$0 = n \times u|_{\partial\Omega}^- - n \times u|_{\partial\Omega}^+ = f = n \times \nabla_T \phi,$$

implying ϕ to be a constant on each $\partial\Omega_j$. Hence,

$$(3.40) \quad \text{Ker}(T + K) = \text{span}\{\chi_{\partial\Omega_1}\} \oplus \dots \oplus \text{span}\{\chi_{\partial\Omega_N}\},$$

and ii) holds.

iii) Since $T\phi$ is a surface divergence of a tangential field for any $\phi \in H^{1/2}(\partial\Omega)$,

$$\langle T\phi, \chi_{\partial\Omega_j} \rangle = \langle n \times S_{\partial\Omega} n \times \nabla_T \phi, \nabla_T \chi_{\partial\Omega_j} \rangle = 0.$$

Also,

$$\langle K\phi, \chi_{\partial\Omega_j} \rangle = k \int_{\Omega_j} \nabla \cdot S_\Omega(n \times \nabla_T \phi) dx,$$

and

$$\nabla \cdot S_\Omega(n \times \nabla_T \phi) = S_\Omega \text{Div}(n \times \nabla_T \phi) = 0.$$

Hence,

$$K\phi, T\phi \in H_0^{-1/2}(\partial\Omega)$$

with every $\phi \in H^{1/2}(\partial\Omega)$, and so

$$R(T + K) \subset H_0^{-1/2}(\partial\Omega).$$

iv) By i) and ii) the codimension of $R(T+K)$ is N . Since the codimension of $H_0^{-1/2}(\partial\Omega)$ is N , the claim follows from iii).

v) By (3.40),

$$H_0^{1/2}(\partial\Omega) \cap \text{Ker}(T+K) = \{0\},$$

from which the injectivity of $T+K$ on $H_0^{1/2}(\partial\Omega)$ follows.

By iv) and v) the integral equation (3.33) is uniquely solvable in $H_0^{1/2}(\partial\Omega)$ for $g \in H_0^{-1/2}(\partial\Omega)$. The claim for u follows now from the computations before the theorem and (3.39). \square

Remark. Suppose we have the obstacle scattering case with incident field u^i ,

$$n \cdot u^s = g$$

on $\partial\Omega$ with $g = -n \cdot u^i$. Now

$$u^s = (\nabla \times + kI)S_{\Omega^s}f$$

and

$$u^i = -(\nabla \times + kI)S_{\Omega}f$$

for

$$f = n \times \nabla_T \phi, \quad \phi = (T+K)^{-1}g.$$

Hence, for the total field $u = u_i + u_s$, the jump formulas imply

$$n \times u|_{\partial\Omega}^+ = n \times u_i|_{\partial\Omega}^- + n \times u^s|_{\partial\Omega}^+ = -f.$$

4 An inverse obstacle scattering problem for Beltrami fields

The basic setting of the inverse obstacle scattering problem of Beltrami fields is similar to the one of the acoustic case. Plane waves

$$u^i(x, \xi, q) = \left(-(\xi \times)^2 q + i\xi \times q \right) e^{ik\xi \cdot x}, \quad \xi \in S^2, \quad q \in \mathbb{R}^3,$$

are used as the incident fields, and the far fields u_∞^s of the scattered fields u^s are measured. The boundary condition for an obstacle is the Neumann boundary condition, the normal component of the total field vanishes,

$$n \cdot u|_{\partial\Omega} = 0, \quad u = u^i + u^s.$$

We always assume that k^2 is not a Dirichlet eigenvalue for the Laplacian in Ω and that k is not a Neumann eigenvalue for $\nabla \times$ in Ω .

Inverse Obstacle Scattering Problem for Beltrami Fields *Given the far field pattern $u_\infty^s(\cdot, \xi, q)$ for each incoming plane wave $u^i(\cdot, \xi, q)$, with all $\xi \in S^2$ and all $q \in \mathbb{R}^3$, and assuming that the scatterer is an obstacle, determine the scatterer Ω .*

Let Ω satisfy the conditions for the unique solvability of the exterior Neumann boundary value problem, Theorem 3.13. Then, for each incoming plane wave, there always exists the unique scattered field, and, therefore, the inverse problem is well defined in this sense. Since the far field depends linearly on the polarization, it is sufficient to know the far field pattern for three linearly independent polarization vectors q .

We will follow the ideas of the acoustic inverse scattering problem for solving the Beltrami field case. First, we prove that the far field data determines the scatterer. Then we show that the singular sources method can be applied for reconstructing the scatterer, and, in particular, we derive the indicator function of type (2.44) for the Beltrami field obstacle scattering case.

The main building blocks that are needed for proving the solvability of the inverse problem are

- a Beltrami field with a singular source term,
- Herglotz waves for Beltrami fields, and
- a Neumann-to-far-field mapping G that sends the Neumann boundary values of radiating exterior solutions to the corresponding far field patterns.

For the singular sources method we also need

- the mixed reciprocity relation connecting plane waves and singular sources.

4.1 Uniqueness of the inverse obstacle scattering problem

4.1.1 A singular Beltrami field

In this section, we introduce a radiating Beltrami field that is singular at one point. We obtain a reciprocity relation and discuss the mirror image principle.

Motivated by the representation formula (3.21), we define

$$(4.1) \quad \Psi_{z,p}(x) = \frac{1}{k}(\nabla_x \times)^2 [\Phi_z(x)p] + \nabla_x \times [\Phi_z(x)p], \quad x, z \in \mathbb{R}^3, \quad p \in \mathbb{C}^3.$$

Note that the representation formula (3.21) can be rewritten with the function $\Psi_{z,p}$ also as

$$(4.2) \quad \left. \begin{array}{l} x \in \Omega : \quad 0 \\ x \in \Omega^s : \quad u^s(x) \end{array} \right\} = \int_{\partial\Omega} \Psi_{y,n \times u^s(y)}(x) dS(y).$$

Since

$$(\nabla \times)^2 [\Phi_z p] = \nabla \nabla \cdot [\Phi_z p] + k^2 \Phi_z p + \delta_z p,$$

we get

$$\nabla \times \Psi_{z,p} = k \nabla \times [\Phi_z p] + (\nabla \times)^2 [\Phi_z p] + \frac{1}{k} \nabla \times (\delta_z p) = k \Psi_{z,p} + \frac{1}{k} \nabla \times (\delta_z p),$$

and so, by Lemma 3.3, $\Psi_{z,p}$ is the radiating Beltrami field with source term

$$\frac{1}{k} \nabla \times (\delta_z p).$$

Call point z the singularity point and p the polarization vector.

For $x \neq z$, denote

$$\xi = \xi(x, z) = \frac{x - z}{|x - z|}, \quad s = |x - z|.$$

Then

$$\Phi_z(x) = g(s)$$

with

$$g(s) = \frac{1}{4\pi} \frac{e^{iks}}{s},$$

and $\Psi_{z,p}$ can be rewritten for $x \neq z$ as

$$(4.3) \quad \Psi_{z,p}(x) = \frac{1}{ks} (sg''(s) - g'(s)) \xi \xi \cdot p + \left(kg(s) + \frac{1}{ks} g'(s) \right) p + g'(s) \xi \times p.$$

Since

$$\xi(z, x) = -\xi(x, z),$$

we get the *reciprocity relation*

$$(4.4) \quad q \cdot \Psi_{x,p}(z) = p \cdot \Psi_{z,q}(x).$$

Denote by $\Psi_{z,p}^s$ the radiating Beltrami field that is scattered from the obstacle Ω with incident field $\Psi_{z,p}$, $z \in \Omega^s$,

$$n \cdot (\Psi_{z,p}^s + \Psi_{z,p}) = 0 \quad \text{on } \partial\Omega.$$

Let $n \in S^2$ be fixed and consider scattering from the plane T_n ,

$$T_n = \{x \mid n \cdot x = 0\}.$$

Suppose z is in the positive half-space, $z_n = n \cdot z > 0$.

First, let the polarization be $p = n$. Then

$$n \cdot \Psi_{z,n}(x) = \frac{1}{ks} (sg''(s) - g'(s)) (\xi \cdot n)^2 + kg(s) + \frac{1}{ks} g'(s).$$

If

$$Jz = -(n \times)^2 z - z_n n$$

is the mirror point with respect to the plane T_n , then for $x \in T_n$,

$$n \cdot \Psi_{Jz,n}(x) = n \cdot \Psi_{z,n}(x).$$

Moreover, since $\Psi_{Jz,n}$ solves the Beltrami equation in the positive half-space, we get the *mirror image principle*,

$$(4.5) \quad \Psi_{z,n}^s(x) = \Psi_{Jz,-n}(x).$$

When computing an estimate for $n \cdot \Psi_{Jz,n}^s(z)$, we note that

$$\xi = \xi(z, Jz) = n$$

and

$$s = |z - Jz| = 2z_n,$$

and hence we get

$$n \cdot \Psi_{z,n}^s(z) = n \cdot \Psi_{Jz,-n}(z) = -\frac{1}{k}g''(s) - kg(s) = -g(s)\frac{2}{ks^2}(1 - is).$$

Hence,

$$(4.6) \quad |n \cdot \Psi_{z,n}^s(z)| \sim \frac{1}{z_n^3} \quad \text{as } z_n \rightarrow 0.$$

For general surfaces, consider the reminder function

$$u_h = \Psi_{z,n_x}^s - \Psi_{Jz,n_x}, \quad x \in \partial\Omega, \quad z = x + hn_x.$$

We show that

$$\sup |u_h| \leq C \frac{1}{h^{2+\alpha}}$$

with $\alpha < 1$, and so, the singularity estimate (4.6) holds also in this case: Consider the local coordinates $y = (y', \psi(y'))$ as in the proof of Theorem 3.13. Let

$$g_h(y) = n(y) \cdot (\Psi_{z,n_0}(y) - \Psi_{Jz,n_0}(y))$$

be the boundary value of the reminder. Fix α , $0 < \alpha < 1$. A straight-forward but rather long computation⁷ shows

$$|h^{2+\alpha}[g_h(y_1) - g_h(y_2)]| \leq C|y_1 - y_2|^\alpha,$$

⁷Use expression (4.3). The key is that for $s = |y - z|$, $Jz = |y - Jz|$, it holds

$$\left| \frac{1}{s^n} - \frac{1}{Js^n} \right| \leq C \frac{1}{s^{n-1}}.$$

where the constant C does not depend on h . Hence, $h^{2+\alpha}g_h \in C^{0,\alpha}(\partial\Omega)$ with

$$\|h^{2+\alpha}g_h\|_{0,\alpha} \leq C,$$

where $C^{0,\alpha}(\partial\Omega)$ is the Hölder space with norm $\|\cdot\|_{0,\alpha}$. Since the pseudo-differential operators act between the Hölder spaces as with the Sobolev spaces, [42, p. 268], and $(T + K)^{-1}$ is of degree -1 by the proof of Theorem 3.13,

$$\phi_h = (T + K)^{-1}(h^{2+\alpha}g_h) \in C^{1,\alpha}(\partial\Omega),$$

and

$$\|\phi_h\|_{1,\alpha} \leq C\|h^{2+\alpha}g_h\|_{0,\alpha} \leq C.$$

By [13, Theorem 6.12],

$$h^{2+\alpha}u_h = (\nabla \times S_{\Omega^s} + kI)(n \times \nabla_T \phi_h) \in C^{0,\alpha}(\mathbb{R}^3 \setminus \Omega)$$

with

$$\|h^{2+\alpha}u_h\|_{0,\alpha} \leq C\|\phi_h\|_{1,\alpha} \leq C.$$

This proves the claim.

For a tangential source polarization p ,

$$n \cdot p = 0,$$

the situation is more complicated. Now

$$(4.7) \quad n \cdot \Psi_{z,p}(x) = \frac{1}{ks} (sg''(s) - g'(s))(n \cdot \xi)(\xi_T \cdot p) + g'(s)(n \times \xi_T) \cdot p,$$

where

$$\xi_T = -(n \times)^2 \xi.$$

When z is replaced by Jz , then the sign of $n \cdot \xi$ changes, but this appears only in the first term of (4.7). Hence, as in the plane wave case (3.27), p should be replaced by

$$(4.8) \quad \tilde{p} = (p \cdot \hat{\xi}_T)\hat{\xi}_T - p \cdot (n \times \hat{\xi}_T)(n \times \hat{\xi}_T).$$

Then $\Psi_{Jz,\tilde{p}}(x)$, defined by (4.3) with p replaced by \tilde{p} and ξ with $J\xi$, satisfies the boundary condition. However, now also $\tilde{p} = \tilde{p}(x)$ depends on x , and it turns out that the function

$$v(x) = \Psi_{Jz,\tilde{p}(x)}(x)$$

does not satisfy the Beltrami equation.

As a summary, we have a mirror image principle for a normal polarization but not for a tangential polarization. This is the reason why we need to have all polarizations q in the inverse obstacle scattering problem instead of just one polarization to guarantee that some of the polarizations are normal to the boundary point that we are approaching.

4.1.2 Herglotz waves

Define the *Herglotz-Beltrami field* by

$$(4.9) \quad Ug(x) = \int_{S^2} u^i(x, \xi, g(\xi)) dS(\xi), \quad g \in L^2(S^2)^3,$$

where u^i is the plane wave

$$u^i(x, \xi, p) = \left(-(\xi \times)^2 p + i\xi \times p \right) e^{ik\xi \cdot x}.$$

Lemma 4.1 *Suppose k^2 is not a Dirichlet eigenvalue of Ω . Let $z \in \Omega^s$ and $p \in \mathbb{C}^3$ be fixed. The function $\Psi_{z,p}$ and its derivatives can be approximated uniformly in $\bar{\Omega}$ by Herglotz-Beltrami fields, and one has the estimate*

$$\sup_{x \in \bar{\Omega}} |\partial^\alpha (\Psi_{z,p} - kU(pf))(x)| \leq C_{A_z, \alpha} \|\Phi_z - Hf\|_{L^2(\partial A_z)}, \quad f \in L^2(S^2),$$

where A_z is an approximation domain and Hf is the scalar Herglotz wave function. The constant $C_{A_z, \alpha}$ depends on distance as

$$C_{A_z, \alpha} \leq Cd(\partial A_z, \Omega)^{-|\alpha|-4}.$$

Proof. Since

$$\left(-(\xi \times)^2 p + i\xi \times p \right) e^{ik\xi \cdot x} = \frac{1}{k} \left[\frac{1}{k} (\nabla \times)^2 (e^{ikx \cdot \xi} p) + \nabla \times (e^{ikx \cdot \xi} p) \right],$$

we can rewrite

$$(4.10) \quad kU(pf)(x) = \left(\frac{1}{k} (\nabla \times)^2 + \nabla \times \right) (pv_f)(x),$$

where v_f is the scalar Herglotz wave function with scalar density f ,

$$v_f(x) = \int_{S^2} e^{ikx \cdot \xi} f(\xi) dS(\xi).$$

Hence,

$$\Psi_{z,p} - kU(pf) = \left(\frac{1}{k} (\nabla \times)^2 + \nabla \times \right) (p(\Phi_z - v_f)).$$

Now, the claim follows by applying Lemma 2.3 for $K = \bar{\Omega}$ and $\Omega = A_z$ with the differential operator

$$\partial^\alpha \left(\frac{1}{k} (\nabla \times)^2 + \nabla \times \right) (p \cdot)$$

operating on the function $\Phi_z - v_f$. □

Remark. By the density of the scalar Herglotz waves (Lemma 2.2) there are $f_m \in L^2(S^2)$ such that

$$\|Hf_m - \Phi_z\|_{L^2(A_z)} \rightarrow 0$$

as $m \rightarrow \infty$. Hence, the singular field Ψ_z can be approximated in $\overline{\Omega}$ by the Herglotz-Beltrami fields when $z \in \Omega^s$.

There is a close connection between the far fields of radiating Beltrami fields u^s , the L^2 -adjoints of Herglotz-Beltrami waves and the incoming plane waves. Let $U_{\partial\Omega}f$ be a Herglotz-Beltrami field on $\partial\Omega$,

$$(4.11) \quad U_{\partial\Omega}f = (Uf)|_{\partial\Omega}, \quad f \in L^2(S^2)^3.$$

Since

$$\begin{aligned} & \int_{\partial\Omega} g(x) \cdot \int_{S^2} \overline{u^i(x, \xi, f(\xi))} dS(\xi) dS(x) \\ &= \int_{S^2} \overline{f(\xi)} \cdot \left(-(\xi \times)^2 + i\xi \times \right) \int_{\partial\Omega} e^{-ikx \cdot \xi} g(x) dS(x) dS(\xi), \end{aligned}$$

for $f \in L^2(S^2)^3$, $g \in L^2(\partial\Omega)^3$, we see that the L^2 -adjoint of $U_{\partial\Omega}$ is

$$(4.12) \quad U_{\partial\Omega}^*g(\xi) = \left(-(\xi \times)^2 + i(\xi \times) \right) \int_{\partial\Omega} e^{-ikx \cdot \xi} g(x) dS(x), \quad g \in L^2(\partial\Omega)^3.$$

Lemma 4.2 *Let u^s be a radiating Beltrami field in Ω^s . Then*

$$u_\infty^s(\hat{x}) = kU_{\partial\Omega}^*(n \times u^s)(x),$$

and

$$p \cdot u_\infty^s(\hat{x}) = k \int_{\partial\Omega} u^i(y, -\hat{x}, p) \cdot (n \times u^s)(y) dS(y).$$

Proof. Recall that the far field of the single layer potential is

$$S_\infty\phi(\xi) = \int_{\partial\Omega} e^{-ik\xi \cdot x} \phi(x) dS(x).$$

By (3.6), the far field of $\Psi_{z,p}$ is

$$\Psi_{z,p,\infty}(\hat{x}) = k(-(\hat{x} \times)^2 + i\hat{x} \times)(e^{-ik\hat{x} \cdot z} p).$$

By combining this with the representation formula (4.2), we get

$$\begin{aligned} u_\infty^s(\hat{x}) &= \int_{\partial\Omega} \Psi_{y, n \times u^s(y), \infty}(\hat{x}) dS(y) \\ &= k \int_{\partial\Omega} \left(-(\hat{x} \times)^2 + i\hat{x} \times \right) [e^{-ik\hat{x} \cdot y} (n \times u^s)(y)] dS(y), \end{aligned}$$

which proves the first formula.

The second formula follows from the previous calculation,

$$\begin{aligned} p \cdot u_\infty^s(\hat{x}) &= k \int_{\partial\Omega} p \cdot \left[-(\hat{x} \times)^2 + i(-\hat{x} \times) \right]^T [e^{ik(-\hat{x}) \cdot y} (n \times u^s)(y)] dS(y) \\ &= k \int_{\partial\Omega} \left[-(\hat{x} \times)^2 + i(-\hat{x} \times) \right] (e^{ik(-\hat{x}) \cdot y} p) \cdot (n \times u^s)(y) dS(y). \end{aligned}$$

□

4.1.3 Neumann-to-far-field mapping

Define the Neumann-to-far-field mapping G as the operator that maps the normal boundary component of a radiating Beltrami field to the corresponding far field pattern,

$$G : g = n \cdot u^s \mapsto u_\infty^s.$$

Lemma 4.3 *The Neumann-to-far-field mapping G is bounded from $H_0^{1/2}(\partial\Omega)$ to $L_T^2(S^2)$, and*

$$(4.13) \quad Gg = kU_{\partial\Omega}^* f,$$

where

$$f = (n \times \nabla_T)(T + K)^{-1}g, \quad g = n \cdot u^s.$$

Proof. Let u^s be a radiating solution with $g = n \cdot u^s$ on the boundary $\partial\Omega$. By Theorem 3.13,

$$u^s = (\nabla \times + kI)S_{\Omega^s} f,$$

with

$$f = (n \times \nabla_T)(T + K)^{-1}g,$$

and hence, by (3.6),

$$(Gg)(\hat{x}) = u_\infty^s(\hat{x}) = k(I + i\hat{x} \times)S_\infty f(\hat{x}).$$

But

$$\hat{x} \cdot u_\infty^s(\hat{x}) = 0$$

again by (3.6), since

$$\nabla \cdot u^s = 0,$$

and so

$$(I + i\hat{x} \times)S_\infty f = (-\hat{x} \times)^2 + i\hat{x} \times S_\infty f,$$

and

$$Gg = kU_{\partial\Omega}^* f.$$

The boundedness follows from the boundedness of the operators

$$\begin{aligned} H^{1/2}(\partial\Omega) &\hookrightarrow H^{-1/2}(\partial\Omega), \\ (T + K)^{-1} &: H_0^{-1/2}(\partial\Omega) \rightarrow H^{1/2}(\partial\Omega), \\ n \times \nabla_T S_{\partial\Omega} &: H^{1/2}(\partial\Omega) \rightarrow TH^{-1/2}(\partial\Omega), \\ (-\hat{x} \times)^2 + i\hat{x} \times S_\infty &: TH^{-1/2}(\partial\Omega) \rightarrow L_T^2(S^2). \end{aligned}$$

□

4.1.4 The uniqueness result

Now, we have the building blocks for proving the solvability for the inverse problem. The proof itself very much follows the proof of the corresponding acoustic result.

Theorem 4.4 *The data of the inverse obstacle scattering problem for Beltrami fields determines Ω uniquely.*

Proof. As in the acoustic case, suppose that the far field patterns of the incident Beltrami plane waves for the obstacles Ω_1 and Ω_2 coincide. Denote by G_j the corresponding Neumann-to-far-field mappings, $j = 1, 2$. Again, let E be the unbounded component of the exterior $\mathbb{R}^3 \setminus (\overline{\Omega_1} \cup \overline{\Omega_2})$, and fix $z \in E$ for a while. We will show that if $\Psi_{z,p,j}^s$ is the radiating solution for

$$(4.14) \quad \begin{cases} \nabla \times \Psi_{z,p,j}^s = k \Psi_{z,p,j}^s & \text{in } \Omega_j^s, \\ n \cdot \Psi_{z,p,j}^s = -n \cdot \Psi_{z,p} & \text{on } \partial\Omega_j, \end{cases}$$

$j = 1, 2$, then

$$\Psi_{z,p,1}^s = \Psi_{z,p,2}^s \quad \text{in } E.$$

By the density result, Lemma 4.1, there are $g_m \in L^2(S^2)$, $m = 1, 2, \dots$, such that Herglotz-Beltrami fields

$$U(g_m p) \rightarrow \Psi_{z,p}$$

uniformly in $\overline{\Omega_1 \cup \Omega_2}$. By the continuity of G_j , Lemma 4.3,

$$\Psi_{z,p,j,\infty}^s = -G_j(n \cdot \Psi_{z,p}) = -\lim_m G_j(n \cdot U(g_m p)) = \lim_m \int_{S^2} u_{\infty,j}^s(\cdot, \xi, g_m(\xi)p) dS(\xi).$$

But

$$u_{\infty,1}^s(\cdot, \xi, g_m(\xi)p) = u_{\infty,2}^s(\cdot, \xi, g_m(\xi)p)$$

by the assumption, and so

$$\Psi_{z,p,1,\infty}^s = \Psi_{z,p,2,\infty}^s.$$

By Rellich's Lemma, Lemma 2.1,

$$\Psi_{z,p,1}^s = \Psi_{z,p,2}^s \quad \text{in } E.$$

Suppose that $\Omega_1 \neq \Omega_2$. Without loss of generality, we may assume that there is $z_0 \in (\partial\Omega_1 \cap \partial E) \setminus \partial\Omega_2$, and let $z \in E$ tend to z_0 so that the distance $d(z, \Omega_2)$ stays bounded below by some positive constant. Now, for $p = n = n(z_0)$,

$$|n \cdot \Psi_{z,p,1}^s(z)| \rightarrow \infty \quad \text{as } z \rightarrow z_0$$

by the mirror image principle, while $|n \cdot \Psi_{z,p,2}^s(z)|$ stays bounded, since the boundary value $n \cdot \Psi_{z,n}$ stays bounded on $\partial\Omega_2$ in z . This contradicts with $\Psi_{z,p,1}^s = \Psi_{z,p,2}^s$ in E , and hence $\Omega_1 = \Omega_2$. \square

4.2 Singular sources method for Beltrami fields

The main goal of this chapter is to obtain an indicator function of type (2.44) for the inverse Beltrami fields obstacle scattering problem.

4.2.1 Mixed reciprocity

Lemma 4.5 *Suppose each component of $\partial\Omega$ is simply connected. Suppose v^i and w^i are Beltrami fields in a neighbourhood of $\overline{\Omega}$, and let v^s and w^s be radiating Beltrami fields with the Neumann boundary condition,*

$$n \cdot (v^i + v^s)|_{\partial\Omega} = 0 = n \cdot (w^i + w^s)|_{\partial\Omega}.$$

Denote

$$v = v^i + v^s, \quad w = w^i + w^s,$$

the total fields. Then the following equalities hold:

$$(4.15) \quad \int_{\partial\Omega} (n \times v^i) \cdot w^i dS = 0,$$

$$(4.16) \quad \int_{\partial\Omega} (n \times v^s) \cdot w^s dS = 0,$$

$$(4.17) \quad \int_{\partial\Omega} (n \times v) \cdot w dS = 0,$$

$$(4.18) \quad \int_{\partial\Omega} (n \times v^i) \cdot w^s dS = \int_{\partial\Omega} (v^s) \cdot (n \times w^i) dS.$$

Remark. Before proving the lemma, we remark that it is important not to have the complex conjugate in (4.16). Namely, by Lemma 3.8, the right-hand side would be non-zero for non-trivial $w^s = v^s$ if we had the complex conjugate. Note also that $\overline{v^s}$ solves still the Beltrami equation but not the radiation condition.

Proof. The first equation (4.15) follows as

$$\begin{aligned} \int_{\partial\Omega} (n \times v^i) \cdot w^i dS &= \int_{\Omega} (\nabla \times v^i) \cdot w^i dx - \int_{\Omega} v^i \cdot (\nabla \times w^i) dx \\ &= \int_{\Omega} (k v^i \cdot w^i - v^i \cdot (k w^i)) dx \\ &= 0. \end{aligned}$$

For (4.16), apply (4.15) with $\Omega_R = B(0, R) \setminus \overline{\Omega}$ to get

$$\int_{\partial\Omega} (n \times v^s) \cdot w^s dS = \int_{\partial B(0,R)} (\hat{x} \times v^s) \cdot w^s dS(x).$$

Since

$$(\hat{x} \times v^s) \cdot w^s = -v^s \cdot (\hat{x} \times w^s),$$

we get

$$\begin{aligned}
 \widehat{x} \times v^s \cdot w^s &= \frac{1}{2} ((\widehat{x} \times v^s) \cdot w^s - v^s \cdot (\widehat{x} \times w^s)) \\
 &= \frac{1}{2} ((\widehat{x} \times v^s + iv^s) \cdot w^s - v^s \cdot (\widehat{x} \times w^s + iw^s)) \\
 &= o\left(\frac{1}{R^2}\right)
 \end{aligned}$$

by the radiation condition as $R = |x| \rightarrow \infty$. Hence, (4.16) holds.

For the equation (4.17), the Neumann boundary conditions for v and w imply

$$Div(n \times v) = 0 \quad \text{and} \quad Div(n \times w) = 0,$$

and so there exist potentials ψ and ϕ with

$$v = \nabla_T \psi, \quad w = \nabla_T \phi.$$

Here we need the topological assumption of $\partial\Omega$. Now,

$$\begin{aligned}
 \int_{\partial\Omega} (n \times v) \cdot w dS &= \int_{\partial\Omega} (n \times \nabla_T \psi) \cdot \nabla_T \phi dS \\
 &= \int_{\partial\Omega} Div(\phi(n \times \nabla_T \psi)) dS - \int_{\partial\Omega} \phi Div(n \times \nabla_T \psi) dS \\
 &= 0,
 \end{aligned}$$

because $\partial(\partial\Omega) = \emptyset$ and $Div(n \times \nabla_T) = 0$.

The last equation (4.18) follows by applying (4.15) - (4.17) to

$$(n \times v) \cdot w = (n \times v^i) \cdot w^i + (n \times v^s) \cdot w^s + (n \times v^s) \cdot w^i + (n \times v^s) \cdot w^s.$$

□

The mixed reciprocity relation relates the scattered fields of the plane waves and of the singular sources. The formula (4.18) together with the representation formula and the relation between the radiating solutions and Beltrami plane waves in Lemma 4.2 are the key for the mixed reciprocity relation.

Theorem 4.6 (*Mixed reciprocity*) *Suppose each component of $\partial\Omega$ is simply connected. Then we have*

$$(4.19) \quad p \cdot \Psi_{z,q,\infty}^s(\xi) = kq \cdot u^s(z, -\xi, p),$$

where $z \in \Omega^s$, $\xi \in S^2$ and $p, q \in \mathbb{R}^3$.

Proof. First, if v^s is a radiating Beltrami field in the exterior domain Ω^s , then by the representation formula (4.2) and reciprocity (4.4),

$$p \cdot v^s(x) = \int_{\partial\Omega} p \cdot \Psi_{y, n \times v^s(y)}(x) dS(y) = \int_{\partial\Omega} (n \times v^s(y)) \cdot \Psi_{x,p}(y) dS(y)$$

for $x \in \Omega^s$. Now, apply Lemma 4.2 with $u^s = \Psi_{z,p}^s$ and the formula (4.18) to get

$$\begin{aligned} p^T \Psi_{z,q,\infty}^s(\xi) &= k \int_{\partial\Omega} u^i(y, -\xi, p) \cdot (n \times \Psi_{z,q}^s)(y) dS(y) \\ &= k \int_{\partial\Omega} (n \times u^s(y, -\xi, p)) \cdot \Psi_{z,q}(y) dS(y) \\ &= kq \cdot u^s(z, -\xi, p). \end{aligned}$$

□

4.2.2 Approximating fields

Theorem 4.7 *Let $z \in \Omega^s$ and let A_z be an approximation domain. Define*

$$(4.20) \quad E(F, G) = \int_{S^2} G(\xi) \cdot U_\infty^s(F)(-\xi) dS(\xi), \quad F, G \in L^2(S^2)^3,$$

where $U^s(F)$ is the scattered Beltrami field of the Herglotz-Beltrami field $U(F)$. Then

$$(4.21) \quad |E(fq, gp) - q \cdot U^s(gp)(z)| \leq C \|g\|_{L^2(S^2)} \|Hf - \Phi_z\|_{L^2(\partial A_z)},$$

where $f, g \in L^2(S^2)$, $p, q \in S^2$, and Hf is the scalar Herglotz wave on ∂A_z . The constant $C = C_{A_z}$ depends on the distance $d(\partial A_z, \Omega)$ as

$$C_{A_z} \leq Cd(\partial A_z, \Omega)^{-5}.$$

Proof. By the mixed reciprocity formula (4.19)

$$\begin{aligned} kq \cdot U^s(gp)(z) &= \int_{S^2} kq \cdot u^s(z, \xi, p) g(\xi) dS(\xi) \\ &= \int_{S^2} p \cdot \Psi_{z,q,\infty}^s(-\xi) g(\xi) dS(\xi), \end{aligned}$$

and so

$$\begin{aligned} |kE(fq, gp) - kq \cdot U^s(gp)(z)| &= \left| \int_{S^2} g(\xi) p \cdot (kU_\infty^s(fq) - \Psi_{z,q,\infty}^s)(-\xi) dS(\xi) \right| \\ &\leq \|g\|_{L^2(S^2)} \|kU_\infty^s(fq) - \Psi_{z,q,\infty}^s\|_{L^2(S^2)}. \end{aligned}$$

The last term can be estimated with the Neumann-to-far-field mapping,

$$\begin{aligned} \|kU_\infty^s(fq) - \Psi_{z,q,\infty}^s\|_{L^2(S^2)} &= \left\| G \left(kn \cdot U^s(fq) - n \cdot \Psi_{z,q}^s \right) \right\|_{L^2(S^2)} \\ &= \left\| G \left(kn \cdot U(fq) - n \cdot \Psi_{z,q} \right) \right\|_{L^2(S^2)} \\ &= \|G\|_{H^{1/2} \rightarrow L^2} \|kn \cdot U(fq) - n \cdot \Psi_{z,q}\|_{H^{1/2}(\partial\Omega)}, \end{aligned}$$

and by Lemma 4.1,

$$\|kn \cdot U(fq) - n \cdot \Psi_{z,q}\|_{H^{1/2}(\partial\Omega)} \leq C\|kU(fq) - \Psi_{z,q}\|_{H^1(\Omega)} \leq C_{A_z}\|Hf - \Phi_z\|_{L^2(\partial A_z)},$$

where

$$C_{A_z} \leq Cd(\partial A_z, \Omega)^{-5}.$$

This proves the theorem. \square

Remark. If f and g are given scalar valued functions, $E(fq, gp)$ can be computed from the far field data,

$$E(fq, gp) = \int_{S^2} g(\xi)p \cdot \int_{S^2} u_\infty^s(-\xi, \eta, q)f(\eta)dS(\eta)dS(\xi).$$

Corollary 4.8 *Let $z \in \Omega^s$ and $\epsilon > 0$. If $f_m \in L^2(S^2)$ are such that*

$$Hf_m \rightarrow \Phi_z \quad \text{in } L^2(\partial A_z),$$

then

$$(4.22) \quad E(f_m q, gp) \rightarrow q \cdot U^s(gp)(z),$$

for $p, q \in S^2$, $g \in L^2(S^2)$, and

$$(4.23) \quad \lim_{k \rightarrow \infty} \left(\lim_{m \rightarrow \infty} E(f_m q, f_k p) \right) = \lim_{k \rightarrow \infty} q \cdot U^s(f_k p)(z) = q \cdot \Psi_{z,p}^s(z).$$

Proof. The first limit (4.22) is clear by Theorem 4.7.

By Lemma 2.3,

$$\left| \Psi_{z,p}^s(z) - U^s(f_k p)(z) \right| \leq C_{d(z, \partial\Omega)} \|\Psi_{z,p}^s - U^s(f_k p)\|_{L^2(\partial\Omega)} \leq C \|n \cdot \Psi_{z,p}^s - n \cdot U^s(f_k p)\|_{H^{1/2}(\partial\Omega)},$$

since the tangential component of a scattered Beltrami field depends continuously on the normal component by Theorem 3.13. As in the proof of the previous theorem,

$$\|n \cdot \Psi_{z,p}^s - n \cdot U^s(f_k p)\|_{H^{1/2}(\partial\Omega)} \leq C \|Hf_k - \Phi_z\|_{L^2(\partial A_z)}.$$

This proves the claim since $Hf_k \rightarrow \Phi_z$ in $L^2(\partial A_z)$. \square

Define

$$(4.24) \quad I(z) = \sup_{p \in S^2} \left| p \cdot \Psi_{z,p}^s(z) \right|, \quad z \in \Omega^s.$$

This will be the indicator function for the inverse obstacle scattering problem. By the previous corollary,

$$\lim_{k \rightarrow \infty} \left(\lim_{m \rightarrow \infty} E(f_m p, f_k p) \right) = p \cdot \Psi_{z,p}^s(z).$$

If $f = g = f_m$, the estimate (4.21) takes the form

$$|q \cdot \Psi_{z,q}^s(z) - E(f_m q, f_m p)| \leq C \|f_m\|_{L^2(S^2)} \|Hf_m - \Phi_z\|_{L^2(\partial A_z)}.$$

But for this we do not have control in general. When $\|Hf_m - \Phi_z\|$ becomes small, the norm $\|f_m\|$ usually grows. This is the reason why we had to fix f_k first.

Corollary 4.9 *Let $\delta > 0$. There is a bound $M_\delta > 0$ such that*

$$I(z) \leq M_\delta$$

for $z \in \Omega^s$ with $d(z, \partial\Omega) > \delta$. For $z_0 \in \partial\Omega$,

$$\lim_{z \rightarrow z_0} I(z) = \infty, \quad z \in \Omega^s.$$

Proof. By continuity,

$$M_\delta = \sup_{d(z, \partial\Omega) > \delta} \sup_{p \in S^2} |p \cdot \Psi_{z,p}^s(z)|$$

is bounded. Let $z_0 \in \partial\Omega$. If Pz is the normal projection of z onto $\partial\Omega$ for z close to z_0 , then by the mirror image principle (4.6)

$$I(z) = \sup_{p \in S^2} |p \cdot \Psi_{z,p}^s(z)| \geq |n(Pz) \cdot \Psi_{z,n(Pz)}^s(z)| \geq C(Pz) |z_n|^{-3}$$

with $z_n = z - Pz$. Because constant $C(Pz)$ depends continuously of the boundary, it is bounded below $C(Pz) \geq C > 0$ in a neighbourhood of z_0 . This proves the claim. \square

4.2.3 Translating the singularity point

Next, we deduce the formulas explaining how the Herglotz density should be changed when the approximation domain is rotated and translated. This can be found in [36], but we present it here for the sake of completeness. If the approximation domain for each z can be chosen by a translation and a rotation, then the limits in (4.24) are uniform in a computational domain; see below.

Let M be a real and unitary 3×3 -matrix. Define

$$R_M f(\xi) = f(M\xi).$$

We show that if f_0 is a regularized solution for

$$H_{\partial A_0} f = \Phi_0,$$

then $R_{M^T} f_0$ is a regularized solution for

$$H_{\partial(MA_0)} f = \Phi_0.$$

Since

$$\int_{S^2} e^{ik(Mx)\cdot\xi} f(\xi) dS(\xi) = \int_{S^2} e^{ikMx\cdot M\eta} f(M\eta) dS(\eta) = H_{\partial A_0}(R_M f)(x), \quad x \in \partial A_0,$$

it holds that for $y = Mx \in \partial(MA_0)$,

$$\begin{aligned} H_{\partial(MA_0)}(R_{M^T} f)(y) &= \int_{S^2} e^{ik(Mx)\cdot\xi} R_{M^T} f(\xi) dS(\xi) \\ &= H_{\partial A_0}(R_M R_{M^T} f)(x) \\ &= H_{\partial A_0} f(x). \end{aligned}$$

Moreover,

$$\Phi_0(y) = \Phi_0(Mx) = \Phi_0(x),$$

so $R_{M^T} f_0$ is a regularized solution for

$$H_{\partial(MA_0)} f = \Phi_0.$$

For translations, define

$$\tau_z(x) = x + z,$$

and

$$e_z(\xi) = e^{ikz\cdot\xi},$$

which is a bounded function on S^2 . Then, for $y = x + z \in \tau_z \partial A_0 = \partial A_0 + z$, it holds that

$$\begin{aligned} H_{\partial(\tau_z A_0)}(e_{-z} f)(y) &= \int_{S^2} e^{ik(x+z)\cdot\xi} e_{-z}(\xi) f(\xi) dS(\xi) \\ &= H_{\partial A_0} f(x). \end{aligned}$$

Since also

$$\Phi_z(y) = \Phi_z(x + z) = \Phi_0(x),$$

the function $e_{-z} f_0$ is a regularized solution for

$$H_{\partial(\tau_z A_0)} f = \Phi_z.$$

Now, if the domain

$$(4.25) \quad A_z = \tau_z M A_0$$

is a rotated and translated domain (in this order) and if f_0 is a regularized solution for

$$H_{\partial A_0} f = \Phi_0,$$

then

$$(4.26) \quad f_z = \tau_{-z} R_{M^T} f_0$$

is a regularized solution for

$$H_{\partial A_z} f = \Phi_z$$

with

$$\|H_{\partial A_z} f_z - \Phi_z\|_{L^2(\partial A_z)} = \|H_{\partial A_0} f_0 - \Phi_0\|_{L^2(\partial A_0)}$$

and

$$\|f_z\|_{L^2(S^2)} = \|f_0\|_{L^2(S^2)}.$$

Thus, we want to choose the approximation domain A_z for each $z \in \Omega^s$ so that it is of the form (4.25) with some rotation matrix $M(z)$. Of course, this is impossible for all $z \in \Omega^s$, since A_0 is bounded and A_z has to contain Ω , and therefore, we need to restrict points z to some bounded computational domain D . For example,

$$D = [-R, R] \times [-R, R] \times [-R, R] \subset \mathbb{R}^3$$

with some $R > 0$. Note that this is not any real restriction since some bounded computational domain is always chosen in this kind of problems. Call Ω *approximable* with A_0 in D , if for every $z \in D \setminus \Omega$ with $d(z, \partial\Omega) \geq d(0, \partial A_0)$ there exists a rotation matrix $M(z)$ such that

$$A_z = \tau_z M(z) A_0$$

is an approximation domain. This sets some requirements for the shape of the scatterer that depend on the shape of the base approximation domain A_0 . The next theorem states that for an approximable domain Ω , the indicator function can be approximated uniformly in a strict exterior domain.

Theorem 4.10 *Let $\rho > 0$ and denote*

$$\Omega_\rho = \{ x \in \mathbb{R}^3 \mid d(x, \Omega) < \rho \}.$$

Suppose that Ω_ρ is approximable by A_0 in a computational domain D . Let $f_m \in L^2(S^2)$ be such that

$$H_{\partial A_0} f_m \rightarrow \Phi_0$$

in $L^2(\partial A_0)$. Define

$$f_{z,m} = \tau_{-z} R_{M(z)^T} f_m.$$

Then, for every $\rho > 0$,

$$\lim_k \left(\lim_m E(f_{m,z} q, f_{k,z} p) \right) = p \cdot \Psi_{z,p}^s(z)$$

uniformly in $D \setminus \Omega_\rho$.

Proof. That Ω_ρ is approximable by A_0 in D means that

$$d(\partial A_z, \partial \Omega) \geq \rho$$

for each approximation domain A_z , $z \in D \setminus \Omega_\rho$. Let $z \in D \setminus \Omega_\rho$. By (4.21) and the proof of Corollary 4.8,

$$\begin{aligned} & \left| q \cdot \Psi_{z,p}^s(z) - E(f_{z,m}q, f_{z,k}p) \right| \\ & \leq \left| q \cdot \Psi_{z,p}^s(z) - q \cdot U^s(f_{z,k}p)(z) \right| + \left| q \cdot U^s(f_{z,k}p)(z) - E(f_{z,m}q, f_{z,k}p) \right| \\ & \leq C_{d(\partial A_z, \partial \Omega)} \|Hf_{z,k} - \Phi_z\|_{L^2(\partial A_z)} + C_{d(\partial A_z, \partial \Omega)} \|f_{z,k}\|_{L^2(S^2)} \|Hf_{z,m} - \Phi_z\|_{L^2(\partial A_z)} \\ & \leq C_\rho \|Hf_k - \Phi_0\|_{L^2(\partial A_0)} + C_\rho \|f_k\|_{L^2(S^2)} \|Hf_m - \Phi_0\|_{L^2(\partial A_0)}, \end{aligned}$$

where the last expression does not depend on z . \square

5 Numerical experiments

In this section, we explain the numerical methods and present some examples. First, in Section 5.1, we describe the forward far field solver which computes the far field of the scattered field when an incident field is given. Then, in Section 5.2, we consider the implementation of the inverse problem. Finally, we give some test examples and discuss the results. All examples are computed with MATLAB.

5.1 The far field solver

The far field solver computes the far field

$$u_\infty^s(\cdot, \eta, p)$$

on S^2 when an incident plane wave

$$u^i(\cdot, \eta, p), \quad \eta \in S^2, \quad p \in \mathbb{R}^3,$$

is given and the boundary of the obstacle is discretized. The solver consists of two steps. First, we solve the boundary integral equation of Theorem 3.13 with

$$g = -n \cdot u^i(\cdot, \eta, p)$$

to get

$$\phi = (T + K)^{-1}g,$$

or

$$f = (n \times \nabla_T)(T + K)^{-1}g.$$

The second step is to compute the integral operator $U_{\partial \Omega}^*$ (see Lemma 4.3) to get the far field

$$u_\infty^s(\xi, \eta, p) = kU_{\partial \Omega}^* f.$$

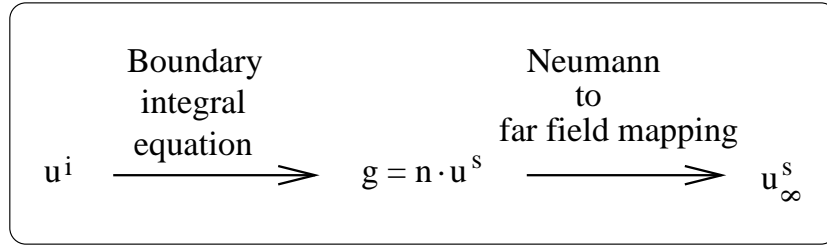


Figure 5: Scheme of the far field solver.

5.1.1 Discretized obstacles and boundary functions

An obstacle Ω is described by defining a triangularization of the boundary $\partial\Omega$. Fix a finite number of points $x_j \in \partial\Omega$, $j = 1, \dots, N_x$, and define triangles (elements) $E_i \subset \partial\Omega$, $i = 1, \dots, N_E$, with points x_j 's as their nodes. As open sets,

$$E_i \cap E_j = \emptyset$$

for $i \neq j$, and with closures,

$$\cup_i \overline{E}_i = \partial\Omega.$$

The sides of two elements have to match along the whole side if at all.

In practice, we define the obstacles via a triangularization. First, we compute a triangularization for the surface S^2 . The triangularization is described by a $3 \times N_x$ node matrix X and a $3 \times N_E$ element matrix E . The node matrix consists of the node points on S^2 ,

$$X_{:,j} = x_j \in \mathbb{R}^3,$$

and of the element matrix E ,

$$E_{:,i} = \text{node indices of the corners of element } E_i.$$

To get an obstacle with a different shape, we transform the S^2 surface nodes x_j with a suitable mapping, while keeping the element matrix E unchanged. Now, the obstacle is defined by

$$(5.1) \quad \partial\Omega = \cup_i \overline{E}_i.$$

This is a single-component obstacle with a piecewise linear boundary. A multi-component obstacle can be obtained by attaching node and element matrices of disjoint single-component obstacles.

On the boundary $\partial\Omega$, we have to define scalar functions ϕ and tangential vector fields of type

$$n \times \nabla_T \phi.$$

For the scalar functions, define the standard linear basis functions. Denote by ϕ_j the basis function which is associated to the node x_j and which is linear in each element,

$$(5.2) \quad \phi_j(x_i) = \begin{cases} 1, & j = i, \\ 0, & j \neq i. \end{cases}$$

The functions ϕ_j span piecewise linear and continuous functions on the triangularization. To represent approximations for the prescribed tangential fields, define

$$(5.3) \quad \psi_j = n \times \nabla_T \phi_j.$$

Since the unit outer normal n and $\nabla_T \phi_j$ are well defined on each element, ψ_j is well defined separately on each element, on which it is a constant vector.

Discretization sets a limit on how rapidly changing functions we are able to give reasonable approximations. Hence, the discretization has to be proportional to the wave length so that the waves of this length and with limited amplitudes can be represented in the discretization. Note that when computing simulated data for the inverse problem, all incident fields are plane waves for which the amplitudes are bounded by

$$| -(\xi \times)^2 p + i\xi \times p | \leq \sqrt{2}|p|.$$

5.1.2 Solving the boundary integral equation

System matrix The aim is to solve the equation (3.29). We write the numerical equation for

$$f = n \times \nabla \phi,$$

for which the boundary integral equation is

$$-Div(n \times S_{\partial\Omega} f) + kn \cdot S_{\partial\Omega} f = g.$$

Approximate

$$f = \sum_{i=1}^{N_x} f_i \psi_i,$$

where coefficients $f_i \in \mathbb{C}$ are the unknown variables to be solved and ψ_i are defined by (5.3). By using the functions ϕ_j (see (5.2)) as test functions, we get

$$\int_{\partial\Omega} (n \times S_{\partial\Omega} f) \cdot \nabla_T \phi_j dS + k \int_{\partial\Omega} \phi_j n \cdot S_{\partial\Omega} f dS = \int_{\partial\Omega} \phi_j g dS,$$

or

$$- \int_{\partial\Omega} S_{\partial\Omega} f \cdot \psi_j dS + k \int_{\partial\Omega} \phi_j n \cdot S_{\partial\Omega} f dS = \int_{\partial\Omega} \phi_j g dS.$$

This can be written in a matrix form,

$$(5.4) \quad MF = G,$$

where

$$F = (f_i)_{i=1}^{N_x}$$

are the coefficients of the function f ,

$$G_j = \int_{\partial\Omega} \phi_j g dS, \quad j = 1, \dots, N_x,$$

and the entries of the system matrix are

$$M_{ji} = - \int_{\partial\Omega} \psi_j \cdot S_{\partial\Omega} \psi_i dS + k \int_{\partial\Omega} \phi_j n \cdot S_{\partial\Omega} \psi_i dS.$$

Note that M is a full $N_x \times N_x$ square matrix.

Invertibility The matrix equation (5.4) is not invertible since we have not taken into account the kernel of the operator $T + K$ of (3.29) but approximated the equation so far just in whole $H^{1/2}(\partial\Omega)$. By Theorem 3.13 and its proof, the kernel is spanned by the characteristic functions of the boundary components. Let $F^\alpha = (F_i^\alpha)$ be associated to the component $\partial\Omega^\alpha$ of the boundary $\partial\Omega$,

$$F_i^\alpha = \begin{cases} 1, & x_i \in \partial\Omega^\alpha \\ 0, & \text{otherwise.} \end{cases}$$

Now,

$$\sum_{i=1}^{N_x} F_i^\alpha \psi_i = \sum_{i=1}^{N_x} n \times \nabla_T (F_i^\alpha \phi_i) = n \times \nabla_T \chi_{\partial\Omega^\alpha} = 0,$$

and so

$$MF^\alpha = 0.$$

Hence, let m be the number of the components of $\partial\Omega$. Now, the equation (5.4) can be inverted by taking the singular value decomposition,

$$M = U' \text{diag}(s) V, \quad s = (s_1, \dots, s_{N_x}),$$

where $s_1 \geq s_2 \geq \dots \geq s_{N_x} \geq 0$, and U, V are orthonormal matrices, and computing the pseudoinverse

$$M^+ = V' \text{diag}(s^+) U,$$

where

$$s^+ = (1/s_1, 1/s_2, \dots, 1/s_{N_x-m}, 0, \dots, 0).$$

The solution coefficients are then

$$F = M^+ G.$$

Note that one needs to compute the pseudoinverse only once, and thereafter coefficients F for each incoming plane wave can be computed just by one matrix-vector multiplication, provided the corresponding G_j 's are computed.

Computing integrals The expressions for G_j and M_{ji} involve integrals that are computed numerically as follows. An integral over the boundary $\partial\Omega$ is the sum of integrals over the surface elements,

$$\int_{\partial\Omega} = \sum_i \int_{E_i}.$$

For G_j we use the one-point approximation

$$\int_{E_i} \phi_j g dS \approx A_i \phi_j(y_i) g(y_i),$$

where y_i is the midpoint of the element E_i ,

$$y_i = \frac{x_{E(1,i)} + x_{E(2,i)} + x_{E(3,i)}}{3},$$

and A_i is the area of the element i . Note that $\phi_j(y_i) = 1/3$ at the midpoint y_i if $y_i \in \text{supp}(\phi_j)$ and zero otherwise.

The exterior integrals for M_{ji} are also computed with the one-point approximation. For this, we need the value $(S_{\partial\Omega}\psi_i)(y_m)$ at each midpoint y_m of the element E_m , $m = 1, \dots, N_E$, which is a singular integral. Since ψ_i is a constant vector on each element,

$$(S_{\partial\Omega}\psi_i)(y_m) = \sum_{\ell} \int_{E_{\ell}} \Phi_{y_m} \psi_i dS = \sum_{\ell} \psi_i(E_{\ell}) \int_{E_{\ell}} \Phi_{y_m} dS.$$

The value for

$$S_{m\ell} = \int_{E_{\ell}} \Phi_{y_m} dS$$

is computed numerically. If y_{α}^{ℓ} are the integral points in E_{ℓ} and w_{α}^{ℓ} the corresponding integral weights,

$$\sum_{\alpha} w_{\alpha}^{\ell} = A_{\ell},$$

we approximate

$$\int_{E_{\ell}} \Phi_{y_m} dS \approx \sum_{\alpha} w_{\alpha}^{\ell} \Phi_{y_m}(y_{\alpha}^{\ell}).$$

The number and location of the integral points on E_{ℓ} vary depending on the distance between the singularity point y_m and the element. When $\ell = m$, the integral is singular, and we set the integral points like polar coordinates around the singularity point y_i . If $\ell \neq m$ but E_{ℓ} is close to y_m , the number of the integral points is high. When E_{ℓ} is far from y_m , we use a smaller number of integral points (one). See Figure 6 for an example of distributing points y_{α}^{ℓ} for the single layer integral. Finally, M_{ji} with one-point approximation is

$$M_{ji} \approx \sum_{m,\ell} (-\psi_j(E_m) \cdot \psi_i(E_{\ell}) + k\phi_j(y_m)n(E_m) \cdot \psi_i(E_{\ell})) S_{m\ell} A_m.$$

5.1.3 The far field

When the discretized solution f for

$$-Div(n \times Sf) + kn \cdot Sf = g$$

is given by

$$f = \sum_{j=1}^{N_x} f_j \psi_j,$$

the far field is the adjoint Herglotz-Beltrami wave $kU_{\partial\Omega}^* f$, see Lemma 4.3. With one-point integral approximation,

$$\begin{aligned} kU_{\partial\Omega}^* f(\xi) &= \sum_j k \left(-(\xi \times)^2 + i(\xi \times) \right) \int_{\partial\Omega} e^{-ik\xi \cdot y} \psi_j(y) dS(y) f_j \\ &\approx \sum_{j,\ell} k A_\ell e^{-ik\xi \cdot y_\ell} \left(-(\xi \times)^2 + i(\xi \times) \right) \psi_j(E_\ell) f_j. \end{aligned}$$

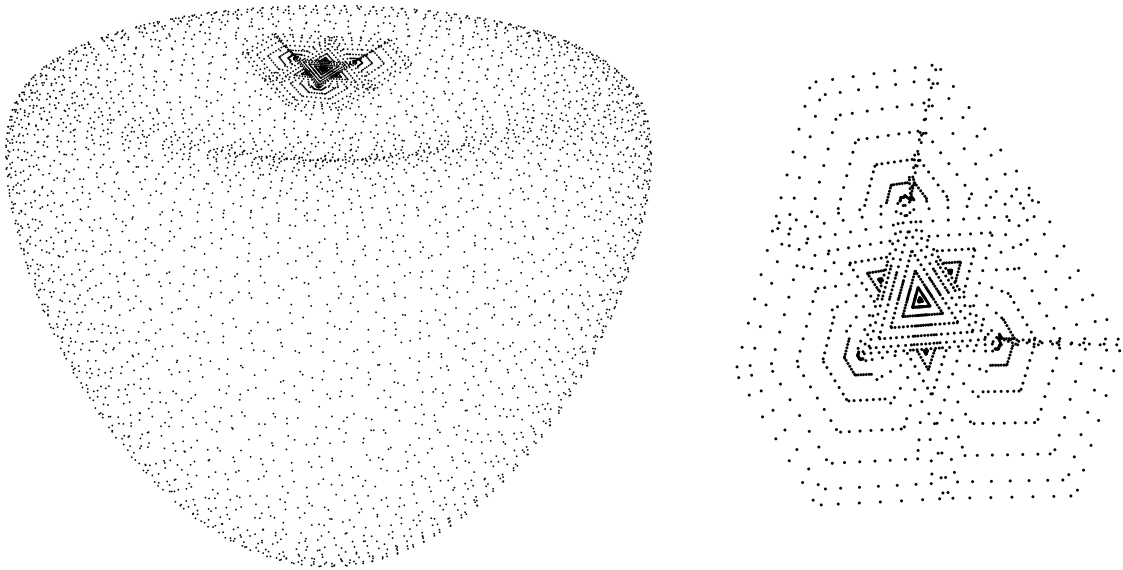


Figure 6: An example of integration points on the surface of an obstacle for computing the single layer potential. On the right-hand side are those elements that are close to the singularity point.

5.2 Reconstructing the obstacle

The inverse obstacle scattering problem for Beltrami fields is to reconstruct an approximation for the obstacle Ω when the far field data

$$u_\infty^s(\xi, \eta, p), \quad \xi, \eta, p \in S^2$$

is given. The reconstruction procedure consists of the following three main parts:

1. The scalar Herglotz density solver for the ill-posed equation

$$H_{\partial A_z} f = \Phi_z$$

with a given approximation domain A_z ;

2. The computation of the indicator function $I(z)$, see (4.24) and (4.20);
3. Some scanning algorithm, namely, a procedure of choosing an approximation domain for each z in the computational domain.

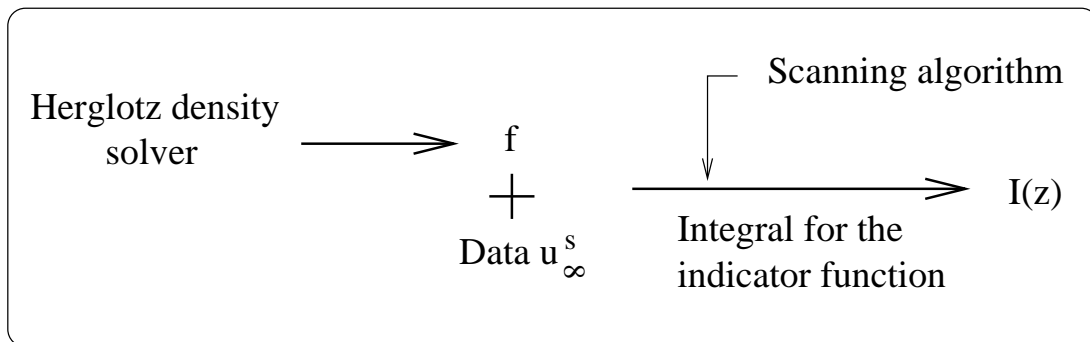


Figure 7: Scheme of the reconstruction algorithm.

The Herglotz density solver part, Part 1 above, does not depend on the (noisy) far field measurement data. The equation can, in principle, be solved with arbitrarily good accuracy. Naturally, this is not quite the case when implying a numerical algorithm. Since we only need to solve the scalar Herglotz density, this part does not particularly depend on that the reconstruction is made for the Beltrami fields

Solving the Herglotz density f is a slow operation. But, by choosing each approximation domain A_z so that it is just a rotation and translation of some base approximation domain A_0 as in Section 4.2.3, one needs to solve the Herglotz density only once. Moreover, if the base approximation domain is chosen so that it satisfies certain symmetry properties, the ill-posed integral equation between two-dimensional surfaces S^2 and ∂A_0 can be reduced to an integral equation over one-dimensional domains. This yields to an improvement in accuracy and computational costs, since now one does not have to solve the integral equation over surfaces.

To compute the indicator function, one has to compute the double limit over Herglotz densities f for which Hf approximates Φ_0 . Recall that the reason for two separate limits was that the estimate in Theorem 4.7 for $E(fq, gp)$ depends on $\|g\|$; see also discussion after Corollary 4.8. Also, decreasing the regularization parameter leads to heavier oscillations of the Herglotz densities, which can destroy the numerical integration (4.20) when computing the indicator function. Note that this integral (4.20) has (noisy) data as its integral kernel. Hence, we use one fixed density f , which is solved from the equation with some accuracy, but for which $\|f\|$ is not very large (now $\|f\|$ has the role of $\|g\|$ in Theorem 4.7). Here we see the ill-posedness of the inverse problem in practice.

In choosing the approximation domains, there are two different approaches. One is to start from a clear part of the computational domain in which we *a priori* know that the scatterer is not located. Then enlarge this clear area someway until the whole empty part of the computational domain is scanned. Another way to choose the approximation domains is to use some cumulative algorithm. For each z one uses many domains A_z that sometimes do not even satisfy the assumptions for an approximation domain but so that eventually the result is satisfactory. This approach is motivated by the standard back projection methods of X-ray tomography and is described further in Section 5.2.3.

5.2.1 Solving the Herglotz density of the singular source

Suppose that the base approximation domain A_0 is rotationally symmetric around, say, the x_1 -axis,

$$MA_0 = A_0,$$

for

$$M = \begin{pmatrix} 1 & 0 & 0 \\ 0 & \cos(\theta) & -\sin(\theta) \\ 0 & \sin(\theta) & \cos(\theta) \end{pmatrix}, \quad \theta \in [0, 2\pi].$$

This holds, for example, if A_0 is a cone domain pointing into the direction e_1 . Now, ∂A_0 is determined by a one-dimensional set

$$(5.5) \quad L = \{ (x_1, x_2, 0) \in \partial A_0 \mid x_2 \geq 0 \}$$

with

$$\partial A_0 = \cup_{\theta} M(\theta)L.$$

Since Φ_0 is also symmetric around the x_1 -axis, we seek a regularized solution f for

$$H_{\partial A_0} f = \Phi_0,$$

of the form

$$f(\xi) = \varphi(r),$$

$$\xi = (r, \rho(r) \cos(\theta), \rho(r) \sin(\theta)), \quad \rho(r) = \sqrt{1 - r^2}, \quad r \in [-1, 1], \quad \theta \in [0, 2\pi].$$

Then for $x \in L$,

$$\begin{aligned} H_{\partial A_0} f(x) &= \int_{S^2} e^{ikx \cdot \xi} f(\xi) dS(\xi) \\ &= \int_{-1}^1 \int_0^{2\pi} e^{ik(rx_1 + x_2 \rho(r) \cos(\theta))} \varphi(r) d\theta dr \\ &= \int_{-1}^1 e^{ikrx_1} \varphi(r) 2\pi J_0(kx_2 \rho(r)) dr, \end{aligned}$$

where

$$J_0(s) = \frac{1}{2\pi} \int_0^{2\pi} e^{is \cos(\theta)} d\theta$$

is the Bessel function of the first kind and of order zero. Hence, we need to solve the function $\varphi : [-1, 1] \rightarrow \mathbb{C}$ from the one-dimensional integral equation

$$(5.6) \quad H_1 \varphi(x) = \Phi_0(x), \quad x = (x_1, x_2, 0) \in L,$$

where

$$H_1 \varphi(x) = 2\pi \int_{-1}^1 e^{ikrx_1} J_0(kx_2 \rho(r)) \varphi(r) dr.$$

But first, compute the Herglotz wave function v_1^i with a constant density $f = 1$. By the polar symmetry, we need to compute v_1^i only at $x = x_1 e_1$,

$$v_1^i(x_1 e_1) = \int_{S^2} e^{ik\xi_1 x_1} 1 dS(\xi).$$

Since for $\xi = r e_1 + \rho(r) \omega \in S^2$,

$$\omega = (0, \cos(\theta), \sin(\theta)), \quad \rho(r) = \sqrt{1 - r^2},$$

the surface measure is

$$dS(\xi) = \sqrt{1 + |\rho'(r)|^2} \rho(r) dr d\theta = dr d\theta,$$

we get

$$v_1^i(x_1 e_1) = \int_{-1}^1 e^{ikrx_1} dr = 4\pi \frac{\sin(kx_1)}{kx_1}.$$

Hence, by the polar symmetry we get

$$v_1^i(x) = 4\pi \frac{\sin(k|x|)}{k|x|}, \quad x \in \mathbb{R}^3,$$

that is, for the imaginary part we have exactly

$$(5.7) \quad \text{Im} \Phi_0(x) = \frac{k}{(4\pi)^2} H_1 1(x),$$

and only the real part of (5.6) has to be solved numerically.

The equation

$$(5.8) \quad H_1 \varphi = \operatorname{Re} \Phi_0$$

is solved by the collocation method, called also the point matching method. Discretize

$$-1 = r_1 < r_2 < \dots < r_{N-1} < r_N = 1,$$

and let φ_k , be the standard piecewise linear basis function associated to the point r_m , $m = 1, \dots, N$. By representing

$$\varphi = \sum_m \alpha_m \varphi_m,$$

and by asking the equation to hold at the points $x(j) \in L$, $j = 1, \dots, M$, we get for $\alpha = (\alpha_m)$ the system

$$H_1 \alpha = G,$$

where

$$H_{1,jm} = 2\pi \int_{-1}^1 e^{ikrx_1(j)} J_0(kx_2(j)\rho(r)) \varphi_m(r) dr,$$

and

$$G_j = \operatorname{Re} \Phi_0(x(j)).$$

The coefficients α are solved with the Tikhonov regularization. The Tikhonov regularization parameter is chosen manually so that $\|f\|$ is low, compare Figure 14. Finally, the Herglotz density for the complex Φ_0 is

$$(5.9) \quad \varphi = \sum_m \left(\alpha_m + i \frac{k}{(4\pi)^2} \right) \varphi_m.$$

5.2.2 Constructing the indicator function with a given approximation domain

The numerical indicator function I_{num} is computed with a fixed Herglotz density instead of the limits of the Herglotz densities.

To compute the bilinear operator $E(f_z p, f_z p)$ at the point $z \in \mathbb{R}^3$ (z in the computation domain), suppose that the approximation domain is given by

$$A_z = \tau_z M(z) A_0.$$

Suppose also that z is on the axis that is directed

$$\omega = M(z) e_1,$$

and suppose this is also the symmetry axis for A_z . For the cone domain, the cone is opening in the direction $\omega \in S^2$. Now, the approximated Herglotz density for Φ_z is given by

$$f_z = \tau_{-z} R_{M(z)^T} f_0,$$

where

$$f_0(\xi) = \varphi(r), \quad r = \xi_1,$$

is the symmetric approximation of the Herglotz density for Φ_0 on ∂A_0 as described in the previous chapter. Then,

$$\begin{aligned} E(f_z p, f_z q) &= \int_{S^2} \int_{S^2} p \cdot u_\infty^s(-\xi, \eta, q) f_z(\eta) f_z(\xi) dS(\eta) dS(\xi) \\ &= \int_{S^2} \int_{S^2} p \cdot u_\infty^s(-\xi, \eta, q) e^{-ikz \cdot \eta} f_0(M(z)^T \eta) dS(\eta) e^{-ikz \cdot \xi} f_0(M(z)^T \xi) dS(\xi) \\ &= \int_{S^2} \int_{S^2} p \cdot u_\infty^s(-\xi, \eta, q) e^{-ikz \cdot \eta} \varphi(\omega \cdot \eta) dS(\eta) e^{-ikz \cdot \xi} \varphi(\omega \cdot \xi) dS(\xi). \end{aligned}$$

To compute this numerically, assume that the sphere S^2 is triangularized and denote by ϕ_j the standard piecewise linear base function associated to the node j as before. Approximate u_∞^s piecewise linearly,

$$p \cdot u_\infty^s(-\xi, \eta, q) \approx \sum_{j, \ell} U_{j\ell}(p, q) \phi_j(\xi) \phi_\ell(\eta),$$

where

$$U_{j\ell}(p, q) = p \cdot u_\infty^s(-\xi_j, \eta_\ell, q).$$

This corresponds to that the measurements are made in pairs $(-\xi_j, \eta_\ell)$. Now the integral takes the form

$$\begin{aligned} \sum_{j, \ell} U_{j\ell}(p, q) \int_{S^2} \int_{S^2} \phi_j(\xi) \phi_\ell(\eta) e^{-ikz \cdot \xi} e^{-ikz \cdot \eta} \varphi(\omega \cdot \xi) \varphi(\omega \cdot \eta) dS(\xi) dS(\eta) \\ = J(z)^T U(p, q) J(z), \end{aligned}$$

where

$$(5.10) \quad J_j(z) = \int_{S^2} \phi_j(\xi) e^{-ikz \cdot \xi} \varphi(\omega \cdot \xi) dS(\xi).$$

The integral for $J_j(z)$ is computed numerically with integration points and weights on S^2 . As a conclusion, to compute the bilinear form, one needs to have the measurement matrix $U(p, q)$, and for each z , to compute the vector $J(z)$ associated to the triangularization.

Finally, the numerical indicator function is by the linearity

$$\begin{aligned} I_{num}(z) &= \max_{n \in S^2} |E(f_z n, f_z n)| \\ &= \max_{n \in S^2} \left| \sum_{j, k} n_j n_k E(f_z e_j, f_z e_k) \right| \\ (5.11) \quad &= \max_{n \in S^2} \left| \sum_{j, k} n_j n_k J(z)^T U(e_j, e_k) J(z) \right|, \end{aligned}$$

where discretized n can be taken, for example, as the nodes of the triangularized unit sphere S^2 .

5.2.3 Some scanning algorithms

The idea in making the reconstruction is to compute the indicator function with some scanning procedure at each grid point z . Then one draws an isosurface picture of the indicator function.

The approximation domains can be chosen in many ways. The algorithms can be divided into two categories - constructive algorithms and cumulative algorithms. A constructive algorithm is such that for each $z \in \Omega^s$, the approximation domain A_z is chosen so that it satisfies the assumptions for such a domain. In cumulative algorithms one computes the indicator function $I(z)$ with many approximation domains A_z for each z . An individual approximation domain might not satisfy the assumptions, but, eventually one is expecting to get a satisfactory reconstruction, maybe with some artefacts. The constructive algorithms are faster, since one needs to compute the indicator function only with one approximation domain at each grid point.

Radial algorithm The radial algorithm is a constructive algorithm which is easy to implement but assumes quite a lot from the scatterer. Suppose that for each point $x \in \partial\Omega$ the scatterer A is approximatable in D with a cone domain from the direction \hat{x} , in other words, if $z \in D \cap \Omega^s$, then

$$A_z = \tau_z M(\hat{z}) A_0$$

satisfies the assumptions for an approximation domain. Note that this implies that $0 \in \Omega$ necessary. Also, Ω has to be connected. Now, for every $z \in D$, compute $I_{num}(z)$, which is small when z is far from Ω and grows when z tends to $\partial\Omega$. To represent the scatterer, draw a picture of the isosurfaces of $I_{num}(z)$ with some large value. For $z \in \Omega$, the assumptions for the approximation domain fail, but still $I_{num}(z)$ is computable and getting some real values.

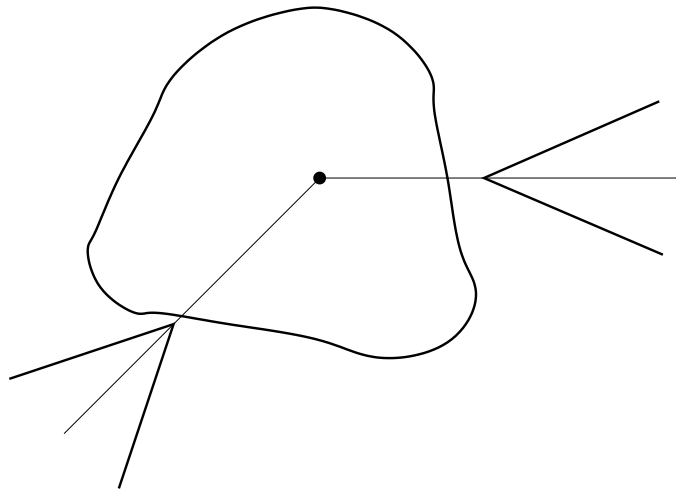


Figure 8: In the radial algorithm the obstacle has to be approximatable radially with a cone.

Back projection algorithm The back projection algorithm (BP) is an example of cumulative algorithms. Suppose that for each point $x \in \partial\Omega$ the scatterer is approximable in D with a cone domain from some direction ξ , that is, if $z \in D \cap \Omega^s$, then

$$A_{z,\xi} = \tau_z M(\xi) A_0$$

satisfies the assumptions for an approximation domain with some ξ . Define the BP indicator function by

$$I_{BP}(z) = \sum_{\xi_n \in S^2} I_{num,\xi_n}(z),$$

where $I_{num,\xi}(z)$ is the indicator function computed with the approximation domain $A_{z,\xi}$. The directions ξ_n run over some discrete set. Since the indicator function becomes large when z gets close to the boundary from some direction from the exterior, the BP indicator function also becomes large then. However, for every z , the assumptions for an approximation domain are not valid from some directions, and hence, $I_{BP}(z)$ can, in principle, be large also for z that is far away from Ω causing some artefacts for the reconstruction.

Compared to the radial algorithm, the back projection algorithm is much heavier computationally, because one is computing the indicator function $I_{num,\xi}$ the number of the directions times.

Maximal scanning algorithm The maximal scanning algorithm is another example of cumulative algorithms. It is very similar to the back projection algorithm, but instead of the sum over the directions, one takes the maximum

$$I_{max}(z) = \max_{\xi \in S^2} I_{num,\xi}(z).$$

5.3 Test cases

The test examples were computed with fat kite domains whose shapes are motivated by the 2D kite shape domains, [36]. A base fat kite is created by transforming a triangularized unit sphere⁸ with mapping

$$S^2 \ni x \mapsto (x_1, x_2, f(x_3)),$$

where

$$f(t) = at^3 + \frac{a-1}{\sqrt{2}}t^2 + t + \frac{1}{\sqrt{2}}, \quad a = \frac{\sqrt{2}-2}{5}.$$

An arbitrary fat kite is then obtained by a rotation, scaling and translation.

We considered two test cases. The first obstacle was a single fat kite and the second obstacle consisted of a pair of fat kite -shaped domains; see Figure 10 and Figure 11.

⁸The triangularization for S^2 is computed with a program of Matti Taskinen and Seppo Järvenpää.

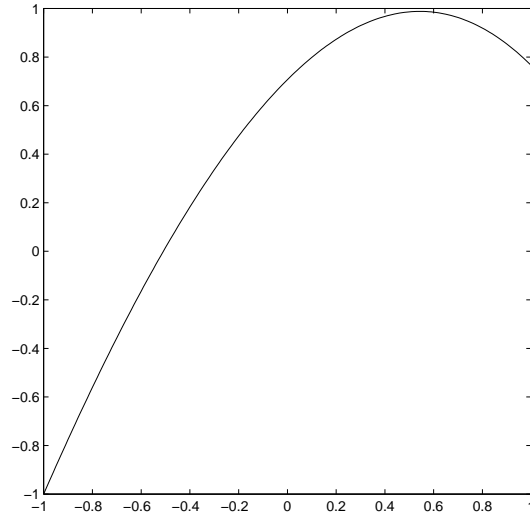


Figure 9: The transform mapping the x_3 -coordinate to get a fat kite from the unit sphere.

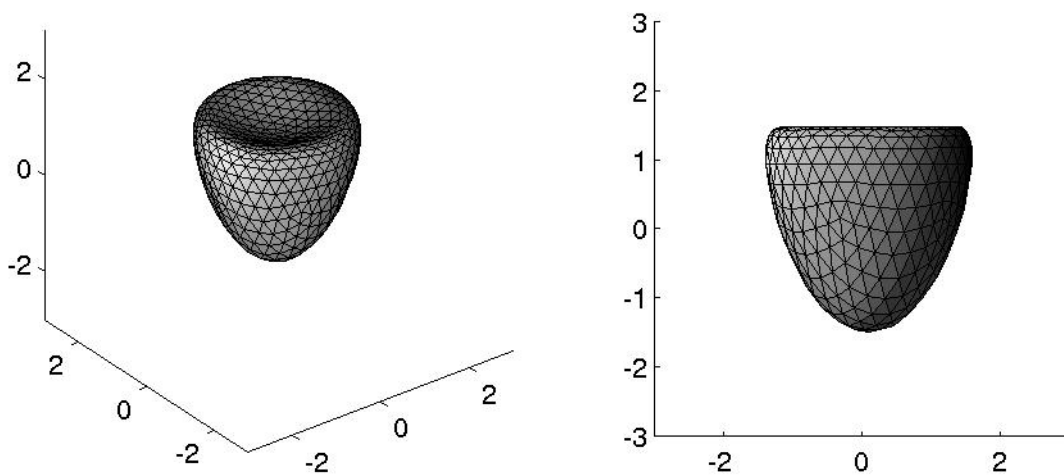


Figure 10: A single fat kite obstacle. The discretization consists of 492 nodes and 980 elements. A base fat kite is translated by the vector $(0.1, 0.2, 0)$ and scaled by the factor 1.5.

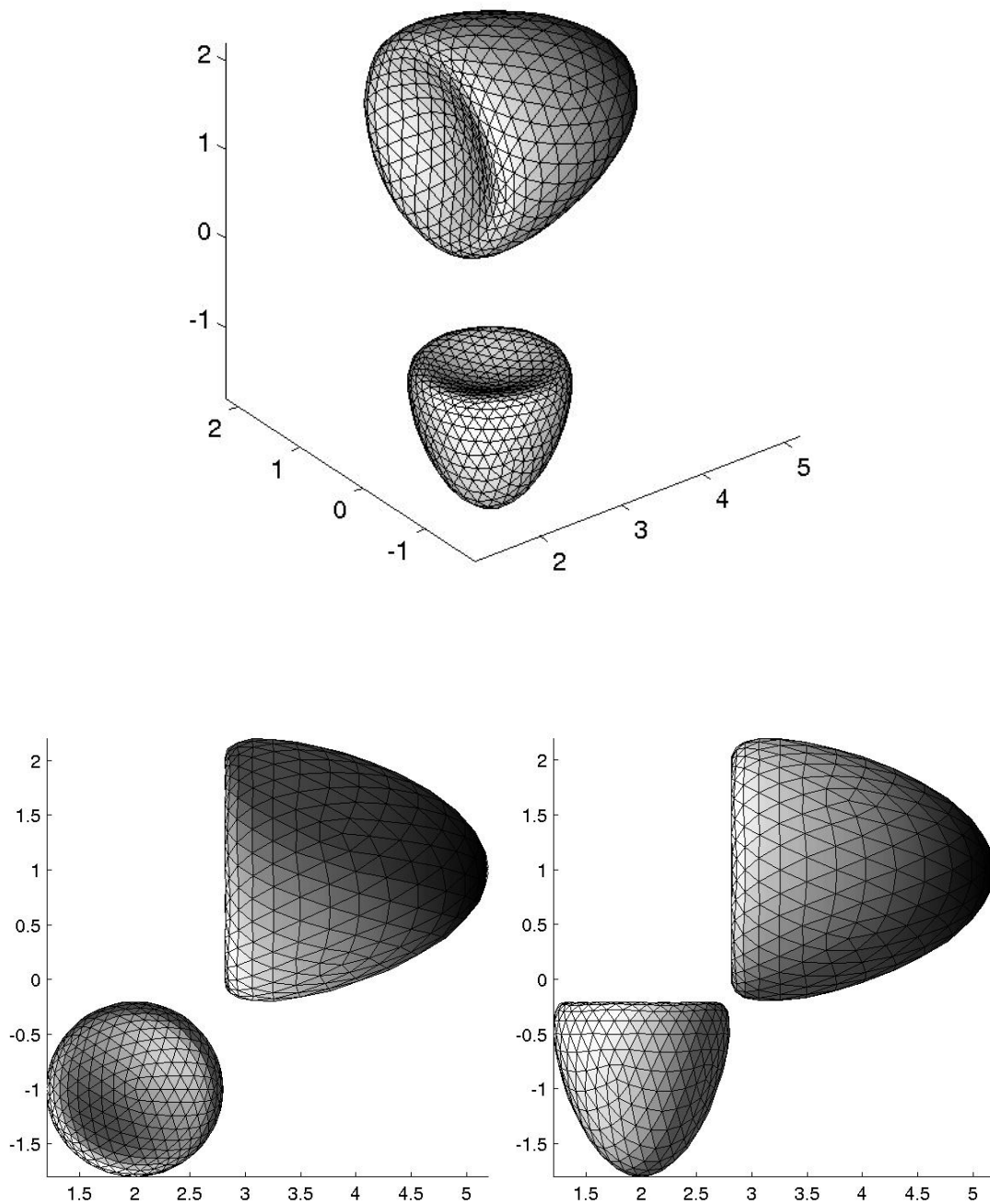


Figure 11: An obstacle consisting of a pair of fat kite -shaped domains whose sizes are slightly different. In the left low image the viewing angle is from above and in the right low image horizontal. Both kites are computed with the same number of elements, causing some difference to the element sizes. The discretization consists of 984 nodes and 1960 elements. For the smaller kite, the base fat kite is translated by the vector $(2, -1, -1)$ and scaled by 0.8. For the larger kite, the translation vector is $(4, 1, 1)$ and the scaling coefficient 1.2. The larger kite was also rotated to open in the direction $(-1, 0, 0)$.

5.3.1 Forward problem

Testing the far field solver is based on the following simple observation. When the singular point z is in the obstacle, then $u^s = \Psi_{z,p}$ is a radiating Beltrami field in the exterior domain. Hence, if we solve f from the boundary integral equation with the right-hand side

$$g_z = n \cdot \Psi_{z,p},$$

then the far field is

$$u_\infty^s = kU_{\partial\Omega}^* f = \Psi_{z,p,\infty},$$

which can be computed directly. Hence, the accuracy of the far field solver can be tested by comparing the boundary integral equation based and numerically solved far field

$$p \cdot kU_{\partial\Omega}^* f(\xi)$$

to known

$$p \cdot \Psi_{z,p,\infty}(\xi) = kp \cdot \left(-(\xi \times)^2 + i(\xi \times) \right) p e^{-ik\xi \cdot z},$$

$\xi \in S^2$.

Results Figure 12 was computed in the two-component case. The wave number was $k = 4$, corresponding to the wave length $\lambda = 2\pi/4 \approx 1.6$. The polarization vector was $p = (\cos(\beta), \sin(\beta), 0)$ with $\beta = 0.5$. The singularity point was at $z = (2, -0.8, -0.9)$. Since the forward problem is well-posed, one can expect a good accuracy for the far field solver. It is hard to see any difference between the true (top left) and the computed (top right) far fields. The relative error (maximum error divided by the maximum absolute value of the true value) is round 1%. One can expect that the numerical error increases if the singularity point z approaches the boundary since the function g_z can no more be approximated well with the given discretization. Note that the test case obstacles were not located at the origin to be able to expose some potential programming errors. For the same reason, the singularity point was not on any symmetricity axis of the kites.

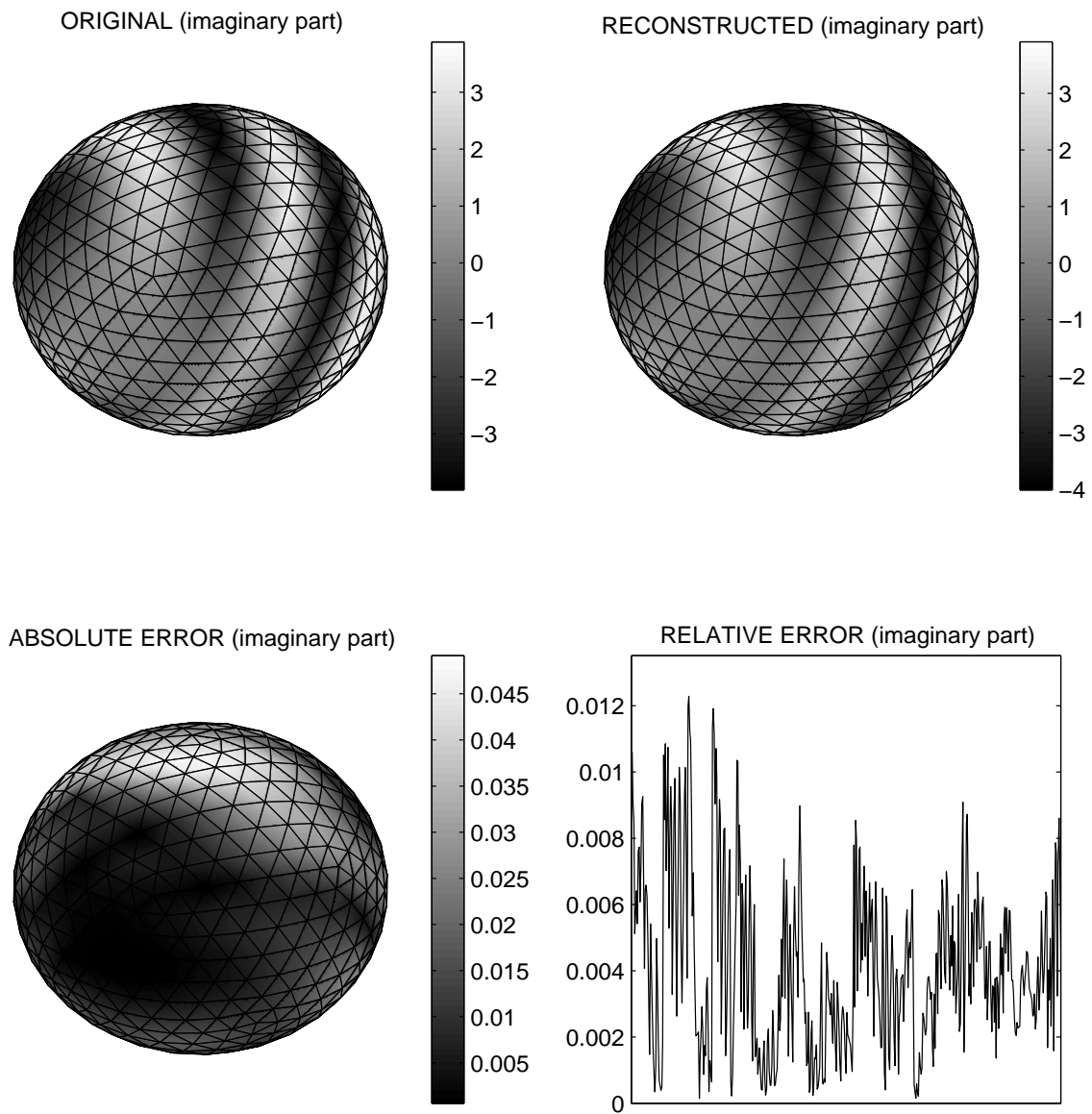


Figure 12: Accuracy of the far field solver, imaginary parts. The far field $p \cdot \Psi_{z,p,\infty}$ is computed at the nodes of the discretized direction surface S^2 . In the top row, the left picture is the truth and the right picture is the reconstructed one. The absolute error of the imaginary part is given in the bottom left image. In the bottom right image, the relative error is plotted as a function of the node indices.

Top	0.14288523793700	0.23263895040999
Bottom 5	0.02302289083348	0.00069725124703
	0.01239024418910	0.00069020016252
	0.01236498907387	0.00014755523225
	0.01204186673852	0.00000000000000
	0.00000000000000	0.00000000000000

Figure 13: Singular values of the system matrix when the obstacle consists of one single component (left column, see Figure 10) or two components (right column, see Figure 11). The top value is the largest singular value. The lower numbers are the five smallest singular values. The theory predicts that the dimension of the kernel $\text{Ker}(T + K)$ equals with the number of the components of the obstacle, see the proof of Theorem 3.13. This fact can be clearly observed also from the singular values.

5.3.2 Inverse problem

The solver for the inverse obstacle scattering problem and its accuracy are tested by examining how well it reconstructs given obstacles. The data is simulated with the forward far field solver. There is no inverse crime since the forward solver based on the boundary element method and the grid points of the inverse problem solver have no connection. The second grid that appears in the computations is the grid of directions $\xi \in S^2$ into which the data is computed. Since these directions ξ can be thought to be the directions of the measurement equipments, they can naturally be assumed to be the same for the forward and the inverse solver. One more point that might too positively affect the results of the inverse algorithms is the general setting of the obstacles. We have tried to eliminate this kind of effects by not locating the obstacles symmetrically around the origin.

In the single-component obstacle case, see Figure 10, we applied the radial algorithm, the back projection algorithm and the maximal scanning algorithm. In the two-component obstacle case, see Figure 11, the radial algorithm was not applicable.

The parameters for the reconstructions were the following:

- The wave number was $k = 4$ as in the forward case.
- The base approximation domain was the cone type domain with radius $R = 10$, see Figure 1. The cone opening angle in two dimensions was $\pi/3$, meaning a $\pi/6$ angle between the x-axis and the two-dimensional line L on the cone part; see (5.5). The distance between the singularity point and A_0 was 0.1.
- The one-dimensional Herglotz density function φ was represented in $N = 542$ points on the interval $[-1, 1]$. The number of the collocation points on L for solving φ from

(5.6) was $M = 541$. The Tikhonov regularizing parameter for (5.6) was 10^{-3} , which was chosen to be a small number for which the norm of the solution does not explode, see Figures 14-16.

- The reconstructions were computed in a $33 \times 33 \times 33$ grid.
- Standard base vectors e_1, e_2, e_3 were used as the normal vectors n over which one maximizes in the formula (5.11).

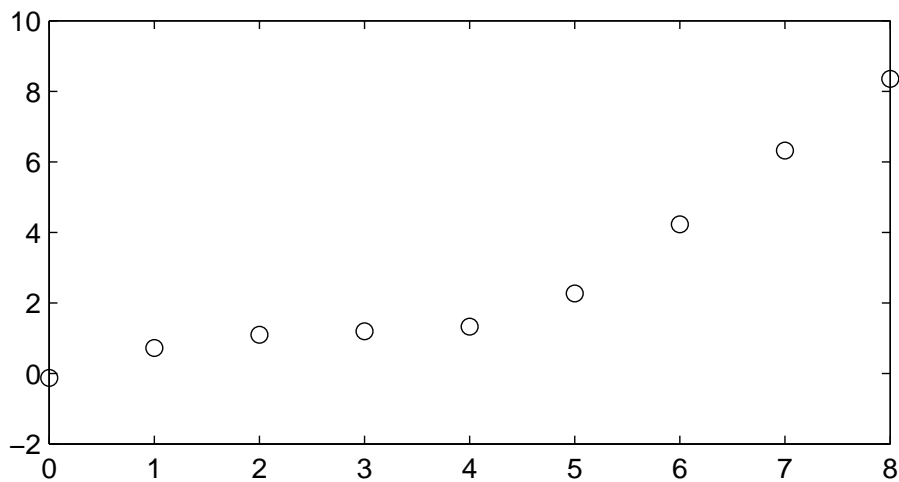


Figure 14: Norm of the Herglotz density φ with respect to the regularizing parameter. In the figure, $\text{Log}\|\varphi\|$ is plotted as a function of j , where $\beta = 10^{-j}$ is the Tikhonov regularization parameter. Since the norm explodes as j gets over four, we have chosen to use the value $\beta = 10^{-3}$ in computing the Herglotz density φ .

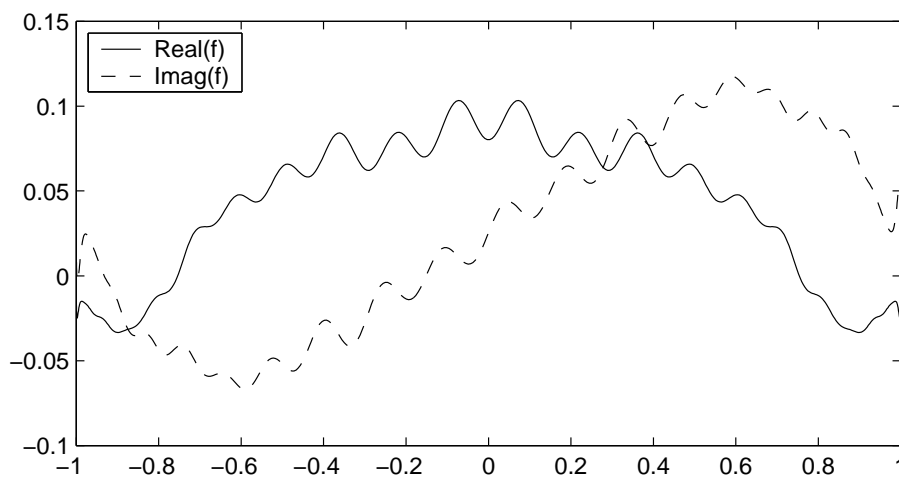


Figure 15: Real and imaginary parts of the Herglotz density $f = \varphi(r)$. Now the function is not oscillating very heavily, so one should be able to estimate the integral (5.10).

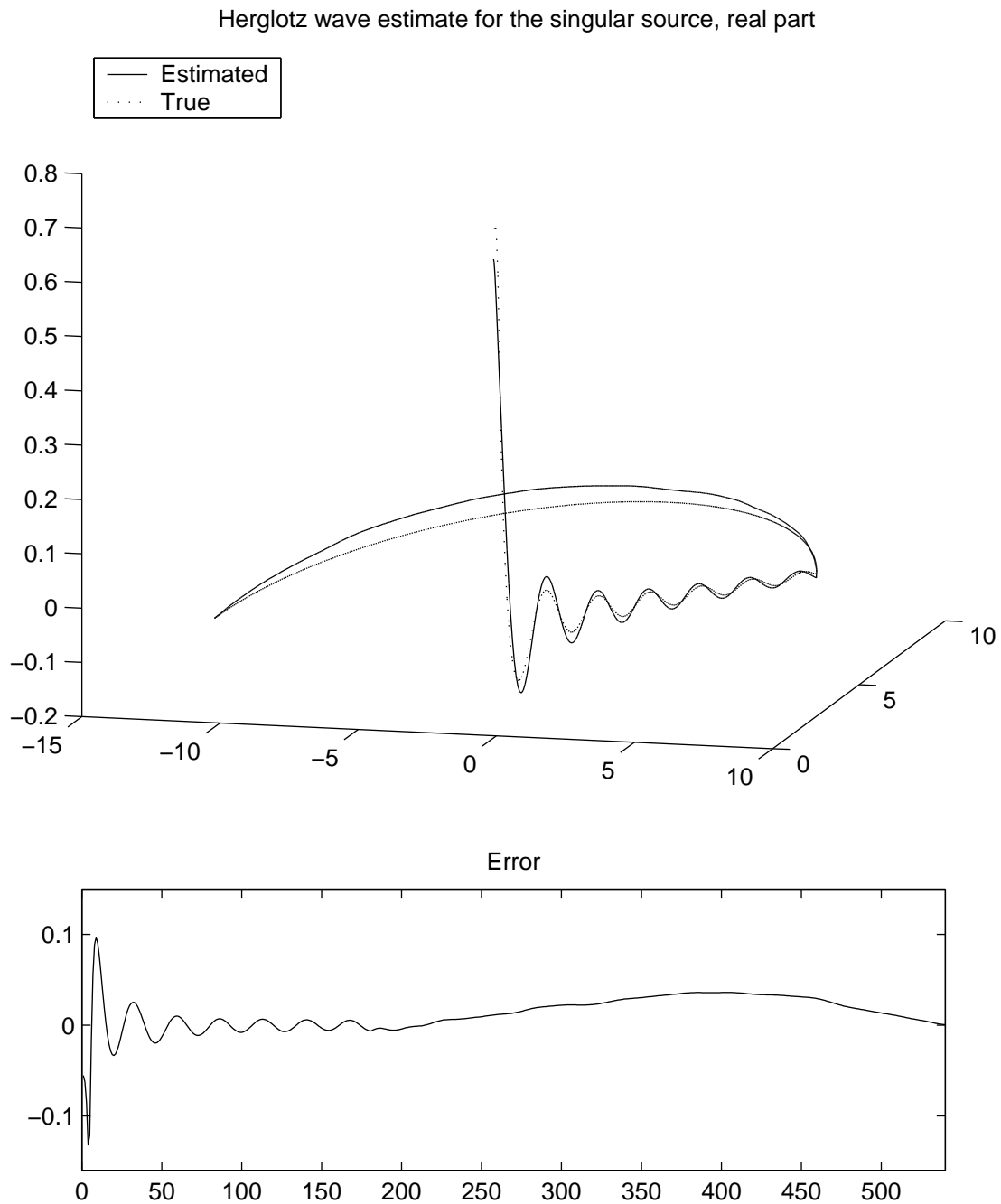


Figure 16: Real part of the true singular source Φ_0 and the Herglotz wave estimate for it on curve L , see (5.5), which determines the cone domain when it is rotated around the x_1 -axis. Naturally, it is hard to approximate the singularity close to the origin. The bottom image is the difference of Φ_0 and the Herglotz wave estimate at the collocation points.

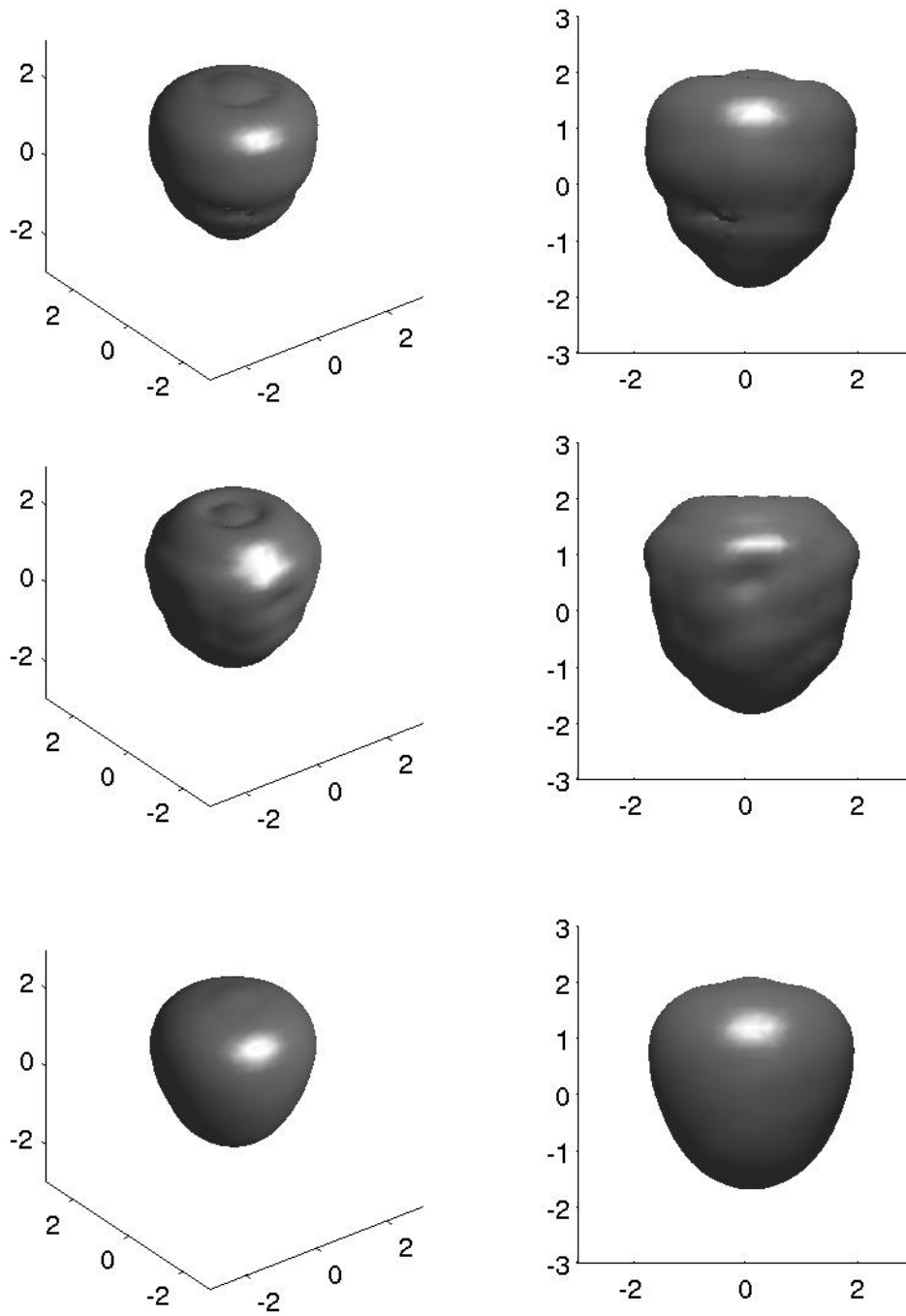


Figure 17: Reconstruction in the single obstacle case with different scanning algorithms. The top row is the radial algorithm, the second row is the maximal scanning algorithm and the bottom row is the BP algorithm. The isosurface value is 50% of the maximum value.

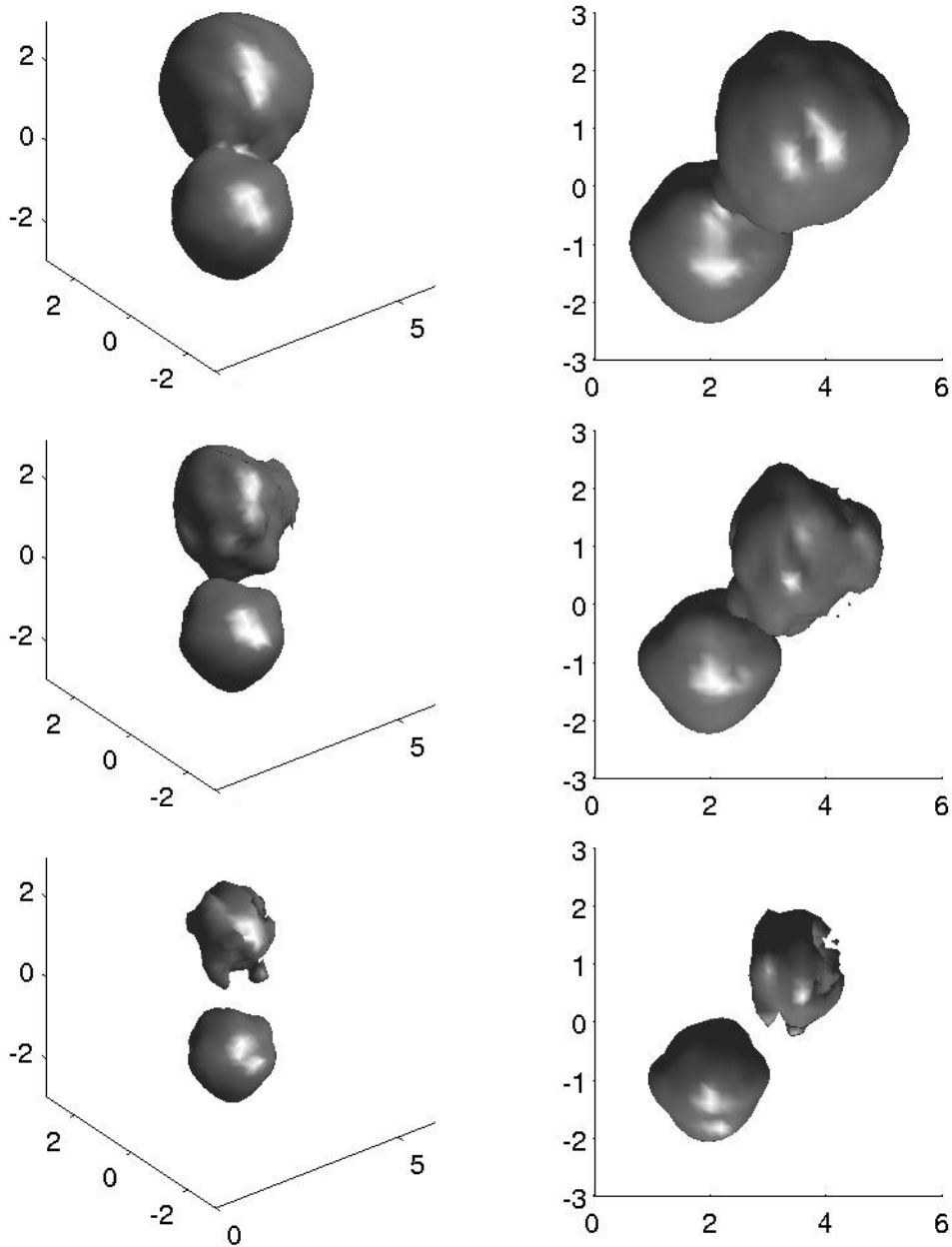


Figure 18: Different isosurface values with the maximal scanning algorithm from two different view angles: In the rows from above, the isosurface values are 40%, 50% and 60% of the maximum value of I_{max} . The bottom row image is the true obstacle.

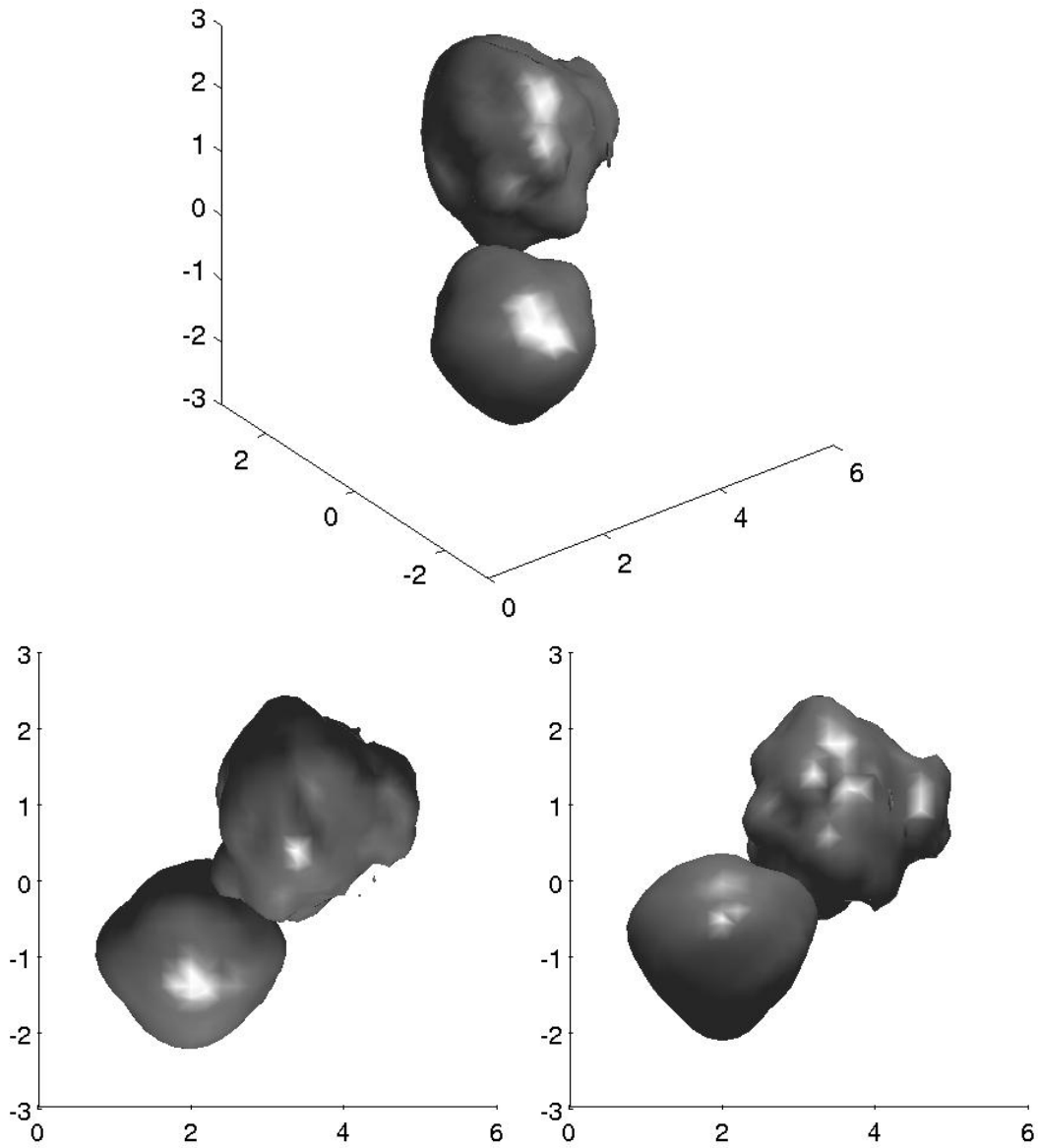


Figure 19: Reconstruction with the maximal scanning algorithm for the two-obstacle case from the same view directions as in Figure 11. The isosurface value is 50% of the maximum value of I_{max} .

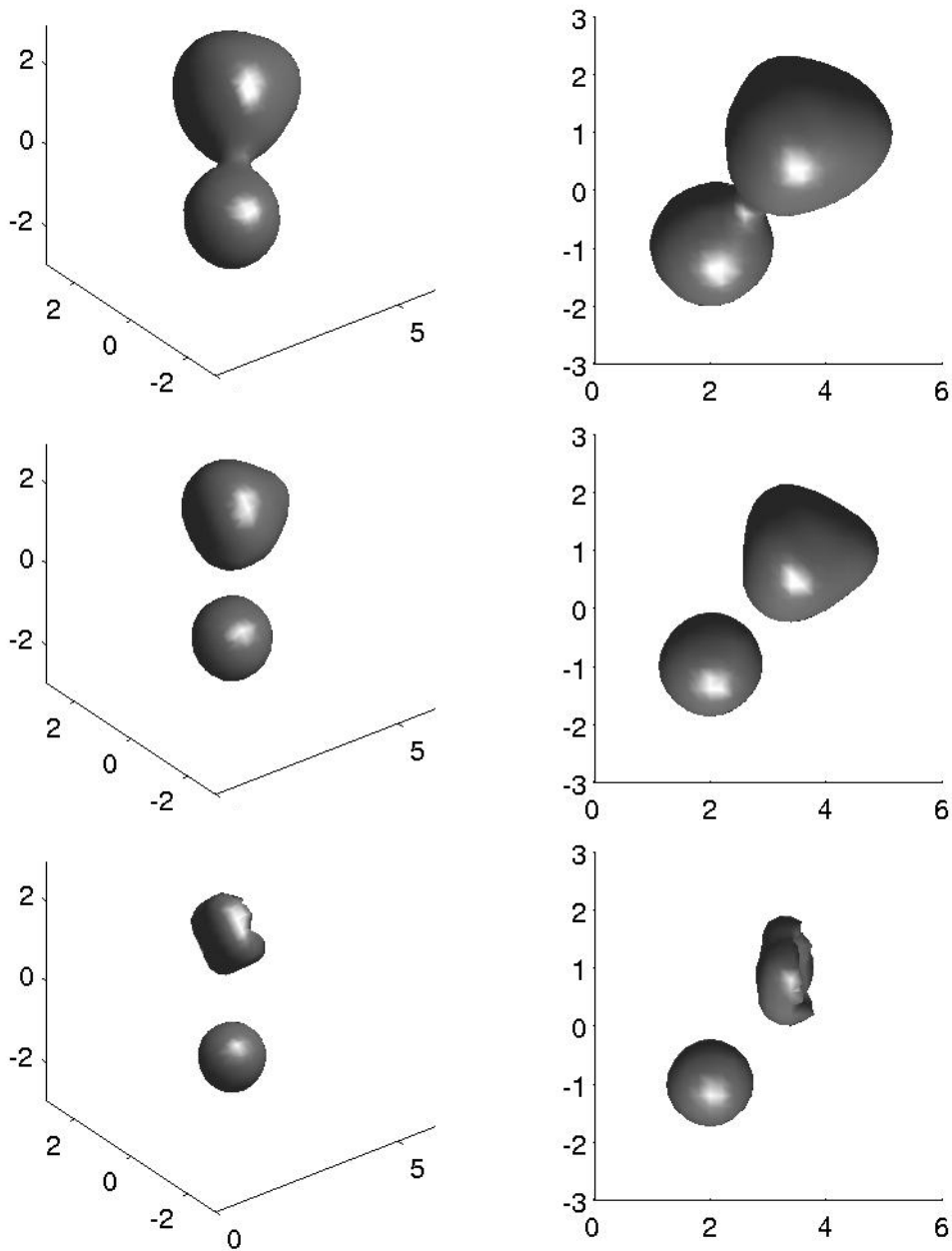


Figure 20: Different isosurface values with the BP algorithm from two different view angles: On the rows from above, the isosurface values are 40%, 50% and 60% of the maximum value of I_{BP} . The bottom row image is the true obstacle.

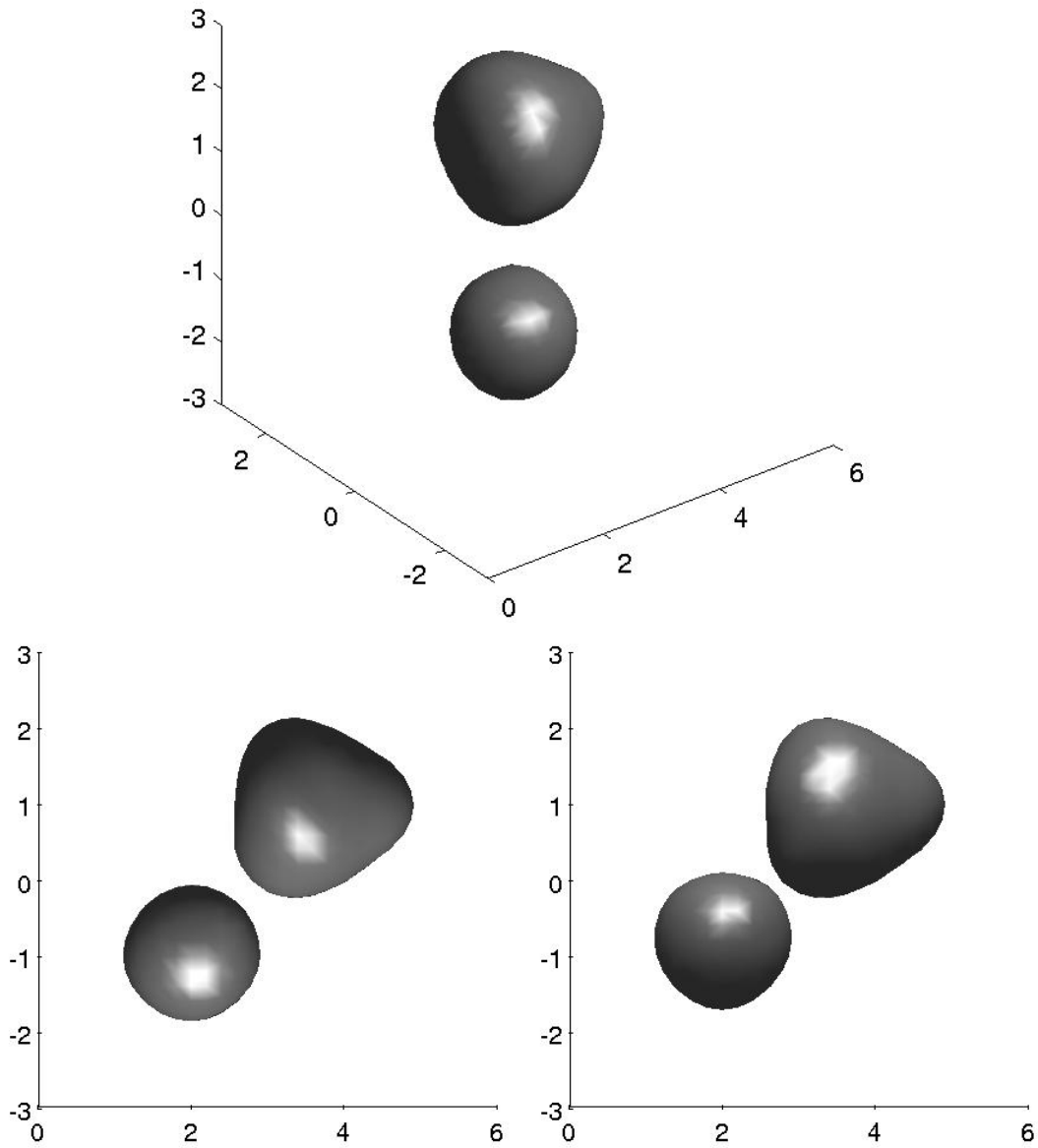


Figure 21: Reconstruction with the BP algorithm for the two-obstacle case from the same view directions as in Figure 11. The isosurface value is 50% of the maximum value of I_{BP} .

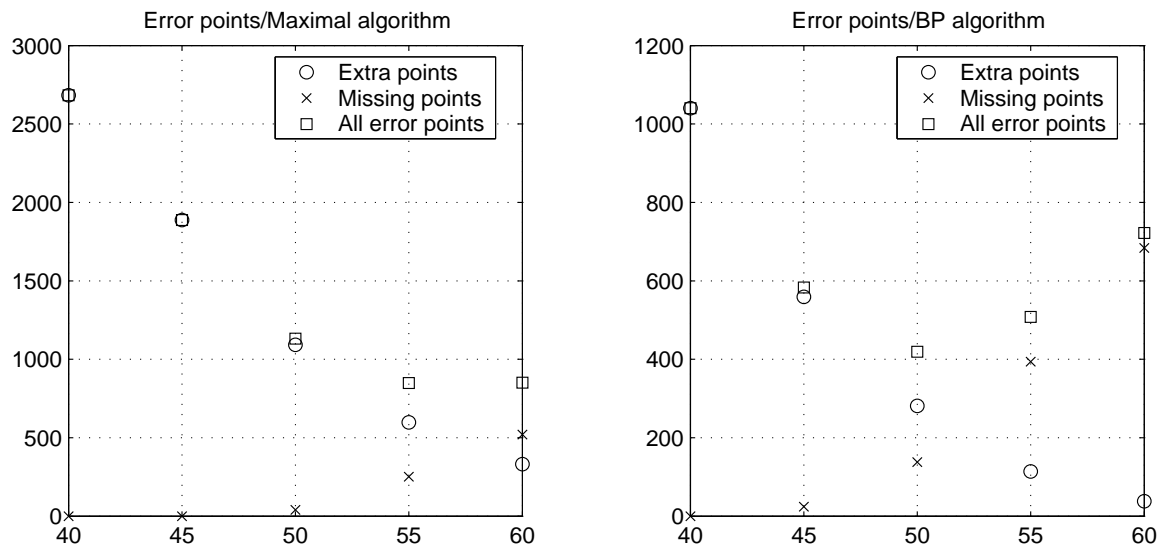


Figure 22: The number of wrongly recovered grid points in terms of the cutting level of the indicator function, the two-obstacle case. The left figure is with the maximal algorithm, the right figure is with the BP algorithm. All together, there are 29791 grid points of which 1050 belong to the scatterer. An extra point is such that the indicator function at the grid point is over the given level, in other words, belongs to the reconstructed scatterer, but the point does not belong to the true scatterer. A missing point is such that the grid point belongs to the true scatterer, but the indicator function at the point is below the given level value. As the cutting level for the indicator function is increased, the number of the extra points is decreasing, whereas the number of the missing points is increasing. The total number of wrongly recovered points (either missing or extra) is marked with a square. The minimum of the error points number is at level 50%, which is consistent with the visual observation. Note, however, that this measure for the reconstruction quality is not very good since there can be points inside the obstacle at which the indicator function is not very large.

Additive noise In practice, data is always noisy. Also the simulated data contains noise, mainly through the boundary element discretization, but next we test the robustness of the reconstruction algorithm by adding normal distributed noise (see Figure 24). The previous reconstructions were made with no extra additive noise.

The additive noise was with 5% noise level, that is, for each measurement value we added ϵ with $\epsilon \sim N(0, \sigma^2)$, where the standard deviation is

$$\sigma = 0.05 \cdot \max_{\xi, \eta, p} |u_{\infty}^s(\xi, \eta, p)|.$$

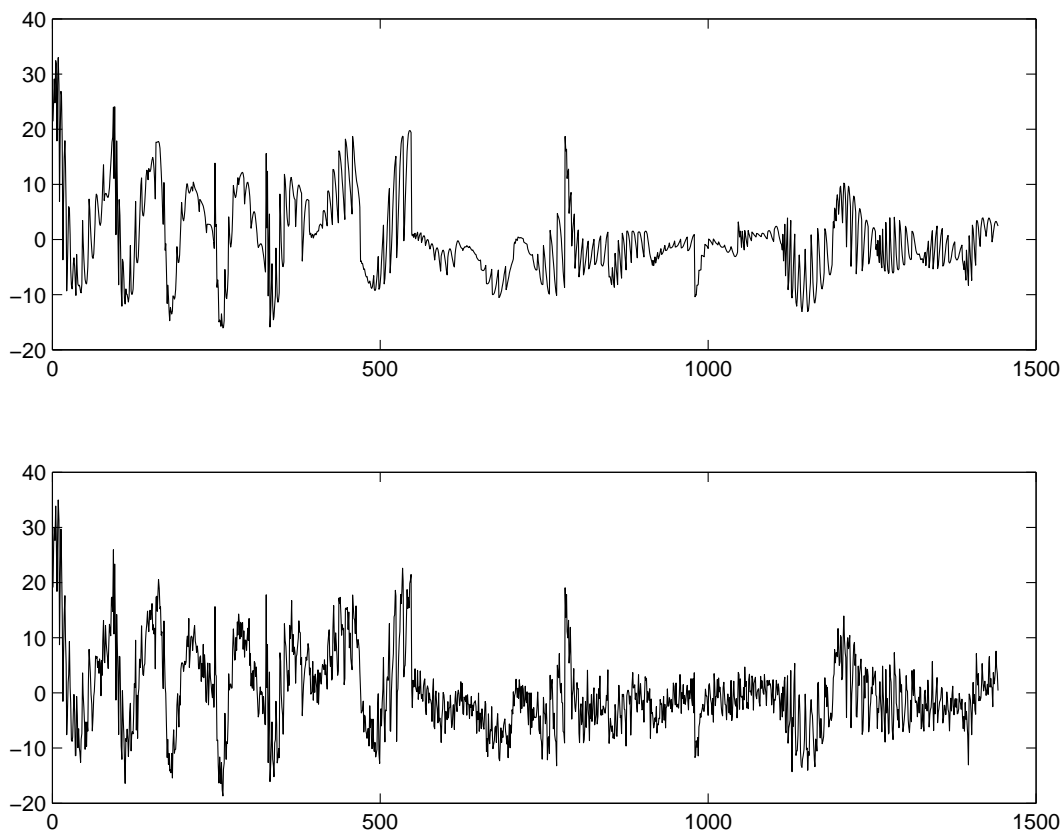


Figure 23: Real part of $u_{\infty}^s(\xi, \cdot)$. Clear data is above and data with 5% additive noise below.

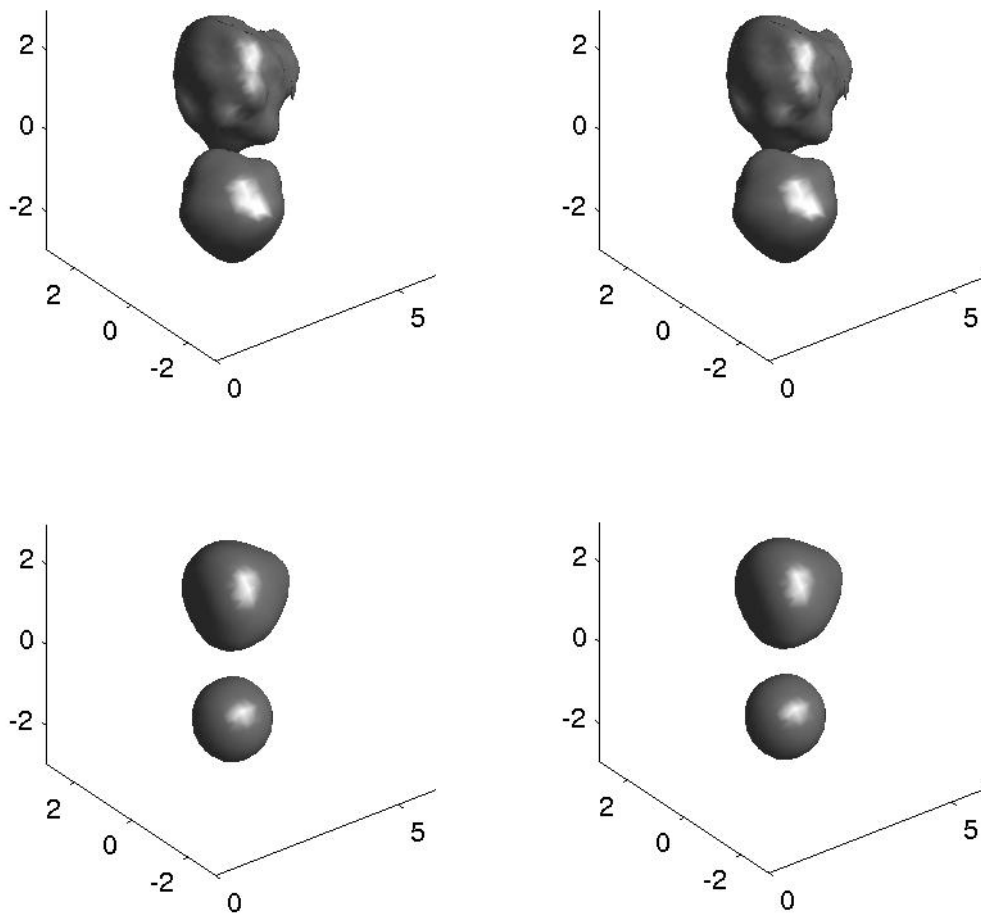


Figure 24: Noise effect. Reconstruction with different scanning algorithms and with 5% additive noise (left column) compared to the reconstructions with no additive noise (right column). The top row is the maximal scanning algorithm and the bottom row is the BP algorithm. The isosurface value is 50% of the maximum value of the indicator function.

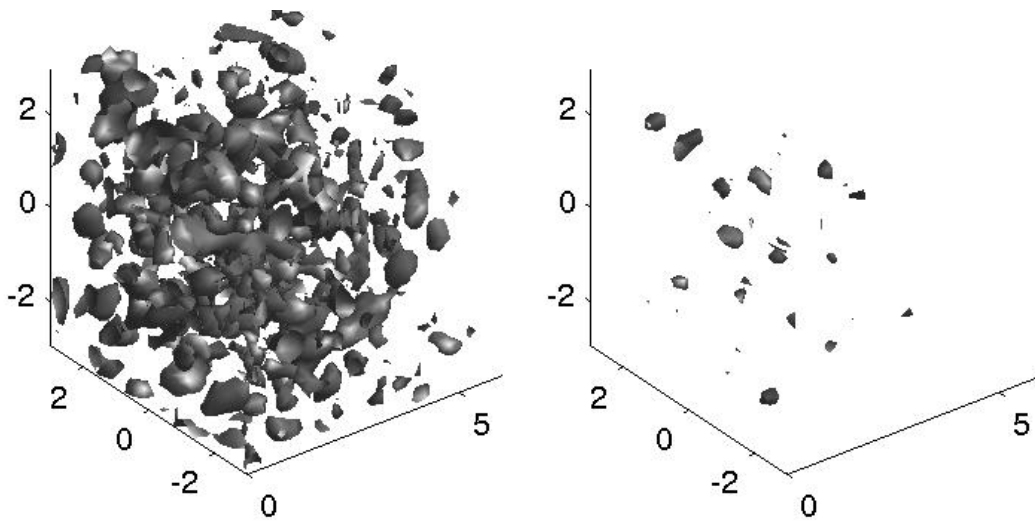


Figure 25: Difference of the indicator function I_{max} with noise and with no noise. The left picture shows the isosurfaces of value 0.1 and the right picture those of value 0.2. We see that the difference is mainly below 0.2. The maximum of I_{max} is set to be 100.

Results The inverse obstacle scattering problem is ill-posed, and one can expect numerical difficulties. However, the reconstructions based on different scanning algorithms give reasonable results. All algorithms find the location and the number of components of the scatterer well. Both cumulative algorithms get through surprisingly well also in the space between the obstacles, which is obviously a difficult place for the cone domain. Between the scanning algorithms, there are differences in the sharpness and smoothness of the reconstructions. Typically, one reconstruction took several hours of computing time on a usual PC machine with our not so well optimized MATLAB codes.

The BP algorithm gives smoothed reconstructions, due to averaging. In the two-obstacle case, one can approximately see the shape of the bigger obstacle, while the smaller obstacle is rounded. The concave part of the obstacle is not seen in the reconstructions.

The maximal algorithm makes sharper or rougher reconstructions when compared to the BP algorithm. The shape of the obstacle is maybe seen better, but at the same time there is much more roughness on the reconstruction. In the one-obstacle case, the concave part is somehow observable in the reconstruction.

The radial scanning algorithm is a constructive algorithm. When the obstacle satisfies the required options, the radial algorithm seems to give as good results as the two cumulative algorithms. The sharpness and roughness of the reconstruction is visually about the same as with the maximal algorithm.

One challenging point is to get the Herglotz wave approximation for the field of the singular source. The corresponding Herglotz wave should not oscillate too heavily. Figure

16 shows that the general behaviour of the Herglotz wave is caught, even if the peak close to the origin is not quite so high as it should be. Also, the oscillation for this density is low, see Figure 15.

Even if the obstacle scattering problem is an ill-posed problem, the reconstruction algorithms seems to manage well with additive noise. It is even hard to see any difference in Figure 24 when the noise is added. An explanation for this is that after the fixed Herglotz density f for approximating Φ_0 is solved (the ill-posed part), then data is integrated against a relatively smooth function f when computing the indicator function.

6 Conclusions

The main purpose of this work is to show that the singular sources method can be applied for the inverse obstacle scattering problem of the Beltrami fields. For this goal, we proved the unique solvability for the exterior Neumann boundary value problem of the Beltrami fields and deduced the formulas that are needed for the singular sources method in this case. We also represented some numerical examples that were computed both for the forward problem and for the inverse problem.

The uniqueness proof for the direct obstacle scattering problem is based on the boundary integral equation approach. The uniqueness, which also leads to the existence according to the Fredholm theory, is obtained from Rellich's Lemma. The numerics for the direct problem follows the theoretical proof, and it is well computable.

The singular sources method was introduced by Potthast in [36]. Earlier, Ikehata presented a probe method that is based on similar ideas, [17, 19]. In this work, the main ideas are translated to the Beltrami field framework. The algorithms were tested with simulated data, and it seems that the method gives feasible reconstructions.

References

- [1] ARENS T.: Linear sampling methods for 2D inverse elastic wave scattering. - *Inverse Problems* 17, 1996, 1445–1464.
- [2] ARENS T.: Why linear sampling works - *Inverse Problems* 20, 2004, 163–173.
- [3] ATHANASIADIS C., G. COSTAKIS and I.G. STRATIS: On some properties of Beltrami fields in chiral media - *Reports on Mathematical Physics* 45, 2000, 257–271.
- [4] BELTRAMI E.: Considerazioni idrodinamiche - *Rend. Ist. Lombardo* 22, 1889, 121–130.
- [5] BOULMEZAOU T.Z., Y. MADAY and T. AMARI: On the linear force-free fields in bounded and unbounded three-dimensional domains - *Math. Model. Numer. Anal* 33, 1999, 359–393.
- [6] BOURDONNAYE A.: Décomposition de $H_{div}^{-1/2}(\Gamma)$ et nature de l'opérateur de Steklov-Poincaré du problème extérieur de l'électromagnétisme - *C. R. Acad. Sci. Paris* 316 Serie I, 1993, 369–372.
- [7] BUFFA A. and P. JR. CIARLET: On traces for functional spaces related to Maxwell's equations Part II: Hodge decompositions on the boundary of Lipschitz polyhedra and applications - *Math. Meth. Appl. Sci.* 24, 2001, 31–48.
- [8] DO CARMO M.: *Riemannian Geometry* - Birkhäuser Boston, 1992.
- [9] COLTON D., J. COYLE and P. MONK: Recent developments in inverse acoustic scattering theory - *SIAM Review* 42, 2000, 369–414.
- [10] COLTON D., H. HADDAR and P. MONK: The linear sampling method for solving the electromagnetic inverse scattering problem - *SIAM Journal of Scientific Computing* 24, 2002, 719–731.
- [11] COLTON D. and A. KIRSCH: A simple method for solving inverse scattering problems in the resonance region - *Inverse Problems* 12, 1996, 383–393.
- [12] COLTON D. and R. KRESS: *Integral Equation Methods in Scattering Theory.* - John Wiley & Sons, 1998.
- [13] COLTON D. and R. KRESS: *Inverse Acoustic and Electromagnetic Scattering Theory* - Springer, 1998.
- [14] DEUTSCH A.J.: Magnetic fields of stars - *Encyclopedia of Physics* Vol. LI, 1958.
- [15] HÖRMANDER L.: *The Analysis of Linear Partial Differential Operators I* - Springer-Verlag, 1990.

- [16] IKEHATA M.: Reconstruction of an obstacle from the scattering amplitude at a fixed frequency - *Inverse Problems* 14, 1998, 949–954.
- [17] IKEHATA M.: Reconstruction of an obstacle from boundary measurements - *Wave Motion* 30, 1999, 205–223.
- [18] IKEHATA M.: Inverse scattering problems and the enclosure method - *Inverse Problems* 20, 2004, 533–551.
- [19] IKEHATA M.: A new formulation of the probe method and related problems - *Inverse Problems* 21, 2005, 413–426.
- [20] KIRSCH A.: Characterization of the shape of a scattering obstacle using the spectral data of the far field operator - *Inverse Problems* 14, 1998, 1489–1512.
- [21] KIRSCH A.: The factorization method for Maxwell’s equations - *Inverse Problems* 20, 2004, S117–S134.
- [22] KIRSCH A.: The factorization method for a class of inverse elliptic problems - *Math. Nachr.* 278, 2005, 248–277.
- [23] KIRSCH A. and R. KRESS: An optimization method in inverse acoustic scattering, in *Boundary Elements IX* - Springer-Verlag, Heidelberg 1987, 3-18.
- [24] KIRSCH A. and R. KRESS: Uniqueness in inverse obstacle scattering - *Inverse Problems* 9, 1993, 285–299.
- [25] KRESS R.: Ein Neumannsches Randwertproblem bei kraftfreien Feldern - *Meth. Verf. math. Phys.* 7, 1972, 81–97.
- [26] KRESS R.: A remark on a boundary value problem for force-free fields - *Journal of Applied Mathematics and Physics (ZAMP)* 28, 1977, 715–722.
- [27] KRESS R.: The treatment of a Neumann boundary value problem for force-free fields by an integral equation method - *Proc. of the Royal Society of Edinburgh* 82A, 1978, 71–86.
- [28] LUKE D.R. and R. POTTHAST: The no response test – a sampling method for inverse scattering problems - *SIAM J. Appl. Math.* 63, 2003, 1292–1312.
- [29] MCLEAN W.: *Strongly Elliptic Systems and Boundary Integral Equations* - Cambridge University Press, 2000.
- [30] OLA P.: Boundary integral equations for the scattering of electromagnetic waves by a homogeneous chiral obstacle - *J. Math. Phys.* 35, 1994, 3969–3980.

- [31] OLA P., L. PÄIVÄRINTA and E. SOMERSALO: An inverse boundary value problem in electrodynamics - *Duke Mathematical Journal* 70, 1993, 617–653.
- [32] OLA P. and E. SOMERSALO: Electromagnetic inverse problem and generalized Sommerfeld potentials - *SIAM J. Appl. Math.* 56, 1996, 1129–1145.
- [33] PICARD R.: Ein Randwertproblem in der Theorie kraftfreier Magnetfelder - *Z. angew. Math. Phys.* 27, 1976, 169–180.
- [34] PICARD R.: On the low frequency asymptotics in electromagnetic theory - *J. Reine Angew. Math.* 394, 1984, 50–73.
- [35] POTTHAST R.: A point source method for inverse acoustic and electromagnetic obstacle scattering problems - *IMA J. Appl. Math.* 61, 1998, 119–140.
- [36] POTTHAST R.: Stability estimates and reconstructions in inverse acoustic scattering using singular sources - *Journal of Comp. and Appl. Mathematics* 114, 2000, 247–274.
- [37] RAMM A. G.: *Scattering by obstacles* - Reidel, 1986.
- [38] SARKOLA E.: A unified approach to direct and inverse scattering for acoustic and electromagnetic waves. - *Annales Academiae Scientiarum Fennicae* 114, 1995.
- [39] SCHIELD M.A., J.W. FREEMAN and A.J. DESSLER: A Source for Field-Aligned Currents at Auroral Latitudes - *Journal of Geophysical Research* 74, 1967, 247-256.
- [40] SERRIN J.: Mathematical principles of classical fluid mechanics. - *Encyclopedia of Physics* Vol. VIII/1, 1959.
- [41] TAYLOR M.: *Partial Differential Equations II* - Springer, 1996.
- [42] TAYLOR M.: *Pseudodifferential Operators* - Princeton University Press, 1981.
- [43] TREVES R.: *Introduction to Pseudodifferential and Fourier Integral Operators* - Plenum Press, 1980.

ANNALES ACADEMIÆ SCIENTIARUM FENNICÆ
MATHEMATICA DISSERTATIONES

101. SARKOLA, EINO, A unified approach to direct and inverse scattering for acoustic and electromagnetic waves. (95 pp.) 1995
102. PARKKONEN, JOUNI, Geometric complex analytic coordinates for deformation spaces of Koebe groups. (50 pp.) 1995
103. LASSAS, MATTI, Non-selfadjoint inverse spectral problems and their applications to random bodies. (108 pp.) 1995
104. MIKKONEN, PASI, On the Wolff potential and quasilinear elliptic equations involving measure. (71 pp.) 1996
105. ZHAO RUHAN, On a general family of function spaces. (56 pp.) 1996
106. RUUSKA, VESA, Riemannian polarizations. (38 pp.) 1996
107. HALKO, AAPO, Negligible subsets of the generalized Baire space $\omega_1^{\omega_1}$. (38 pp.) 1996
108. ELFVING, ERIK, The G -homotopy type of proper locally linear G -manifolds. (50 pp.) 1996
109. HUOVINEN, PETRI, Singular integrals and rectifiability of measures in the plane. (63 pp.) 1997
110. KANKAANPÄÄ, JOUNI, On Picard-type theorems and boundary behavior of quasiregular mappings. (38 pp.) 1997
111. YONG LIN, Menger curvature, singular integrals and analytic capacity. (44 pp.) 1997
112. REMES, MARKO, Hölder parametrizations of self-similar sets. (68 pp.) 1998
113. HÄMÄLÄINEN, JYRI, Spline collocation for the single layer heat equation. (67 pp.) 1998
114. MALMIVUORI, MARKKU, Electric and magnetic Green's functions for a smoothly layered medium. (76 pp.) 1998
115. JUUTINEN, PETRI, Minimization problems for Lipschitz functions via viscosity solutions. (53 pp.) 1998
116. WULAN, HASI, On some classes of meromorphic functions. (57 pp.) 1998
117. ZHONG, XIAO, On nonhomogeneous quasilinear elliptic equations. (46 pp.) 1998
118. RIEPPO, JARKKO, Differential fields and complex differential equations. (41 pp.) 1998
119. SMOLANDER, PEKKA, Numerical approximation of bicanonical embedding. (48 pp.) 1998
120. WU PENGCHENG, Oscillation theory of higher order differential equations in the complex plane. (55 pp.) 1999
121. SILTANEN, SAMULI, Electrical impedance tomography and Faddeev Green's functions. (56 pp.) 1999
122. HEITTOKANGAS, JANNE, On complex differential equations in the unit disc. (54 pp.) 2000
123. TOSSAVAINEN, TIMO, On the connectivity properties of the ρ -boundary of the unit ball. (38 pp.) 2000
124. RÄTTYÄ, JOUNI, On some complex function spaces and classes. (73 pp.) 2001
125. RISSANEN, JUHA, Wavelets on self-similar sets and the structure of the spaces $M^{1,p}(E, \mu)$. (46 pp.) 2002
126. LLORENTE, MARTA, On the behaviour of the average dimension: sections, products and intersection measures. (47 pp.) 2002
127. KOSKENOJA, MIKA, Pluripotential theory and capacity inequalities. (49 pp.) 2002
128. EKONEN, MARKKU, Generalizations of the Beckenbach–Radó theorem. (47 pp.) 2002
129. KORHONEN, RISTO, Meromorphic solutions of differential and difference equations with deficiencies. (91 pp.) 2002

130. LASANEN, SARI, Discretizations of generalized random variables with applications to inverse problems. (64 pp.) 2002
131. KALLUNKI, SARI, Mappings of finite distortion: the metric definition. (33 pp.) 2002
132. HEIKKALA, VILLE, Inequalities for conformal capacity, modulus, and conformal invariants. (62 pp.) 2002
133. SILVENNOINEN, HELI, Meromorphic solutions of some composite functional equations. (39 pp.) 2003
134. HELLSTEN, ALEX, Diamonds on large cardinals. (48 pp.) 2003
135. TUOMINEN, HELI, Orlicz-Sobolev spaces on metric measure spaces. (86 pp.) 2004
136. PERE, MIKKO, The eigenvalue problem of the p -Laplacian in metric spaces (25 pp.) 2004
137. VOGELER, ROGER, Combinatorics of curves on Hurwitz surfaces (40 pp.) 2004
138. KUUSELA, MIKKO, Large deviations of zeroes and fixed points of random maps with applications to equilibrium economics (51 pp.) 2004
139. SALO, MIKKO, Inverse problems for nonsmooth first order perturbations of the Laplacian (67 pp.) 2004
140. LUKKARINEN, MARI, The Mellin transform of the square of Riemann's zeta-function and Atkinson's formula (74 pp.) 2005
141. KORPPI, TUOMAS, Equivariant triangulations of differentiable and real-analytic manifolds with a properly discontinuous action (96 pp.) 2005
142. BINGHAM, KENRICK, The Blagoveščenskii identity and the inverse scattering problem (86 pp.) 2005
143. PIIROINEN, PETTERI, Statistical measurements, experiments and applications (89 pp.) 2005
144. GOEBEL, ROMAN, The group of orbit preserving G -homeomorphisms of an equivariant simplex for G a Lie group (63 pp.) 2005
145. XIAONAN LI, On hyperbolic Q classes (66 pp.) 2005
146. LINDÉN, HENRI, Quasihyperbolic geodesics and uniformity in elementary domains (50 pp.) 2005
147. RAVAIOLI, ELENA, Approximation of G -equivariant maps in the very-strong-weak topology (64 pp.) 2005
148. RAMULA, VILLE, Asymptotical behaviour of a semilinear diffusion equation (62 pp.) 2006

5 €

Distributed by

BOOKSTORE TIEDEKIRJA
 Kirkkokatu 14
 FI-00170 Helsinki
 Finland
<http://www.tsv.fi>

ISBN 951-41-0987-2